CALCULATION OF REALISTIC CHARGED-PARTICLE TRANSFER MAPS*

C E. Mitchell and A. J. Dragt, University of Maryland, USA

Abstract

The stability of orbits in storage and damping rings can depend sensitively on nonlinear fringe-field and high-order-multipole effects in the various beam-line elements. The inclusion of these effects requires a detailed and realistic model of the interior and fringe electric and magnetic fields, including their high spatial derivatives. In the case of magnetic elements a collection of surface fitting methods has been developed for extracting this information accurately from 3-dimensional magnetic field data on a grid, as provided by various 3-dimensional finite element field codes. The virtue of surface methods is that they exactly satisfy the Maxwell equations and are relatively insensitive to numerical noise in the data. These techniques can be used both to compute realistic design orbits and realistic high-order transfer maps about these orbits. An exactly soluble but numerically challenging model field is used to provide a rigorous collection of performance benchmarks.

BACKGROUND

For the design of high-performance storage or damping rings it is essential to have realistic electric and magnetic field information for the various beam-line elements, in order to compute accurate design orbits and high-order transfer maps about the design orbits. Realistic field data can be provided on a grid with the aid of various 3-dimensional finite element codes, sometimes spot checked against measured data. But the computation of high-order transfer maps based on this data appears to pose an insurmountable problem: the calculation of high-order transfer maps requires a knowledge of high derivatives of the field data. The direct calculation of high derivatives based only on grid data is intolerably sensitive to noise (due to truncation or round-off) in the grid data. We will see that this problem can be overcome by the use of surface methods. The effect of numerical noise can be overcome by fitting onto a bounding surface far from the beam axis and continuing inward using the Maxwell equations. While the process of differentiation serves to amplify the effect of numerical noise, the process of continuing inward using the Maxwell equations is *smoothing*. This smoothing is related to the fact that harmonic functions take their extrema on boundaries. When using surface methods, all fits are made to such boundaries. Therefore if these fits are accurate, interior data based on these fits will be even more accurate.

In this paper we will devote our attention to magnetic beam-line elements. (For a treatment of RF cavities, see [1].) Two cases have been treated separately: straight and curved. For straight beam-line elements such as quadrupoles, sextupoles, octupoles, and wiggglers, it is convenient to employ cylindrical surfaces. These surfaces may have circular, elliptical, or rectangular cross sections. We will describe the use of elliptical cylinders. The use of circular and rectangular cylinders is described elsewhere [2, 3, 4]. For the case of curved magnetic elements such as dipoles with large design-orbit sagitta, we will employ the surface of a bent box with straight ends. In all cases the bounding surface will surround the design orbit within the beam-line element and will extend into the fringe-field regions outside the beam-line element, thus taking into account all fringe-field effects as well as all effects within the body of the beam-line element.

For the case of straight beam-line elements it is convenient to describe the magnetic field in terms of a magnetic scalar potential ψ. Then, if one wishes to compute transfer maps in terms of canonical coordinates, one can proceed with the aid of an associated vector potential $\boldsymbol{A}$ computed from ψ. Alternatively, if one wishes to integrate noncanonical equations employing the magnetic field $\boldsymbol{B}$, it can be obtained from the relation $\boldsymbol{B} = \nabla\psi$.

For the case of curved beam-line elements it is convenient to work directly with the vector potential. Its use in the case of canonical coordinates is then immediate. If instead one wishes to integrate noncanonical equations employing the magnetic field $\boldsymbol{B}$, it can be obtained from the relation $\boldsymbol{B} = \nabla \times \boldsymbol{A}$.

In this paper we will first treat the case of straight beam-line elements. For this case a cylindrical multipole expansion for ψ is convenient. In Sections II-III we will describe such an expansion and how it can be computed based on $\boldsymbol{B}$ data provided on a grid and interpolated onto the surface of an elliptical cylinder. In Section IV we will treat the case of curved beam-line elements. In this case $\boldsymbol{A}$ will be computed based on both $\boldsymbol{B}$ and ψ data provided on a grid and interpolated onto the surface of a bent box.

CYLINDRICAL HARMONIC EXPANSIONS

In a current-free region the magnetic field $\boldsymbol{B}$ is curl free, and can therefore can be described in terms of a magnetic scalar potential. Because $\boldsymbol{B}$ is also divergence free, ψ must obey the Laplace equation $\nabla^2\psi = 0$. A general solution ψ satisfying the Laplace equation in cylindrical coordinates

* Work supported by U.S. Department of Energy Grant DE-FG02-96ER40949.

CONSTRUCTION OF LARGE-PERIOD SYMPLECTIC MAPS BY INTERPOLATIVE METHODS *

Robert L. Warnock † and Yunhai Cai‡
SLAC National Accelerator Laboratory, Stanford University, Menlo Park, CA 94025, USA
James A. Ellison§
Dept. of Mathematics and Statistics, University of New Mexico, Albuquerque, NM 87131, USA

Abstract

The goal is to construct a symplectic evolution map for a large section of an accelerator, say a full turn of a large ring or a long wiggler. We start with an accurate tracking algorithm for single particles, which is allowed to be slightly non-symplectic. By tracking many particles for a distance S one acquires sufficient data to construct the mixed-variable generator of a symplectic map for evolution over S, given in terms of interpolatory functions. Two ways to find the generator are considered: (i) Find its gradient from tracking data, then the generator itself as a line integral. (ii) Compute the action integral on many orbits. A test of method (i) has been made in a difficult example: a full turn map for an electron ring with strong nonlinearity near the dynamic aperture. The method succeeds at fairly large amplitudes, but there are technical difficulties near the dynamic aperture due to oddly shaped interpolation domains. For a generally applicable algorithm we propose method (ii), realized with meshless interpolation methods.

1. INTRODUCTION

The method of differential algebra, giving automatic differentiation of functions defined by complex algorithms, allows the construction of the truncated Taylor series of a map defined by a tracking code. After this method was implemented by Martin Berz [1], the option of producing a Taylor map eventually became a feature of several tracking codes. The Taylor map is not symplectic, but some codes use the Taylor coefficients to produce the mixed-variable generator of a symplectic map, itself represented as a truncated power series [2]. Another way is to use the Taylor coefficients to form the symplectic "jolt factorization" of Irwin, Abell, and Dragt [3]. The Taylor map, symplectified or not, is good at small phase space amplitudes, but has a range of usefulness at larger amplitudes that varies with the type of accelerator lattice considered. It appears to be fairly useful for hadron rings, but can fail badly for electron rings with stronger nonlinearity near the dynamic aperture. In this paper we choose such a lattice for a demanding test of mapping methods.

* Work supported in part by U.S. Department of Energy contracts DE-AC02-76SF00515 and DE-FG-99ER41104.
† warnock@slac.stanford.edu; also affiliated with LBNL and UNM.
‡ yunhai@slac.stanford.edu
§ ellison@math.unm.edu

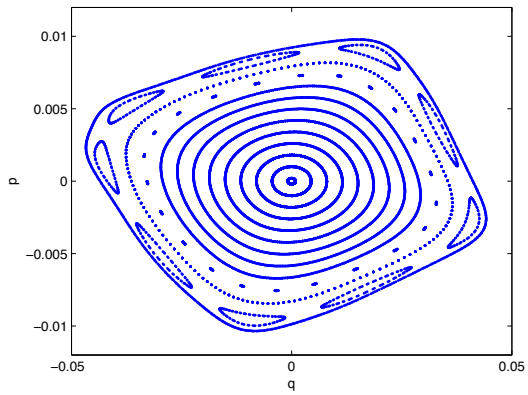

Figure 1: Phase plot from element-by-element tracking, 1000 turns, $\nu_x = 16.23$.

For our example the Taylor map fails at large amplitudes. For a striking illustration we choose a tune $\nu_x = 16.23$. Element-by-element tracking gives the plot of Fig.1 on a Poincaré section at a fixed position in the ring; p is dimensionless and q is in meters. The corresponding plot from iteration of the 10th order Taylor map is shown in Fig.2. The prominent 9th order island chain is only vaguely visible, and there is spurious stochasticity. The result is not improved by going to 13th order. The symplectified Taylor map [2] shows islands and gets rid of the stochasticity, but the shape of phase contours is all wrong. Changing to a better tune of $\nu_x = 15.81$, for which the lattice has a much larger dynamic aperture, we find that the Taylor map still breaks down at about the same amplitude.

One can easily see, however, that producing a more successful map when the Taylor series fails is not out of the question. A spline fit to one-turn tracking data on a grid of initial conditions gives a map which produces the plot of Fig.3 in 1000 iterations. To graphical accuracy it agrees with the tracking map of Fig.1, but the symplectic condition is badly violated at large amplitudes: the determinant of the map's Jacobian differs from 1 at some points by as much as 0.004. Nevertheless it does not do badly over 10^5 iterations, as is seen in Fig.4. The main features of the phase plot persist correctly, but fuzziness appears near ends of the islands. By 10^6 turns there is a clear failure, with spurious damping, whereas phase curves including the islands are sharply defined in tracking for 10^6 turns. The spline is a tensor product B-spline interpolating tracking

HIGHLY SCALABLE NUMERICAL METHODS FOR SIMULATION OF SPACE CHARGE DOMINATED BEAMS *

J. Xu #, B. Mustapha, P. N. Ostroumov, and J. A. Nolen, Argonne National Laboratory, Argonne, IL 60439, USA

ABSTRACT

Beam dynamic simulations with kinetic model have been conducted. We have successfully parallelized a PIC solver, TRACK, and developed new Vlasov solvers. For the PIC solver, particles are distributed evenly on different processors and space charge effect has been counted by solving Poisson's equation on a finite mesh. Several Poisson solvers have been developed using Fourier method in Cartesian coordinate system, Fourier Spectral Element in Cylindrical coordinate system, Wavelet method, Spectral Element Method (SEM) on structured and unstructured grids. Domain decomposition (DD) has been used to parallelize these solvers. Different Poisson solvers have been developed for simulating space charge dominated beams. These solvers have been incorporated into PTRACK and Vlasov solvers. PTRACK has now widely been used for large scale beam dynamics simulations in linear accelerators. For the Vlasov solver, Semi-Lagrangian method and time splitting scheme have been employed to solve Vlasov equation directly in 1P1V and 2P2V phase spaces. Similarly, DD has been used for parallelization of Vlasov solvers.

INTRODUCTION

Plasma and charged particle simulations have great importance in science. There are three different approaches to simulate plasmas: the microscopic model, the kinetic model and the fluid model. In the microscopic model, each charged particle is described by 6 variables (x, y, z, v_x, v_y, v_z). Therefore, for N particles, there are 6N variables in total. This requires solving the Vlasov equation in 6N dimensions, which exceeds the capability of current supercomputers for large N. On the other end is the fluid model which is the simplest because it treats the plasma as a conducting fluid with electromagnetic forces exerted on it. This leads to solving the Magneto-hydrodynamics (MHD) equations in 3D (x, y and z). MHD solves for the average quantities, such as density and charge, which makes it difficult to describe the fine structure in the plasma. Between these two models is the kinetic model, which solves for the charge density function by solving the Boltzmann or Vlasov equations in 6 dimensions (x, y, z, v_x, v_y, v_z). The Vlasov equation describes the evolution of a system of particles under the effects of self-consistent electromagnetic fields. This paper deals with the kinetic model.

* This work was supported by the U.S. Department of Energy, Office of Nuclear Physics, under Contract No. DE-AC02-06CH11357.
#jin_xu@anl.gov

There are two different ways to solve the kinetic model. The most popular one is to represent the beam bunch by macro particles and push the macro particles along the characteristics of the Vlasov equation. This is the so called Particle-In-Cell (PIC) method, which utilizes the motion of the particles along the characteristics of the Vlasov equation using a Lagrange-Euler approach [1, 2]. The PIC method has the advantages of speed and easy implementation, but similar to MHD, it is hard to calculate fine structures in the plasma. Furthermore, there is noise associated with the finite number of particles in the simulation. This noise decreases very slowly, as $1/\sqrt{N}$, when the number of particles N is increased. The other way to solve the kinetic model is to solve the Vlasov equation directly. This can overcome the shortcomings of the PIC method. We have applied SEM which can achieve high order accuracy and developed scalable Poisson and Vlasov solvers. This paper reports our work using both models. In order to describe space charge effects, several Poisson solvers have been developed.

BEAM DYNAMIC SIMULATION WITH PIC SOLVER

In the last several years, we have parallelized a PIC solver, TRACK, which has been developed in physics division at ANL. Parallel algorithm and detailed benchmark results can be in [2, 3, 4]. Recently PTRACK has been used for an one-to-one RFQ simulation of FNAL proton driver. Totally 865M charged particles have been simulated from 50 keV to 2.5 MeV in 325 MHz radio frequency quadrupole of a proton driver at FNAL. Figure 1 is the comparison in $(\phi, \Delta W/W)$ plane. This result provides much more accurate information and useful to the design optimizations. Now PTRACK has been used as workhorse for large scale optimizations.

PARALLEL POISSON SOLVERS

Fourier Method

$$\phi(x,y,z,t) = \sum_{m=-M/2}^{M/2-1} \sum_{p=-P/2}^{P/2-1} \sum_{n=-N/2}^{N/2-1} \phi(m,p,n,t) e^{-i\alpha m x} e^{-i\beta p y} e^{-i\gamma n z}$$

This is the most standard method for solving the Poisson's equation in Cartesian coordinate system. The potential has been expanded in Fourier series in all three directions. Periodic and Dirichlet zero boundary conditions have been applied in all three directions. Three different domain decomposition methods have been implemented as shown in Fig.2. Using model C, it is easy to use tens of thousands of processors with relatively small grid for space charge calculation. Since

OVERVIEW OF (SOME) COMPUTATIONAL APPROACHES IN SPIN STUDIES

F. Lin, A.U. Luccio, N.D. Malitsky, W.M. Morse, Y.K. Semertzidis, BNL, Upton, NY, USA
C.J.G. Onderwater, University of Groningen, NL-9747AA Groningen, the Netherlands
Y.F. Orlov, R. Talman, Cornell University, Ithaca, NY, USA

Abstract

In the proposed electric dipole moment (EDM) experiment, with an estimated spin coherence time of 1000 s, the spin precession due to an EDM of 10^{-29} e.cm will produce a change in the vertical spin component of approximately 10 μrad during the storage time. Such high sensitivity needs an highly accurate and reliable simulation environment of the beam and spin behavior during the storage time. Therefore, several spin-related accelerator simulation programs have been considered. The paper surveys the computational algorithms of these approaches and discusses their comprehensive analysis from multiple perspectives.

INTRODUCTION

Introduced by Uhlenbeck and Goudsmit to explain the result of Stern-Gerlach experiments, spin has become a fundamental concept and plays an important role in the interactions of elementary particles. To study the various related phenomena, different experiment environments are required. For example, to study spin dependence in the interactions at the quark and gluon level, one employs collision of intense beams of polarized protons at high energy. The Relativistic Heavy Ion Collider (RHIC) at Brookhaven National Lab provides a unique facility for this study. Here, polarized protons can be collided with 50 to 500 GeV center of mass energy. The design calls for an intensity of 2×10^{11} protons per bunch with a polarization of 70%. When the polarized beam is produced from the source, accelerated by several pre-acceleration facilities, injected and ramped in RHIC to the required energy, numerous spin resonances due to the interaction of the magnetic moment and external electromagnetic fields can deteriorate the polarization. Hence, the spin dynamics have to be understood and solutions have to be proposed to preserve the polarization during the acceleration and storage.

Recently, another quest for physics beyond the Standard Model (SM) represents a major effort in basic physics research. A non-vanishing EDM is a violation of Time-Reversal (T) and Parity (P) symmetries, and under the assumption of CPT invariance also violates the CP symmetry. Because the Electric Dipole Moment (EDM) values predicted by most extensions to the SM are many orders of magnitude larger than those of the SM itself and close to present experimental sensitivity levels, EDM experiments have become very sensitive probes for new physics, such as new sources of CP violation.

A completely new approach to EDM studies is based on a charged polarized particle storage ring [1, 2]. A non-zero EDM will affect the observed spin precession, resulting in the eventual change of the polarization. This technique promises a significant sensitivity improvement, reaching down to 10^{-29} e.cm in 10^7 s of physics running time. In such a long time running, the polarization of the beam has to be maintained, which requires the spin dynamics systematic errors need to be tightly controlled.

The most general description of spin motion under the influence of external electromagnetic fields is

$$\frac{d\vec{S}}{dt} = \mu\vec{S} \times \vec{F}_\mu(\vec{B}, \vec{\beta} \times \vec{E}) + d\vec{S} \times \vec{F}_d(\vec{E}, \vec{\beta} \times \vec{B}). \quad (1)$$

Here, the spin vector $\vec{S}$ is in the particle rest frame, $\vec{B}$ and $\vec{E}$ stand for the laboratory magnetic field and electric field, respectively. The first term, representing the spin precession due to the magnetic dipole moment $\mu = g\frac{e}{2mc}$, has been explored in previous accelerator experiments, for example at RHIC. The second term is the spin precession due to the electric dipole moment $d = \eta\frac{e}{2mc}$, which is proposed for study in the EDM experiment.

The design, optimization, and commissioning of modern accelerator complexes rely on dedicated beam studies based on advanced numerical approaches. Analysis of the spin motion required further development of conventional accelerator codes by augmenting positional coordinates with spin coordinates and combining the Lorentz and Thomas-BMT equations. However, such composite spin-orbital applications do not affect the basic computational framework, especially given that particle orbits are essentially independent of spin orientation (Stern-Gerlach forces are negligible at the high particle energies considered). The same numerical approaches are applicable and can be divided into two major categories: tracking and mapping. The list of successful implementations of these approaches is very long and this paper does not presume to cover all of them. Its primary goal is rather practical: to build an open simulation environment addressing the challenging EDM experiment. The correction of spin (g-2) frequency was selected as an initial benchmark application.

EQUATIONS OF MOTION

Present beam simulation programs have usually considered only the first term of Eq.(1) dealing with the spin procession due to the magnetic dipole moment. This term with

AN EFFICIENT 3D SPACE CHARGE ROUTINE WITH SELF-ADAPTIVE DISCRETIZATION *

G. Pöplau†, U. van Rienen, Rostock University, Rostock, Germany

Abstract

Precise and fast 3D space charge calculations for bunches of charged particles are still of growing importance in recent accelerator designs. A widespread approach is the particle-mesh method computing the potential of a bunch in the rest frame by means of Poisson's equation. Whereas an adaptive discretization of a bunch is often required for efficient space charge calculations in practice, such a technique is not implemented in many computer codes.

In this paper we present a new approach to an adaptive discretization which is based on the multigrid technique. The goal is that the error estimator needed for the adaptive distribution of mesh lines can be calculated directly from the multigrid procedure. The algorithm was implemented in the software package MOEVE and investigated for several particle distributions. It turns out that the adaptive discretization technique performs very efficiently.

INTRODUCTION

The simulation of the dynamics of high-brightness charged particle bunches demand the fast calculation of 3D non-linear space charge fields with an accuracy that matches the quality of the bunch. The particle-mesh method is a widespread model for space charge calculations. Here, adaptive discretization techniques are often required in order to satisfy both computational demands: accuracy and fast performance. Nevertheless, adaptive discretizations are implemented only in a few software packages together with space charge calculations. For instance, the FFT Poisson solver that is often applied allows only an equidistant mesh. An adaptive discretization following the particle density distribution is implemented in the GPT tracking code (General Particle Tracer, Pulsar Physics) together with a multigrid Poisson solver of the software package MOEVE (**M**ultigrid for n**o**n-**e**quidistant grids to sol**v**e Poisson's **e**quation) [5, 11]. The disadvantage of this approach is that it does not provide a hierarchical construction of meshes which could be used directly by the multigrid algorithm.

In this paper we present a new approach to an adaptive discretization which is based on the multigrid technique. The goal is that the error estimator needed for the adaptive distribution of mesh lines can be calculated directly from the multigrid procedure. The algorithm has been implemented within the framework of the software package MOEVE. It will be investigated for several particle distributions among them a particle distribution which occured during simulations for the European XFEL [1].

* Work supported by DFG under contract number RI 814/18-1

† gisela.poeplau@uni-rostock.de

3D SPACE CHARGE MODEL

The space charge model we consider here is the particle-mesh method. The distribution of particles in a bunch is modeled as distribution of macro particles. Assuming that the energy of the macro particles is within the same range the space charge field is calculated in the rest frame of the bunch. After the transformation into the rest frame a mesh is constructed around the particles of the bunch and the charge of the particles is assigned to the mesh points. Now, the potential φ can be obtained from Poisson's equation given by

$$\begin{aligned} -\Delta\varphi &= \frac{\varrho}{\varepsilon_0} && \text{in } \Omega \subset \mathbb{R}^3, \\ \varphi &= 0 && \text{on } \partial\Omega_1, \\ \frac{\partial\varphi}{\partial n} + \frac{1}{r}\varphi &= 0 && \text{on } \partial\Omega_2, \end{aligned} \tag{1}$$

where ϱ the space charge distribution, ε_0 the dielectric constant and r the distance between the centre of the bunch and the boundary. Usually, the domain Ω is a rectangular box constructed around the bunch. On the surface $\partial\Omega = \partial\Omega_1 \cup \partial\Omega_2$ ($\partial\Omega_1 \cap \partial\Omega_2 = \emptyset$) perfectly conducting boundaries ($\partial\Omega_1$) or open boundaries ($\partial\Omega_2$) can be applied. For space charge calculations within a beam pipe the domain Ω is assumed to be a cylinder with elliptical cross section. A detailed description of the 3D space charge model can be found in [8] and the model with elliptical shaped beam pipe in [4], respectively.

For the solution of the Poisson equation we applied the discretization with second order finite differences. This leads to a linear system of equations of the form

$$L_h u_h = f_h, \tag{2}$$

where u_h denotes the vector of the unknown values of the potential and f_h the vector of the given space charge density at the grid points. The step size h indicates a certain refinement level and the operator L_h is the discretization of the Laplacian.

THE POISSON SOLVERS OF MOEVE

The software package MOEVE has been developed for space charge calculations. It involves several iterative Poisson solvers among them the state-of-the-art multigrid Poisson solvers MG (multigrid) and MG-PCG (multigrid preconditioned conjugate gradients). These algorithms provide optimal convergence, i. e. the number of iteration steps

IMPEDANCE ESTIMATION BY PARABOLIC PARTIAL DIFFERENTIAL EQUATION FOR RECTANGULAR TAPER*

N. Okuda, The University of Tokyo, Tokyo, Japan
K. Yokoya, KEK, Tsukuba, Japan

Abstract

The mesh calculation based on the paraxial approximation can be much faster than ordinary methods when the bunch is very short. There are two reasons. One is to be able to choose the longitudinal mesh size independent of the bunch length. The other is that the problem can be solved as an initial-value problem in spite of frequency domain calculation.

However, the accuracy of the results by the approximation is not clear generally. It will be shown that the approximation is valid for rectangular tapered chamber in some frequency range.

INTRODUCTION

Recently, the calculation of wake field and the impedance has become more important because new accelerators require high current and much required fineness. In many cases they are usually calculated numerically by simulation using a mesh.

There are many methods of mesh calculation. The finite-difference time domain (FDTD) [1] and the finite integration technique (FIT) [2] are popular.

The mesh computation based on the paraxial approximation [3] can be much faster than ordinary methods if the bunch length is very short. The approximation has used in geometrical optics. Since several years ago, it has also used for beam field. The calculation of Coherent Synchrotron Radiation (CSR) by paraxial approximation give good results[4][5]. In Ref.[3], the analytical solution of geometric wake impedances by paraxial approximation are shown. They are that for axisymmetric geometry.

In these proceedings, numerical 3D calculation will be shown. The vertical impedance for rectangular tapered chamber is computed. It agrees with the analytic solution in the appropriate frequency.

The smaller angle taper should be better because the wave at small angle is dominant.

We will focus only on short range wake and completely conducting wall in this proceeding. Resistive wall is not considered. MKSA unit is used in these proceedings.

* Work supported by KEK and by Global COE Program "the Physical Sciences Frontier", MEXT, Japan.

IMPEDANCE

In these proceedings, special transformed fields for arbitrary function $\tilde{f}(x,y,z,t)$ are defined by

$$\tilde{f}(x,y,z,t) = \frac{1}{2\pi}\int \grave{f}(x,y,z,k)e^{-ik(ct-z)}dk. \quad (1)$$

Tilde means original value and 'grave' ($\grave{f}$) means the transformed value satisfying the equation above. This is like Fourier transform. However, the factor e^{ikz} has to be noticed.

The wake effect is able to be represented by impedance. Conventional vertical impedance is

$$Z_y = \frac{-i}{cqy_s}\int_{-\infty}^{\infty} dz \left[\grave{E}_y + c\grave{B}_x\right]_{\boldsymbol{r}_w=\boldsymbol{r}_s=(0,y_s)}, \quad (2)$$

where q is a charge, $\boldsymbol{r}_s = (x_s, y_s)$ is an offset of source particle, $\boldsymbol{r}_w = (x_w, y_w)$ is an offset of witness particle, y_s is small, and $\grave{E}_y, \grave{B}_x$ are the special transformed fields defined by Eq.(1). We will omit grave ($\grave{f} \to f$) from now on.

PARAXIAL APPROXIMATION

In this study, paraxial approximation is used. iIt is valid if the wave propagates at small angle θ from z axis, as shown in Figure 1.

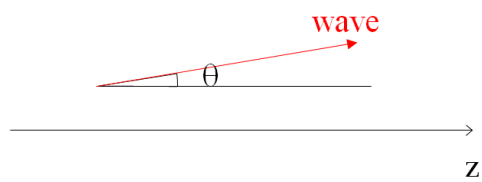

Figure 1: 'Paraxial' means the wave angle θ is small.

We will consider $c\tau \ll g$, where $\tau = (z_s - z_w)/c$ and g is the transverse minimum distance from beam axis. For rectangular chamber whose hight is smaller than width, g is the smallest half hight. In this range, backward or large angle propagating waves cannot take effect. Therefore, $\theta \ll 1$ can be assumed. Suppose $c\tau(\ll g)$ is bunch length, the waves of $\theta \geq 1$ which generated by a bunch don't catch up with the same bunch. When considering wake effect for bunch itself, paraxial approximation is valid for very short bunch length.

APPLYING AN HP-ADAPTIVE DISCONTINUOUS GALERKIN SCHEME TO BEAM DYNAMICS SIMULATIONS*

S. Schnepp†, Graduate School of Computational Engineering, TU Darmstadt, Germany
E. Gjonaj‡, T. Weiland§, Institut für Theorie Elektromagnetischer Felder, TU Darmstadt, Germany

Abstract

An adaptive high order discontinuous Galerkin (DG) scheme for performing beam dynamics simulations is presented. We elaborate on h- and p-adaptations, the former modifying the actual size of computational elements and the latter the dimension of the associated approximation space. The efficiency and stability of the adaptation techniques are emphasized. The scheme is applied in order to perform hp-adaptive beam dynamics simulations. We compare the results with the analytical solution and demonstrate that the adaptive scheme requires significantly less computational resources for obtaining a certain accuracy.

INTRODUCTION

The problem of self-consistent simulations of short relativistic particle bunches in long accelerator structures exhibits a pronounced multi-scale character. The adequate resolution of the THz space charge fields excited by short ultra-relativistic bunches requires mesh spacings in the micrometer range. On the other hand, the discretization of complete accelerator sections using such fine meshes results in a prohibitive number of Degrees of Freedom (DoF). Due to the spatial concentration of the particles and the excited space charge fields, the application of time-adaptive mesh refinement is an emerging idea. We reported on the implementation of time-adaptive mesh refinement for the Finite Integration Technique (FIT) [1]. Based on this work, an adaptive discontinuous Galerkin (DG) code was implemented. Within the DG method, the electromagnetic field solution is approximated elementwise, employing a set of basis functions. This provides two options for adapting the local accuracy of the DG approximation. First, the size of the grid elements can be varied. This is referred to as h-adaptation. Additionally, the maximum order of the employed basis functions can be modified, which is referred to as p-adaptation. Combining both options yields an hp-adaptive method. The twofold refinement mechanisms of the hp-adaptive DG method offer maximum freedom for the approximation of the electromagnetic field solution.

* The work of S. Schnepp is supported by the 'Initiative for Excellence' of the German Federal and State Governments and the Graduate School of Computational Engineering at Technische Universität Darmstadt.

† schnepp@gsc.tu-darmstadt.de
‡ gjonaj@temf.tu-darmstadt.de
§ weiland@temf.tu-darmstadt.de

DISCONTINUOUS GALERKIN METHOD FOR MAXWELL'S EQUATIONS

Spatial Discretization Procedure

Given a decomposition of the computational domain Ω into N non-overlapping, hexahedral elements $\{C_i\}$, $i = 1..N$, a set of linearly independent basis functions $\{\varphi_i^p\}$, $p = 0..P$ for every cell is defined, where P denotes the highest order employed. The basis functions are required to be continuous within the cell C_i and vanish otherwise

$$\varphi_i^p(\mathbf{r}) = \begin{cases} \varphi^p(\mathbf{r}), & \mathbf{r} \in C_i, \\ 0, & \text{otherwise.} \end{cases} \quad (1)$$

Subsequently, the space and time continuous electromagnetic field quantities **E** and **H** are approximated in the form

$$\mathbf{E}(\mathbf{r},t) \approx \widetilde{\mathbf{E}}(\mathbf{r},t) = \sum_i \widetilde{\mathbf{E}}_i(\mathbf{r},t) = \sum_{i,p} e_i^p(t)\varphi_i^p(\mathbf{r}), \quad (2)$$

$$\mathbf{H}(\mathbf{r},t) \approx \widetilde{\mathbf{H}}(\mathbf{r},t) = \sum_i \widetilde{\mathbf{H}}_i(\mathbf{r},t) = \sum_{i,p} h_i^p(t)\varphi_i^p(\mathbf{r}), \quad (3)$$

where $\widetilde{\mathbf{E}}$ and $\widetilde{\mathbf{H}}$ denote the approximate field vectors. The numerical DoF are denoted by e_i^p and h_i^p. They are gathered in the vectors **e** and **h**.

Substituting the electromagnetic quantities by their approximations in Faraday's and Ampère's law and applying the Galerkin procedure yields the weak DG formulation [2]. Due to the cell-wise compact support of the basis functions (1), the approximations (2) and (3) will, in general, be discontinuous at element interfaces. Continuity is enforced only in the weak sense via numerical fluxes. Among the different flux definitions, we chose centered fluxes. As demonstrated in [2, 3] this ensures the strict conservation of the electromagnetic energy. Using the naming convention given there and vector notation for all terms, the semidiscrete formulation reads

$$\frac{\mathrm{d}}{\mathrm{d}t}\begin{pmatrix}\mathbf{M}_\epsilon\mathbf{e}\\ \mathbf{M}_\mu\mathbf{h}\end{pmatrix} + \begin{pmatrix}\mathbf{0} & -\mathbf{C}\\ \mathbf{C}^{\mathrm{T}} & \mathbf{0}\end{pmatrix}\begin{pmatrix}\mathbf{e}\\ \mathbf{h}\end{pmatrix} = -\begin{pmatrix}\mathbf{j}\\ \mathbf{0}\end{pmatrix}. \quad (4)$$

The terms $\mathbf{M}_\epsilon$ and $\mathbf{M}_\mu$ are the mass matrices and $\mathbf{C}$ denotes the weak DG curl operator. The vector $\mathbf{j}$ represents the convective currents.

In the particular case of particle accelerator problems, the issue of charge conservation is specially relevant due to the existence of freely moving charges. In [3] it was shown that strict charge conservation is guaranteed if, and only if, a tensor product basis on conforming Cartesian grids is

PORTABLE HIGH PERFORMANCE COMPUTING FOR MICROWAVE SIMULATION BY FDTD/FIT MACHINES*

Yuya Fujita and Hideki Kawaguchi#, Muroran Institute of Technology, Muroran, 050-8585, Japan

Abstract

This paper presents a development of fully customized printed circuit board of a dedicated computer for FDTD/FIT method which is aiming to portable high performance computation for microwave simulation. In the construction of dedicated computer hardware, it is very important to carefully consider parallel properties hidden in the target application scheme of the dedicated computer to achieve its maximum performance. In addition, judgement on tread-off between calculation performance and flexibility for various target applications is also very important in concrete design of the dedicated computer architecture. In this paper, basic concept and concrete design of the FDTD/FIT dedicated computer architecture are described, and a printed circuit board which is manufactured according to these concepts are presented.

INTRODUCTION

Due to strong requirements of high performance computation (HPC) for electromagnetic microwave simulation in not only science but also industry, a method of FDTD or FIT dedicated computer has been actively investigated in the last several years [1-8]. One of most important advantages of the method of dedicated computer in a regime of HPC technologies is possibility of portable computing. That is to say, in most cases, HPC hardware such as supercomputer and PC cluster is installed at apart from user computers because such the HPC hardware are basically multi-user system, therefore those kinds of HPC environment are not familiar with industrial applications such as microwave simulation connecting with CAD system which are usually carried out in user personal computers. Then the method of the dedicated computer is one of powerful solutions to those requirements. Especially appearance of large size rewritable LSI hardware such as FPGA and GPU, very useful LSI design tool and low price Printed Circuit Board (PCB) development service enhance such the activities of dedicated computer researches. Authors also have been working in development of dedicated computers of the FDTD or FIT method for high performance computation in microwave simulation [5-8]. The method of dedicated computer allows us to construct highly optimized hardware architecture and high performance computation dedicated into the calculation scheme of the target application by comparably small size hardware. Especially a problem of Neumann bottleneck related to memory access overhead, which is essential problem for achievement of HPC in Neumann architecture based computer system, can be avoidable in the method of dedicated computer. This paper presents a design of the dedicated computer specialized into FDTD / FIT method and its hardware implement.

*Work supported by JSPS Grants-in-Aid for Scientific Research (No. 21560345)

#kawa@mmm.muroran-it.ac.jp

PARALLEL PROPETIES HIDDEN IN FDTD METHOD AND CONCEPTUAL DESIGN OF DEDICATED COMPUTER

Parallel properties hidden in FDTD method

To achieve efficient computation in use of dedicated computer, we need to embed parallel properties hidden in the FDTD method ((1) and (2)) into the hardware architecture of the dedicated computer.

$$\begin{aligned}
E_{x\,i,j,k}^{\,n+1} &= E_{x\,i,j,k}^{\,n-1} + \frac{\Delta t}{\varepsilon \Delta l}\left[H_{z\,i,j,k}^{\,n} - H_{z\,i,j-1,k}^{\,n} - H_{y\,i,j,k}^{\,n} + H_{y\,i,j,k-1}^{\,n}\right], \\
E_{y\,i,j,k}^{\,n+1} &= E_{y\,i,j,k}^{\,n-1} + \frac{\Delta t}{\varepsilon \Delta l}\left[H_{x\,i,j,k}^{\,n} - H_{x\,i,j,k-1}^{\,n} - H_{z\,i,j,k}^{\,n} + H_{z\,i-1,j,k}^{\,n}\right], \\
E_{z\,i,j,k}^{\,n+1} &= E_{z\,i,j,k}^{\,n-1} + \frac{\Delta t}{\varepsilon \Delta l}\left[H_{y\,i,j,k}^{\,n} - H_{y\,i-1,j,k}^{\,n} - H_{x\,i,j,k}^{\,n} + H_{x\,i,j-1,k}^{\,n}\right],
\end{aligned} \quad (1)$$

$$\begin{aligned}
H_{x\,i,j,k}^{\,n} &= H_{x\,i,j,k}^{\,n-1} - \frac{\Delta t}{\mu \Delta l}\left[E_{z\,i,j+1,k}^{\,n} - E_{z\,i,j,k}^{\,n} - E_{y\,i,j,k+1}^{\,n} + E_{y\,i,j,k}^{\,n}\right], \\
H_{y\,i,j,k}^{\,n} &= H_{y\,i,j,k}^{\,n-1} - \frac{\Delta t}{\mu \Delta l}\left[E_{x\,i,j,k+1}^{\,n} - E_{x\,i,j,k}^{\,n} - E_{z\,i+1,j,k}^{\,n} + E_{z\,i,j,k}^{\,n}\right], \\
H_{z\,i,j,k}^{\,n} &= H_{z\,i,j,k}^{\,n-1} - \frac{\Delta t}{\mu \Delta l}\left[E_{y\,i+1,j,k}^{\,n} - E_{y\,i,j,k}^{\,n} - E_{x\,i,j+1,k}^{\,n} + E_{x\,i,j,k}^{\,n}\right],
\end{aligned} \quad (2)$$

There are roughly three kinds of parallel properties in the FDTD method,

- dataflow property in the FDTD calculation structure
- parallel calculation of x-, y-, z- three field components
- parallel calculation of different grid field components

The FDTD dedicated computer implementing all of these parallel properties (we call this "full dataflow architecture FDTD/FIT machine") indeed gives us extremely high performance computation, however its hardware size is quite large and especially 3D FDTD machine will be impossible in the next several years even beyond remarkable progress of recent LSI technology [6]. Accordingly the FDTD/FIT dedicated computer based on the first two parallel properties is practical solution in the present LSI technology (we call this "memory architecture FDTD/FIT machine").

Design of memory architecture FDTD machine

The figure 1 shows an overview of the FDTD/FIT dedicated computer architecture. The hardware mainly consists of two parts, calculation and memory modules. All components of electromagnetic field values, material

HIGH-ORDER DIFFERENTIAL ALGEBRA METHODS FOR PDEs INCLUDING RIGOROUS ERROR VERIFICATION

Shashikant Manikonda† Martin Berz‡ and Kyoko Makino‡
†Physics Division, Argonne National Laboratory, Argonne, IL 60439
‡Department of Physics and Astronomy, Michigan State University, East Lansing, MI 48824

Abstract

Many processes in Physics can be described by Partial Differential equations (PDE's). For various practical problems, very precise and verified solutions of PDE are required; but with conventional finite element or finite difference codes this is difficult to achieve because of the need for an exceedingly fine mesh which leads to often prohibitive CPU time. We present an alternative approach based on high-order quadrature and a high-order finite element method. Both of the ingredients become possible through the use of Differential Algebra techniques. Further the method can be extended to provide rigorous error verification by using the Taylor model techniques. Application of these techniques and the precision that can be achieved will be presented for the case of 3D Laplace's equation. Using only around 100 finite elements of order 7, verified accuracies in the range of 1E-7 can be obtained.

INTRODUCTION

Many problems in physics and engineering require the solution of the three dimensional ($3D$) Laplace equation

$$\Delta\psi\left(\vec{r}\right)=0 \text{ in the bounded volume } \Omega\subset \mathtt{R}^3 \qquad (1)$$

It is well known that under mild smoothness conditions for the boundary $\partial\Omega$ of Ω, the Laplace equation admits unique solutions if either ψ or its derivative normal to $\partial\Omega$ are specified on the entire boundary surface $\partial\Omega$. In many typical applications, not only the normal derivative of ψ but indeed the entire gradient $\vec{\nabla}\psi$ is known on the surface; for example, in the magnetostatic case the entire field $\vec{B}=\vec{\nabla}\psi$ is measured, and not merely whatever component happens to be normal to the surface under consideration. The corresponding problem of determining ψ based on the knowledge of the field $\vec{\nabla}\psi\left(\vec{r}\right)=\vec{f}\left(\vec{r}\right)$ on the surface $\partial\Omega$ is referred to as the Helmholtz problem.

Analytic closed form solutions for the 3D case can usually only be found for special problems with certain regular geometries where a separation of variables can be performed. However, in most practical 3D cases, numerical methods are the only way to proceed. Frequently the finite difference or finite element approaches are used to find the approximations of the solution on a set of points in the region of interest. But because of their relatively low approximation order, for the problem of precise solution of PDEs, the methods have very limited success because of the prohibitively large number of mesh points required. For reference, codes like the frequently used TOSCA [1, 2] can usually solve 3D Laplace problems with a relative accuracy of 10^{-4} with meshes of size about 10^{-6}[3]. Furthermore, direct validation of such methods is often very difficult.

In the following we develop a new method based on the Helmholtz theorem and the Taylor model methods[4, 5] and the corresponding tools in the code COSY Infinity [6, 7] to find a validated solution of the Laplace equation starting from the field boundary data. The final solution is provided as a set of local Taylor models, each of which represents an enclosure of a solution for a sub-box of the volume of interest.

THEORY AND IMPLEMENTATION

The Helmholtz Approach

We begin by representing the solution of the Laplace equation via the Helmholtz vector decomposition theorem [8, 9, 10, 11, 12, 13], which states that any vector field $\overrightarrow{B}$ which vanishes at infinity can inside Ω be written as the sum of two terms

$$\overrightarrow{B}\left(\vec{x}\right)=\vec{\nabla}\times\vec{A}_t\left(\vec{x}\right)+\vec{\nabla}\phi_n\left(\vec{x}\right), \text{ where} \qquad (2)$$

$$\phi_n\left(\vec{x}\right)=\frac{1}{4\pi}\int_{\partial\Omega}\frac{\vec{n}\left(\vec{x}_s\right)\cdot\overrightarrow{B}\left(\vec{x}_s\right)}{|\vec{x}-\vec{x}_s|}ds-\frac{1}{4\pi}\int_{\Omega}\frac{\vec{\nabla}\cdot\overrightarrow{B}\left(\vec{x}_v\right)}{|\vec{x}-\vec{x}_v|}dV$$

$$\vec{A}_t\left(\vec{x}\right)=-\frac{1}{4\pi}\int_{\partial\Omega}\frac{\vec{n}\left(\vec{x}_s\right)\times\overrightarrow{B}\left(\vec{x}_s\right)}{|\vec{x}-\vec{x}_s|}ds+\frac{1}{4\pi}\int_{\Omega}\frac{\vec{\nabla}\times\overrightarrow{B}\left(\vec{x}_v\right)}{|\vec{x}-\vec{x}_v|}dV.$$

Here $\partial\Omega$ is the surface which bounds the volume Ω. $\vec{x}_s$ denotes points on the surface $\partial\Omega$, and $\vec{x}_v$ denotes points within Ω. $\vec{n}$ is the unit vector perpendicular to $\partial\Omega$ that points away from Ω, and $\vec{\nabla}$ denotes the gradient with respect to $\vec{x}_v$.

The first term is usually referred to as the solenoidal term, and the second term as the irrotational term. Because of the apparent similarity of these two terms to the well-known vector- and scalar potentials to $\vec{B}$, we note that in the above representation, it is in general not possible to utilize only one of them; for a given problem, in general both ϕ_n and $\vec{A}_t$ will be nonzero.

For the special case that $\vec{B}=\vec{\nabla}V$, we have $\vec{\nabla}\times\vec{B}=0$; furthermore, if V is a solution of the Laplace equation $\vec{\nabla}^2V=0$, we have $\vec{\nabla}\cdot\overrightarrow{B}=0$. Thus in this case, all the volume integral terms vanish, and $\phi_n\left(\vec{x}\right)$ and $\vec{A}_t\left(\vec{x}\right)$ are

COMPUTATIONAL BEAM DYNAMICS FOR A HIGH INTENSITY RING: BENCHMARKING WITH EXPERIMENT IN THE SNS*

J. Holmes, S. Cousineau, and V. Danilov, ORNL, Oak Ridge, TN 37831, U.S.A.
Z. Liu, Indiana University, Bloomington, IN 47405, U.S.A.

Abstract

As the Spallation Neutron Source (SNS) continues to ramp toward full intensity, we are acquiring a wealth of experimental data. Much effort is being applied to understand the details of the beam accumulation process under a variety of experimental conditions. An important part of this effort is the computational benchmarking of the experimental observations. In order to obtain quantitative agreement between the calculations and the observations, and hence a full understanding of the machine, a great deal of care must be taken to incorporate all the relevant experimental parameters into the calculation. These vary from case to case, depending upon what is being studied. In some of these cases, the benchmarks have been critical in unearthing flaws in the machine and in guiding their mitigation. In this paper, we present the results of benchmarks with a variety of experiments, including coupling in beam distributions at low intensities, space charge effects at moderate intensities, and a transverse instability driven by the impedance of the ring extraction kickers.

INTRODUCTION

The Spallation Neutron Source continues to make impressive progress toward its full operating power of 1.44 MW. In the most recent run, SNS operated at a sustained power of 865 kW during production. At the current applied energy of 930 MeV, this corresponds to nearly 10^{14} protons on target per pulse. In recent dedicated high intensity studies, 1.55×10^{14} protons (24.8 μC) were injected stably into the ring, extracted, and transported to the target. This is the first time the SNS ring has exceeded its design beam intensity of 1.5×10^{14} protons per pulse. Although we are able to operate in production mode at 865 kW with acceptably low losses (< 10^{-3} total beam loss and 10^{-4} uncontrolled beam loss), losses in the high intensity studies are much higher. In order to achieve acceptable losses as we continue to increase the beam intensity, we must gain a detailed understanding of the underlying beam dynamics.

Another reason to thoroughly understand the SNS ring beam dynamics is to avoid instabilities. In several studies, including the one that achieved the record beam intensity, we found that we can easily induce instabilities in the ring. In order to do so, a number of measures are typically taken. These include various combinations of the following: ring RF buncher voltages are modified, or turned off altogether, so that coasting beams are accumulated; the choppers may be turned off to provide continuous beam with no gap; the chromatic sextupoles are activated in order to zero the ring chromaticity; and the ring tunes may be altered to induce the resistive wall instability. So far, three independent instabilities have been observed. The frequency signatures of these instabilities strongly suggest 1) a low frequency resistive wall instability at ~100 kHz, 2) a transverse (extraction kicker) impedance-induced instability in the 4→10 MHz range, and 3) a broad e-p instability in the 20→100 MHz range. The slow-growing resistive wall instability occurs only when the tunes are set below integer values, such as $5.8 < \nu_{x,y} < 6$. Because SNS is operated nominally with $\nu_x = 6.23$ and $\nu_y = 6.20$, the resistive wall instability will not be a problem. The extraction kicker instability has been observed only for a continuous coasting beam under the condition of zero chromaticity and with the beam stored for several milliseconds. It is not expected to be a problem for SNS as currently designed, but it could arise at the higher powers being considered for an SNS upgrade. The e-p instability has been observed the most frequently and under a wide variety of conditions. It is likely to present the greatest challenge as we push the intensity frontier. The observations of these instabilities have been discussed in Refs. [1,2], and preliminary simulation results have been shown in Refs. [3-5].

In order to gain a quantitative understanding of the beam dynamics in the SNS ring, it is necessary to apply careful numerical simulation. We carry this out using the ORBIT Code [6], which was written with high intensity rings and transfer lines in mind. We now present the results of benchmarks with a variety of experiments, including coupling in beam distributions at low intensities, space charge effects at moderate intensities, and the transverse instability driven by the impedance of the ring extraction kickers. We begin with a low-intensity study that revealed the presence of x-y coupling in the extraction septum magnet and follow this work through to its present state of benchmarking with low and intermediate intensity beams with injection painting. We then present the results of a careful study of the observed extraction kicker induced instability. Lacking from this paper will be any results of e-p instability simulation. We are actively pursuing this work on a number of fronts, but have not yet obtained results beyond those previously presented [3,4]. Throughout this paper we stress the necessity of attention to detail as well as the interplay between theory, experiment, and computation required for successful and accurate simulation.

* ORNL/SNS is managed by UT-Battelle, LLC, for the U.S. Department of Energy under contract DE-AC05-00OR22725.

COMPARISON OF DIFFERENT SIMULATION CODES WITH UNILAC MEASUREMENTS FOR HIGH BEAM CURRENTS

L. Groening, W. Barth, W. Bayer, G. Clemente, L. Dahl, P. Forck, P. Gerhard,
I. Hofmann, M.S. Kaiser, M. Maier, S. Mickat, T. Milosic, G. Riehl, H. Vormann,
S. Yaramyshev, GSI, D-64291 Darmstadt, Germany
D. Jeon, SNS, ORNL, Oak Ridge, TN 37831, USA
D. Uriot, CEA IRFU, F-91191 Gif-sur-Yvette, France
R. Tiede, Goethe University, Frankfurt a.M., Germany

Abstract

The GSI Univeral Linear Accelerator UNILAC can accelerate all ion species from protons to uranium. Hence its DTL section is equipped with e.m. quadupoles allowing for a wide range of field strength along the section. During the last years various campaigns on the quality of high current beams at the DTL exit as a function of the applied transverse focusing have been performed. Measurements were compared with up to four different high intensity beam dynamics codes. Those comparisons triggered significant improvement of the final beam quality. The codes were used to prepare an ambitious and successful beam experiment on the first observation of a space charge driven octupolar resonance in a linear accelerator.

INTRODUCTION

In the last decades many beam dynamics computer codes were developed [1] in order to simulate emittance growth along a linac. Several benchmarking studies among codes have been performed [2, 3, 4] generally assuming idealized conditions as initial Gaussian distributions, equal transverse emittances, matched injection into a periodic lattice, and small longitudinal emittance with respect to the rf-bucket size. In case of an operating linac generally not all of these conditions are met. To apply simulation codes to a realistic environment a benchmark activity was started aiming at simulations of beam emittance measurements performed at a DTL entrance and exit, respectively. The studies were performed at the GSI UNILAC [5]. For the simulations four different codes were used: DYNAMION [6], PARMILA [7], TraceWin [8], and LORASR [9].

The first benchmarking was done with moderate mismatch with respect to the periodic DTL solution. The zero current transverse phase advance σ_o has been varied from 35° to 90°. A detailed description of this first campaign is given in [10]. A second campaign suggested in [11] aimed at exploration of the 90° stop-band by varying σ_o from 60° to 130°. In this campaign the mismatch was minimized in order to mitigate the effects of the envelope instability. Ref. [12] is dedicated to this campaign.

EXPERIMENT SET-UP AND PROCEDURE

Intense beams are provided by a MUCIS source at low charge states with the energy of 2.2 keV/u. An RFQ followed by two IH-cavities (HSI section) accelerates the ions to 1.4 MeV/u using an rf-frequency of 36 MHz. A subsequent gas-stripper increases the average charge state of the ion beam. Final acceleration to 11.4 MeV/u is done in the Alvarez DTL section operated at 108 MHz. The increase of rf-frequency by a factor of three requires a dedicated matching section preceding the DTL. It comprises a 36 MHz re-buncher for longitudinal bunch compression, a 108 MHz re-buncher for final bunch rotation, a quadrupole doublet for transverse compression, and a quadrupole triplet for final transverse beam matching.

The Alvarez DTL comprises five independent rf-tanks. Transverse beam focusing is performed by quadrupoles in the F-D-D-F mode. Each drift tube houses one quadrupole. The periodicity of the lattice is interrupted by four inter-tank sections, where D-F-D focusing is applied. Acceleration is done -30° from crest in the first three tanks and -25° from crest in the last two tanks.

Figure 1 presents the schematic set-up of the experiments. Beam current transformers are placed in front of

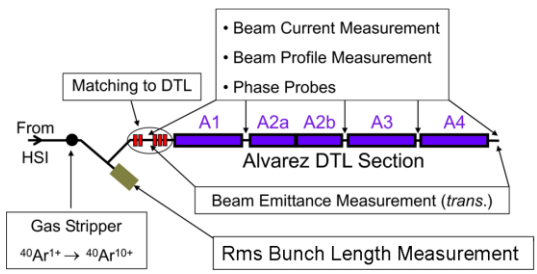

Figure 1: Schematic set-up of the experiments.

and behind the DTL as well as horizontal and vertical slit/grid emittance measurement devices. The total accuracy of each rms emittance measurement including its evaluation is estimated to be 10%. A set-up to measure the longitudinal rms bunch length is available in front of the DTL [13]. It measures the time of impact of a single ion on a foil. This time is related to a 36 MHz master oscillator. The resolution is 0.3° (36 MHz). Prior to the high intensity measurements a scan with very low beam current was done, demonstrating that no emittance growth occurs in absence of space charge forces. Afterwards the HSI was set to obtain 7.1 mA of $^{40}Ar^{10+}$ in front of the DTL. Horizontal and vertical phase space distributions were measured in front of the DTL. The longitudinal rms bunch length was

BENCHMARKING DIFFERENT CODES FOR THE HIGH FREQUENCY RF CALCULATION*

K. Tian, G. Cheng, F. Marhauser, H. Wang
Thomas Jefferson National Accelerator Facility, Newport News, VA 23606, U.S.A.

Abstract

In this paper, we present benchmarking results for high-class 3D electromagnetic (EM) codes in designing RF cavities today. These codes include Omega3P [1], VORPAL [2], CST Microwave Studio [3], Ansoft HFSS [4], and ANSYS [5]. Two spherical cavities are selected as the benchmark models. We have compared not only the accuracy of resonant frequencies, but also that of surface EM fields, which are critical for superconducting RF cavities. By removing degenerated modes, we calculate all the resonant modes up to 10 GHz with similar mesh densities, so that the geometry approximation and field interpolation error related to the wavelength can be observed.

INTRODUCTION

Numerical EM simulations are very important for designing and optimizing new cavity structures, investigating the RF breakdown fields of cavity operation, and studying beam dynamics in RF cavities. Hence, it is very important to understand the accuracy, limitation, and capability of an EM code before applying an EM code in analyzing such problems. For many advanced problems in superconducting RF cavities, high accuracy is not only demanded for the calculation of resonant frequencies but also for the surface electromagnetic fields. For example, multipacting is still an important factor that limits the performance of a superconducting cavity. To correctly predict the process of multipacting in a cavity, the second emission yields of each impact, which is dependent on the impact energy, has to be calculated accurately. Therefore, an accurate calculation of the surface EM fields is a natural requirement for simulating the multipacting process. Another example is the Lorentz force detuning [6] resulting from the interaction of the rf magnetic field with the rf wall current in superconducting cavities. Because the superconducting cavity wall is relatively thin, at high accelerating fields, the cavity shape could be significantly deformed by the inward radiation pressure on the iris wall and the outward radiation pressure on the equator. It hence is a simulation challenge to simulate the frequency shift due to this effect. Since the radiation pressure is directly calculated from the surface EM fields, the key for an accurate simulation relies on the correct prediction of the surface EM fields.

Several EM codes, either developed by commercial companies or non profit research institutes, are utilized for simulations related to RF cavities. Most of these codes provide good benchmarking results against a simple pillbox cavity for the accuracy of frequency and EM fields. However, a real RF cavity is usually much more complex than the pillbox structure, and normally featured with curved 3-D surface. On the other hand, due to measurement errors and unpredictable operating complexity, it is often difficult to conduct benchmarking comparison between different simulation codes using measured experimental data. In a word, the ideal benchmarking model should have 3-D curved boundaries and can be solved analytically. Spherical cavities are such candidates for the benchmarking study. In this paper, we compare the integrity of results from different EM codes using same spherical cavity models.

ANALYTICAL SOLUTIONS

In this paper, we use r, θ, and φ to denote the radial distance, zenith angle, and azimuth angle in a spherical coordinate system, respectively. As shown in Fig.1, we use two different spherical models for the benchmarking: one is a simple cavity bounded by the perfect conductor at r=a; the other model is formed by subtracting two cones from a concentric sphere (d<r<b). For convenience, throughout this paper, we call the first cavity single sphere, and the second cavity double sphere. We have chosen a=b=10 cm and d=5 cm.

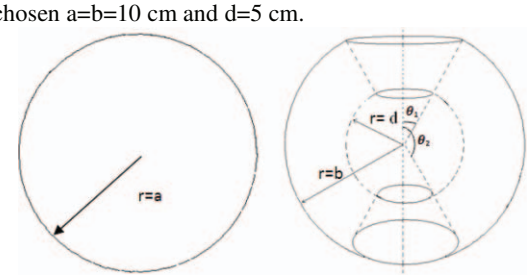

Figure1: Two spherical cavities.

The electromagnetic fields inside a spherical cavity can be obtained by solving Helmholtz equations in spherical coordinates using the Borgnis technique as shown in Ref [7]. For simplicity, we assume that the EM fields, rotationally symmetric, are independent of the azimuthal angle φ. Under this assumption, if we choose the radial direction as the longitudinal direction in a spherical cavity, the EM fields can be classified into TM and TE modes, whose general solutions of EM fields are shown in Equations. (1) and (2), respectively:

*Authored by Jefferson Science Associates, LLC under U. S. DOE Contract No. DE-AC05-06OR23177.
#ktian@jlab.org

SIMULATION STUDIES & CODE VALIDATION FOR THE HEAD-TAIL INSTABILITY WITH SPACE CHARGE

Vladimir Kornilov and Oliver Boine-Frankenheim
GSI, Planckstr. 1, 64291 Darmstadt, Germany

Abstract

The head-tail instability represents a potential intensity limitation for bunched beams in the synchrotrons of the FAIR project. Parametrical studies with numerical simulations over very long time scales are necessary in order to understand the effect of direct space charge, nonlinear synchrotron oscillations and image charges, which are all important in the FAIR synchrotrons. Existing analytic approaches either neglect space charge or describe simplified models, which require a numerical or experimental validation. For our simulation studies we use two different computer codes, HEADTAIL and PATRIC. In this work we verify models for wake-field kicks and space-charge effect using the analytic solution for head-tail mode frequencies and growth rates from the barrier airbag model.

INTRODUCTION

Modern synchrotrons, as SIS-100 and SIS-18 of the FAIR [1] complex, will operate with ion bunches under conditions of strong space charge, $\Delta Q_{\rm sc} \gg Q_s$, or moderate space charge, $\Delta Q_{\rm sc} \gtrsim Q_s$, where $\Delta Q_{\rm sc}$ is the shift of the betatron tune due to space charge and Q_s is the synchrotron tune. Transverse head-tail instability, which is one of the main concerns for the high-intensity operation, can be strongly modified by the effect of space charge. Classical theories, such as the model of Sacherer [2], do not include interactions of a head-tail mode with any incoherent tune spreads. Recent works [3, 4] propose approaches to treat head-tail modes with space charge. However, numerical simulations appear to be indispensable for a comprehensive stability analysis in different beam parameter regimes and with various collective effects taken into account.

A study for head-tail modes with space charge requires extensive parametrical scans of long time scale (tens of thousands of turns) runs. In the case of the weak head-tail instability it is not possible to scale up e.g. the impedance and hence reduce the run time, since mode coupling excites strong head-tail modes above the associated threshold. For reliable stability predictions it is thus necessary to use code modules, in this case primarily space-charge and wake-field implementations, which have been validated accurately, and are applicable for long time scale runs. In the present work we use two different particle tracking codes, `PATRIC` [5] and `HEADTAIL` [6], in order to take the advantage of different kinds of implementations and thus treat the task. The `PATRIC` code, a part of numerical development effort at GSI, was optimised for relatively short-term effects with well-resolved betatron oscillations and exact self-consistent space charge solvers, while the `HEADTAIL` code, created at CERN, was designed historically for longer-term phenomena, including electron-cloud effects, with an option of very fast once-per-turn modus. For the code validation in the range of moderate and strong space charge we suggest to use the model of an airbag bunch in barrier potential. This bunch model, being rather artificial, has a simple analytical solution [7], can be easily implemented in a simulation and, as we demonstrate here, gives very useful insight into physics of head-tail modes with incoherent interactions.

PHYSICAL MODEL

An analytical solution for head-tail modes in bunches with space charge has been derived in Ref. [7]. The model assumes the airbag distribution in phase space and the square-well (barrier) potential and thus a constant line density. The longitudinal momentum distribution has then two opposing flows of particle $\Big[\delta(v_0 - v_{\rm b}) + \delta(v_0 + v_{\rm b})\Big]$, the synchrotron tune in this bunch is $Q_s = v_{\rm b}/2\tau_{\rm b} R f_0$, where $\tau_{\rm b}$ is the full bunch length in radian, R is the ring radius and f_0 is the revolution frequency. The model considers "rigid slices", i.e. only dipole oscillations without transverse emittance variation are included. It is also assumed that all betatron tune shifts are small compared to the bare tune $|\Delta Q| \ll Q_0$. The resulting tune shift due to space

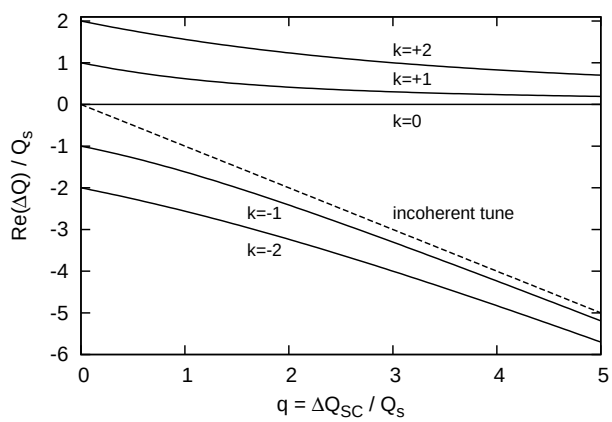

Figure 1: Tune shifts of five head-tail modes versus space charge parameter q as given by the airbag theory Eq. (1), the dashed line is the incoherent betatron tune $Q_0 - \Delta Q_{\rm sc}$.

PROGRESS WITH UNDERSTANDING AND CONTROL OF NONLINEAR BEAM DYANAMICS AT THE DIAMOND STORAGE RING

R. Bartolini, Diamond Light Source Ltd, Oxfordshire, OX11 0DE, UK and John Adams Institute, University of Oxford, OX1 3RH, UK.

Abstract

The Diamond light source started operation for users in January 2007. With the successful commissioning of the nominal optics, delivering a 2.75 nm emittance beam at 3 GeV, we now routinely provide the users with a 250 mA beam with a lifetime of 20 h, exceeding the minimum specified current-lifetime product of 3000 mAh.

Driven by the necessity to guarantee a correct implementation of the nonlinear optics, a significant experimental and theoretical effort is ongoing to understand and improve the nonlinear beam dynamics in the storage ring. The necessity to control the nonlinear beam dynamics is even more urgent with the installation of a large number of small gap (5 mm) in-vacuum insertion device and the need to control the injection efficiency with Top-Up operation. We report here the present status of the analysis of the nonlinear beam dynamics and the main experimental results.

INTRODUCTION

Diamond is a third generation light source which entered in operation in January 2007 [1-2]. The storage ring lattice is a Double Bend Achromat (DBA) where the achromatic condition is broken and dispersion leaks in the straight sections in order to reduce the natural emittance of the machine. The storage ring consists of 24 DBA cells, with ten quadrupoles and seven sextupoles per cell, making a total of 48 dipoles, 240 quadrupoles and 168 sextupoles. The sextupoles are combined function magnets which also have skew quadrupole and dipole correctors in the horizontal and vertical plane. These magnets all have independent power supplies, allowing a large degree of freedom in the choice of both the optimisation and the correction of the linear and nonlinear optics. The ring is also equipped with a set of 7 BPMs per cell providing a total of 168 BPMs, each with turn-by-turn capabilities.

The sextupoles were carefully optimised in order to provide sufficient dynamic aperture and momentum aperture for injection and a Touschek lifetime of at least 10 h for the nominal operating current of 300 mA in a 2/3 fill. Extensive numerical simulations were performed to ensure that the injection efficiency and the Touschek lifetime were maintained even with the complement of IDs planned for Phase-I and Phase-II. Currently this includes ten in-vacuum IDs at 5 mm minimum gap, two superconducting multipole wigglers and an APPLE II device. Two customised optics are also planned in two long straight sections, providing two vertical mini-beta sections with two virtual horizontal focuses.

Striving for the lowest emittance achieved so far in a medium energy machine (2.75 nm), the correct operation of the ring requires a very strict control of the optics of the storage ring. During the commissioning the correct implementation of the linear optics was achieved with the use of the LOCO package [3] and its implementation in the MATLAB Middlelayer [4]. The residual β-beating was reduced to less than 1% peak-to-peak and the nominal emittance of 2.75 nm was measured with very good correction of the linear coupling. The correction is achieved with LOCO by fitting the quadrupoles to match the model and measured orbit response matrix. The required quadrupole gradient corrections are below 2% peak-to-peak and are compatible with the measurements of the quadrupole gradient performed prior to the installation of these magnets.

While the correct implementation of the linear optics is nowadays not unusual in modern third generation light sources, the analysis and correction of the nonlinear model of the storage ring of most modern light sources still stops short of an equivalently good solution [5]. In this context, Diamond has put in place a significant experimental and theoretical effort to provide tools and strategies that allow a correct implementation of the nonlinear model of the storage ring. In this paper we report the current status of the investigation and the main experimental results.

CHARACTERISATION OF THE NONLINEAR BEAM DYNAMICS

The nonlinear dynamics of the storage ring is optimised in order to provide sufficient aperture for injection and adequate Touschek lifetime for the electron beam in the various operating conditions. This is achieved by extending the dynamic aperture and the momentum aperture of the ring. Numerical tracking is ultimately used to validate the optimisation and currently available codes such as Tracy-II [6] or elegant [7] have automated numerical computation of the ring apertures.

It is desirable however to provide dynamical quantities that characterise the nonlinear behaviour of the ring that can be used at the design stage, that can give insight on the beam dynamics and provide further guidelines to the optimisation. When these quantities can be accessed experimentally in the machine, they provide a valuable to tool to compare the nonlinear model of the ring with the real nonlinear behaviour of the beam in the storage ring. The dynamical quantities typically used are the detuning with amplitude and the nonlinear resonance driving terms, which can be computed to the desired perturbative order with codes such as Tracy-II and Mad-X/PTC [8]. A

DESIGN AND CONTROL OF ULTRA LOW EMITTANCE LIGHT SOURCES*

Johan Bengtsson#
BNL, Upton, NY 11973, U.S.A.

Abstract

In the quest for brightness, the horizontal emittance remains one of the main performance parameters for modern synchrotron light sources. A control theory approach that takes the nonlinear dynamics aspects into account, using a few simple (linear) optics guidelines, at an early stage generates robust designs. Modern analytic- and computational techniques enable the optics designer to avoid the fallacy of the traditional approach guided by the Theoretical Minimum Emittance (TME) cell: the "chromaticity wall". In particular, by using an interleaved computational approach with the nonlinear dynamics analyst/model. We also outline how to implement the correction algorithms for a realistic model so that they can be re-used as part of an on-line model/control server for commissioning- and operations of the real system.

TRADE-OFFS: GLOBAL OPTIMIZATION

The (natural) horizontal emittance ε_x originates from the equilibrium:

$$\text{damping} \leftrightarrow \text{diffusion}$$

of three different processes: radiation damping, quantum fluctuations, and IntraBeam Scattering (IBS). One can show that (fundamental limit is IBS):

$$\varepsilon_x \sim \frac{1}{R^2 \cdot P}$$

where R is the bend radius, and P the radiated power.

The design of a synchrotron light source is essentially a matter of balancing the conflicting entities schematiized in Fig. 1 (optimized for Insertion Device (ID) beam lines) [1].

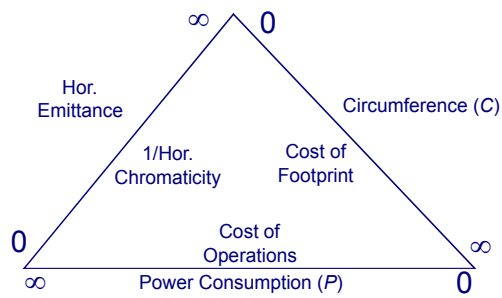

Figure 1: Synchrotron Light Source Optimization.

Traditionally, the approach has been driven by the so-called Theoretical Minimum Emittance (TME) cell [2-3].

However, the approach is misguided (reductionalist), since it only considers the linear optics, i.e., ignores how to control the resulting (linear) chromaticity, and hence does not lead to realistic/robust designs. In particular, it creates an artificial "chromaticity wall" [4]. It also leads to lattices with dispersion at the cavity; which potentially increases the effective transverse beam size due to syncro-betatron coupling (by i.e. operating with finite (linear) chromaticity).

To capture the control aspects of the nonlinear dynamics from the start of the NSLS-II, we have provided the following (linear) optics guidelines [5]:

- max chromaticity per cell,
- min peak dispersion,
- max values for the beta functions.

For an intuitive (systems) approach, see e.g. the MAX-IV conceptual design [6].

WHAT'S KNOWN

The first dedicated third generation light sources were commissioned in the early 80s, i.e., they have been optimized for over 20 years. Basically:

- The horizontal emittance (isomagnetic lattice) is given by

$$\varepsilon_x\,[\text{nm·rad}] = 7.84\times10^{3} \cdot \frac{(E[\text{GeV}])^2 F}{J_x N_b^3}$$

  where N_b is the number of dipoles, $J_x + J_z = 3$, and $F \geq 1$. No dipole gradients => $J_x \sim 1$.
- Generalized Chasman-Green lattices: DBA, TBA, QBA, 7-BA [6].
- Effective emittance => chromatic cells.
- Increasing N_b reduces ε_x but also reduces the peak dispersion, which makes the chromatic correction less effective => "chromaticity wall".
- Damping wigglers (DWs): damping rings and conversion of HEP accelerators [7-8].
- Mini-Gap Undulators (MGUs), Three-Pole-Wigglers (TPWs) inside the DBA [9].

WHAT'S NEW

The NSLS-II design is conservative, i.e., it is based on well known techniques, but the approach is also novel because it combines these in a unique way:

- Use of damping wigglers to reduce horizontal emittance and as high flux X-ray sources => achromatic cells and weak dipoles.
- Medium energy ring (3 GeV) with ~30 DBA cells.
- Vertical orbit stability requirements.
- Generalized higher order achromat.

#bengtsson@bnl.gov
* Work supported by U.S. DOE, Contract No.DE-AC02-98CH10886.

NOVEL METHODS FOR SIMULATING RELATIVISTIC SYSTEMS USING AN OPTIMAL BOOSTED FRAME*

J.-L. Vay†, W. M. Fawley, C. G. Geddes, E. Cormier-Michel, LBNL, Berkeley, CA, USA
D. P. Grote, LLNL, CA, USA

Abstract

It can be computationally advantageous to perform computer simulations in a Lorentz boosted frame for a certain class of systems. However, even if the computer model relies on a covariant set of equations, it has been pointed out that algorithmic difficulties related to discretization errors may have to be overcome in order to take full advantage of the potential speedup. We summarize the findings, the difficulties and their solutions, and show that the technique enables simulations important to several areas of accelerator physics that are otherwise problematic, including self-consistent modeling in three-dimensions of laser wakefield accelerator stages at energies of 10 GeV and above.

INTRODUCTION

In [1], we have shown that the ratio of longest to shortest space and time scales of a system of two or more components crossing at relativistic velocities is not invariant under a Lorentz transformation. This implies the existence of an "optimum" frame of reference minimizing a measure of the ratio of space and time scales. Since the number of computer operations (e.g., time steps), for simulations based on formulations from first principles, is proportional to the ratio of the longest to shortest time scale of interest, it follows that such simulations will eventually have different computer runtimes, yet equivalent accuracy, depending solely upon the choice of frame of reference. The scaling of theoretical speedup was derived for a generic case of two crossing identical rigid particle beams, and for three particle acceleration related problems: particle beams interacting with electron clouds [2], free electron lasers (FEL) [3], and laser-plasma accelerators (LWFA) [4]. For all the cases considered, it was found that the ratio of space and time scales varied as γ^2 for a range of γ, the relativistic factor of the frame of reference relative to the optimum frame. For systems involving phenomena (e.g., particle beams, plasma waves, laser light in plasmas) propagating at large γ, demonstrated speedup of simulations being performed in an optimum boosted frame can reach several orders of magnitude, as compared to the same simulation being performed in the laboratory frame.

We summarize the difficulties and limitations of the method, the solutions that were developed, and the simulations that we have performed to date. We show that the technique enables simulations important to several areas of accelerator physics that are otherwise problematic. For the first time, it allows for direct self-consistent simulations of laser wakefield accelerator stages at 10 GeV and beyond using current supercomputers in a few hours, while the same calculations in the laboratory frame would take years using similar resources and are thus impractical. It also allows simulations of electron cloud effects in high energy physics accelerators (modeled so far with codes based on quasistatic approximations) using more standard Particle-In-Cell methods. This renders these types of simulations accessible to a wider range of existing computer codes, alleviates the added complication due to pipelining when parallelizing a quasistatic code, and removes the approximations of the quasistatic method which may not be applicable in some situations. For free electron lasers, the new technique offers the possibility of calculating self-consistently configurations that are not accessible with standard FEL codes due to the limitations of the approximations that they are based on. Finally, the method may offer a unique way of calculating self-consistently, and in three-dimensions, coherent synchrotron radiation effects which are of great importance in several current and future accelerators.

DIFFICULTIES

Even if the fundamental electrodynamics and particles equations are written in a covariant form, the numerical algorithms that are derived from them may not retain this property and special techniques have been developed to allow simulations in boosted frames. As an example, we considered in [5] an isolated beam propagating in the laboratory frame at relativistic velocity. When applying the effect of the beam field on itself using the Newton-Lorentz equation of motion, the contribution from the radial electric field is largely canceled by the contribution from the azimuthal magnetic field. However, we showed that the so-called 'Boris particle pusher' [6] (which is widely used in PIC codes), does make an approximation in the calculation of the Lorentz force which leads to an inexact cancellation of the electric component by the magnetic component. The magnitude of the error grows with the beam relativistic factor and in practice, it is unacceptably large for simulations of ultra-relativistic charged beams, where the cancellation needs to be nearly complete. The issue was resolved by changing the form of the Lorentz force term in the Boris pusher, and solving analytically the resulting implicit system of equations (see [5] for details).

* Work supported by US-DOE Contracts DE-AC02-05CH11231 and DE-AC52-07NA27344, US-LHC program LARP, and US-DOE SciDAC program ComPASS. Used resources of NERSC, supported by US-DOE Contract DE-AC02-05CH11231.

† jlvay@lbl.gov

MODELING TECHNIQUES FOR DESIGN AND ANALYSIS OF SUPERCONDUCTING ACCELERATOR MAGNETS*

P. Ferracin, LBNL, Berkeley, CA 94720, USA

Abstract

Superconducting magnets for particle accelerators are complex devices requiring the use of sophisticated modelling techniques to predict their performance. A complete description of the magnet behaviour can only be obtained through a multi-physics approach which combines magnetic models, to compute magnetic fields and electro-magnetic forces, mechanical models, to study stresses arising during assembly, cool-down and excitation, and electrical-thermal models, to investigate temperature margins and quench phenomena. This approach is essential in particular for the next generation of superconducting accelerator magnets, which will likely implement strain sensitive conductors like Nb_3Sn and will handle forces significantly larger than in the present LHC dipoles. The design of high field superconducting magnets has benefited from the integration between CAD, magnetic, and structural analysis tools allowing a precise reproduction of the magnet 3D geometry and a detailed analysis of the three-dimensional strain in the superconductor. In addition, electrical and thermal models have made possible investigating the quench initiation process and the thermal and stress conditions of the superconducting coil during the propagation of a quench. We present in this paper an overview of the integrated design approach and we report on simulation techniques aimed to predict and improve magnet behaviour.

INTRODUCTION

The R&D on the next generation of superconducting magnets for particle accelerators is currently focused on quadrupoles and dipoles for future luminosity and energy upgrades of the LHC [1]. Other possible applications include neutrino factories and cable test facilities [2]. These magnets will operate at field approaching 15 T, i.e. beyond the limits of NbTi superconductor, and with stored energies and electro-magnetic (e.m.) forces significantly larger than in the magnets presently used in the LHC. At the moment, Nb_3Sn, the only practical superconductor capable of generating fields higher than 10 T, appears as the best candidate for this future generation of superconducting magnets. However, Nb_3Sn is a brittle and strain-sensitive superconductor whose current carrying capability depends on its strain status [3,4]. As a result, the performance of Nb_3Sn magnets can be strongly affected by the mechanical stresses in the windings during magnet operation. It is therefore mandatory to understand and predict the strain in the superconductor, and devise a support structure capable of minimizing the stresses in the coils from magnet assembly to excitation.

*Supported by the Office of Science, Office of Basic Energy Sciences, U. S. Department of Energy under Contract No. DE-AC02-05CH1123.
#pferracin@lbl.gov

The computation of the mechanical status of the superconducting material is a very complex task, considering all the stages involved in the fabrication of Nb_3Sn coils, like cabling, winding, heat treatment to 650 °C, and epoxy impregnation (Fig. 1). These steps are then followed by magnet assembly, pre-loading, cool-down and powering, which further contribute to the final strain conditions of the Nb_3Sn superconductor.

Figure 1: Nb_3Sn coil after winding (left), after reaction (center), and after impregnation (left).

We present in this paper an overview on modelling works performed in the LBNL Superconducting Magnet Program and aimed at design Nb_3Sn superconducting magnets, predict their behaviour, and analyze and improve quench performance. We start with a description of the tools and techniques adopted, and we then discuss how the models can be used to optimize coil and magnet lay-outs, improve fabrication process, and predict and minimize coil stress from assembly to quench.

INTEGRATED MODELING: TOOLS AND TECHNIQUES

The design and analysis of superconducting magnets can be seen as one single process that integrates different tools to provide a full characterization of the magnet components during assembly, cool-down, magnet excitation and quench. We present in this section an overview of codes and techniques utilized for superconducting magnet design, starting from simplified scaling laws to full 3D magnet models. A complete description of the integrated design approach applied to accelerator magnets can be found in [5].

Coil and Magnet 2D Design

The first step of magnet design consists in a preliminary estimate, through analytical tools or scaling laws, of the amount of conductor required for a given field and aperture [6-8]. Then, the definition of a 2D cross-section of superconducting cable, coil and support structure constitutes the second design step. In this phase, a 2D analysis of the magnetic and mechanical behaviour of the magnet can be performed with programs like Poisson [9], Roxie [10], Opera 2D [11] and ANSYS [12] (Fig. 3). The output of such programs gives field, harmonics and short-sample predictions for the magnet performance, as well as stress in all magnet components.

TRANSIENT, LARGE-SCALE 3D FINITE ELEMENT SIMULATIONS OF THE SIS100 MAGNET*

S. Koch§, T. Weiland‡, Technische Universitaet Darmstadt, D-64289 Darmstadt, Germany
H. De Gersem¶, Katholieke Universiteit Leuven - Campus Kortrijk, B-8500 Kortrijk, Belgium

Abstract

Numerical simulations are frequently used in the design, optimization and commissioning phase of accelerator components. Strict requirements on the accuracy as well as the complex structure of such devices lead to challenges regarding the numerical simulations in 3D. In order to capture all relevant details of the geometry and possibly strongly localized electromagnetic effects, large numerical models are often unavoidable. The use of parallelization strategies in combination with higher-order finite-element methods offers a possibility to account for the large numerical models while maintaining moderate simulation times as well as high accuracy. Using this approach, the magnetic properties of the SIS100 magnets designated to operate within the Facility of Antiproton and Ion Research (FAIR) at the GSI Helmholtzzentrum für Schwerionenforschung GmbH in Darmstadt, are calculated. Results for eddy-current losses under time-varying operating conditions are reported.

INTRODUCTION

For the operation of the heavy-ion synchrotron SIS100 as a part of the FAIR project at GSI, the magnetic flux density in the aperture of the dipole magnets is required to be ramped at rates as high as 4 T/s in order to keep up with the acceleration of the particles. As a consequence, eddy-current effects arising at the end regions of the dipole magnets with respect to the beam orbit, become an important issue in the magnet design and optimization process.

Despite the laminated structure of the iron yoke, eddy currents and, in turn, resistive losses appear in the conductive iron sheets. In the actual design, not only the superconductive current coils are operated at the appropriate temperature of 4.5 K, but also the the ferromagnetic yoke and the mechanical support. As a consequence, the eddy-current losses induced by fast ramping appear in the cold mass of the system. These losses increase the load of the cryogenic system and therefore the power consumption of the facility significantly. Hence, one of the design goals is to reduce the Joule losses inside the magnet to an acceptable level. Several design optimizations aimed at this issue have already been proposed, e.g. in [1], [2], whereas the Nuclotron magnet [3], [4] served as a starting point for the design. These optimizations are based on experiments as well as numerical simulations in 2D and 3D.

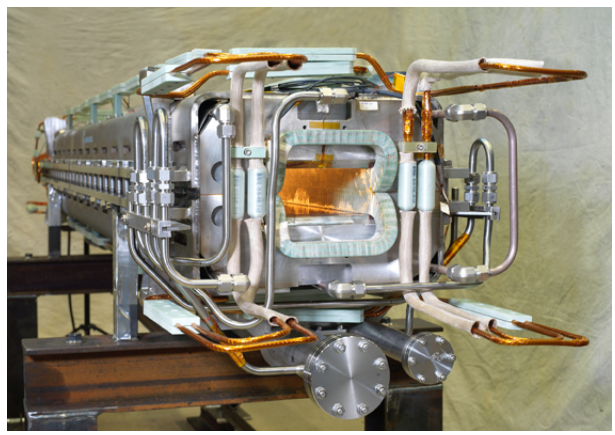

Figure 1: Full-length prototype dipole magnet for the SIS100 including cooling tubes and mechanical assembly (photograph: J. Guse, GSI (www.gsi.de)).

While the original Nuclotron magnet is 1.4 m long [4], the length of the current prototype of the SIS100 dipole shown in Fig. 1 is increased to 2.8 m [5]. Therefore, the number of dipole magnets required to cover the circumference of the synchotron is, in turn, lowered by a factor close to two when compared to a virtual installation of the short magnet. As the major fraction of the eddy currents arises at the end regions of the iron yoke, the resulting overall losses are reduced accordingly. The increased length, however, provides additional challenges regarding numerical simulations when using volume-based discretization methods such as the finite element (FE) method. It leads to larger numerical models which in turn require a longer simulation time and more computational resources. One way to deal with the large numerical models is the use of parallelization techniques. Simulations related to the full length prototype shown in Fig. 1 are carried out using the finite element method in combination with higher-order shape functions. The eddy-current losses in the different parts of the yoke assembly are calculated.

NUMERICAL MODELING

Transient Magnetoquasistatic Formulation

Even though the desired ramping of the aperture field is fast when considering the amount of energy dissipated in the electrically conductive iron yoke, the time variation of

* Work supported by GSI Helmholtzzentrum für Schwerionenforschung GmbH, Darmstadt under contract F&E, DA-WEI1
§ koch@temf.tu-darmstadt.de
‡ thomas.weiland@temf.tu-darmstadt.de
¶ Herbert.DeGersem@kuleuven-kortrijk.be

A PARALLEL HYBRID LINEAR SOLVER FOR ACCELERATOR CAVITY DESIGN

I. Yamazaki*, X. S. Li†, and E. G. Ng‡
Lawrence Berkeley National Laboratory, Berkeley, CA 94720.

Abstract

Numerical simulations to design high-energy particle accelerators give rise to large-scale ill-conditioned highly-indefinite linear systems of equations that are becoming increasingly difficult to solve using either a direct solver or a preconditioned iterative solver alone. In this paper, we describe our current effort to develop a parallel hybrid linear solver that balances the robustness of a direct solver with the efficiency of a preconditioned iterative solver. We demonstrate that our hybrid solver is more robust and efficient than the existing state-of-the-art software to solve these linear systems on a large number of processors.

INTRODUCTION

Numerical simulations to design high-energy particle accelerators [10] give rise to large sparse linear systems of equations that are becoming increasingly difficult to solve using standard techniques [9]. Although significant progress has been made in the development of high-performance direct solvers [2, 4, 11], the dimension of the systems that can be directly factored is limited due to large memory requirements. Preconditioned iterative solvers [3, 14, 16] can reduce the memory requirements, but they often suffer from slow convergence.

To overcome these challenges, a number of parallel hybrid solvers have been developed based on a domain decomposition idea called the Schur complement method [5, 6]. In this method, the unknowns in interior domains are first eliminated using a direct method, and the remaining Schur complement system is solved using a preconditioned iterative method. These hybrid solvers often exhibit great parallel performance because the interior domains can be factored in parallel, and the direct solver is effective to factor the relatively-small interior domain. In addition, the preconditioned iterative solver is shown to be robust to solve the Schur complement systems, where most of the fill occurs, in a number of applications [5, 6]. In particular, for a symmetric positive definite system, the Schur complement has a smaller condition number than the original matrix [15, Section 4.2], and fewer iterations are often needed to solve the Schur complement system. Hence, these hybrid solvers have the potential to balance the robustness of the direct solver with the efficiency of the iterative solver.

Unfortunately, for a highly-indefinite linear system from the accelerator simulation, these existing hybrid solvers often suffer from slow convergence when solving the Schur complement system. This is true especially on a large number of processors because these solvers are designed to achieve good scalability of time to compute the preconditioners, but the quality of the preconditioner often degrades as more processors are used.

To overcome these drawbacks, we have been developing a new implementation of the Schur complement method which provides the robustness and flexibility to solve large highly-indefinite linear systems on a large number of processors [12, 17]. In this paper, we demonstrate the effectiveness of our hybrid solver to solve these linear systems on hundreds of processors using a linear system whose dimension is greater than those used in our previous papers. We also point out how our impelemtnation has been modified since the last publication in order to solve such large linear systems with millions of unknowns.

SCHUR COMPLEMENT METHOD

The Schur complement method is a non-overlapping domain decomposition method, which is also referred to as iterative substructuring. In this method, the original linear system is first reordered into a 2×2 block system of the following form:

$$\begin{pmatrix} A_{11} & A_{12} \\ A_{21} & A_{22} \end{pmatrix} \begin{pmatrix} x_1 \\ x_2 \end{pmatrix} = \begin{pmatrix} b_1 \\ b_2 \end{pmatrix}, \qquad (1)$$

where A_{11} and A_{22} respectively represent *interior domains* and *separators*, and A_{12} and A_{21} are the *interfaces* between A_{11} and A_{22}. By eliminating the unknows associated with the interior domains A_{11} in the bottom part of (1), we obtain the block-triangular system

$$\begin{pmatrix} A_{11} & A_{12} \\ 0 & S \end{pmatrix} \begin{pmatrix} x_1 \\ x_2 \end{pmatrix} = \begin{pmatrix} b_1 \\ \widehat{b}_2 \end{pmatrix}, \qquad (2)$$

where S is the Schur complement defined as

$$S = A_{22} - A_{21} A_{11}^{-1} A_{12}, \qquad (3)$$

and $\widehat{b}_2 = b_2 - A_{21} A_{11}^{-1} b_1$. Hence, the solution of the linear system (1) can be computed by first solving the Schur complement system

$$S x_2 = \widehat{b}_2, \qquad (4)$$

then solving the interior system

$$A_{11} x_1 = b_1 - A_{12} x_2. \qquad (5)$$

Note that interior domains are independent of each other, and A_{11} is a block-diagonal matrix. Hence, the relatively

* ic.yamazaki@gmail.com
† xsli@lbl.gov
‡ egng@lbl.gov

HARD- AND SOFTWARE-BASED ACCELERATION TECHNIQUES FOR FIELD COMPUTATION

Martin Schauer[#], Peter Thoma[*]
[#] CST of America, San Mateo, CA, United States
[*] CST AG, Darmstadt, Germany

Abstract

Due to a high demand in more realistic graphics rendering for computer games and professional applications, commercial, off-the-shelf graphics processing units (GPU) increased their functionality over time. Recently special application programming interfaces (API) allow programming these devices for general purpose computing. This paper will discuss the advantages of this hardware platform for time domain simulations using the Finite-Integration-Technique (FIT). Examples will demonstrate typical accelerations over conventional central processing units (CPU).

Next to this hardware based accelerations for simulations also software based accelerations are discussed. A distributed computing scheme can be used to accelerate multiple independent simulation runs. For memory intense simulations the established Message Passing Interface (MPI) protocol enables distribution of one simulation to a compute cluster with distributed memory access. Finally, the FIT framework also allows special algorithmic improvements for the treatment of curved shapes using the perfect boundary approximation (PBA), which speeds up simulations.

INTRODUCTION

Simulation performance is a frequently discussed topic since users of simulation software want to achieve faster time-to-market in order to gain a competitive advantage. As a prerequisite for the following studies, "performance" needs to be defined first and includes the full design process from the idea to the realization.

1. Pre-processing
   - CAD Modeling / Workflow integration
   - Parameter definition
2. Solver
   - Advanced numerical algorithms
   - High performance computing
3. Post-processing
   - Derive secondary quantities
   - Optimize parameter

It is important to note that on the solver side not only the speed, but also the accuracy of this algorithm needs to be taken into account.

Performance = speed * accuracy

Most of the performance studies in this paper are discussed within the FIT framework [1]. We would also like to emphasize that the right solver choice can speed up the simulation significantly and should therefore be preferred, before hard- and software based acceleration techniques are chosen.

The paper is subdivided into two parts: hardware and software based acceleration techniques. Figure 1 illustrated how these techniques play together in [2].

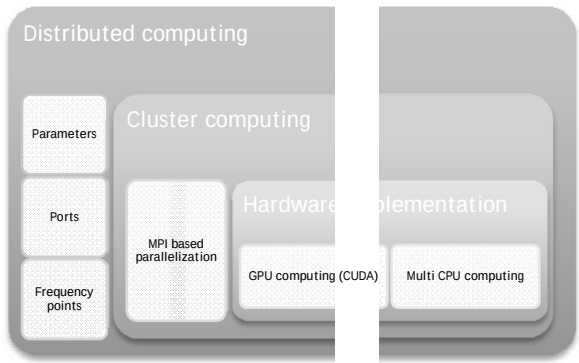

Figure 1: Overview of acceleration techniques and their hierarchy

HARDWARE ACCELERATION TECHNIQUES

Multi-CPU/multi-core is a classical hardware acceleration technique. In the recent years GPU computing emerged as a competing technique. In terms of performance we need to distinguish between algorithms with a high count of operations per memory access and algorithms with a low count.

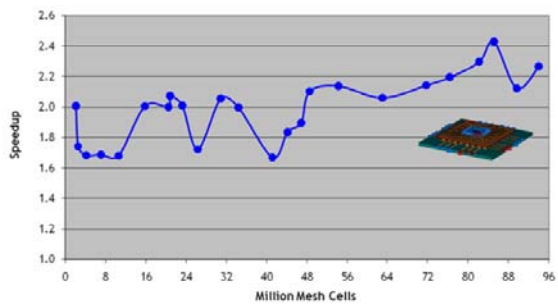

Figure 2: Simulation speed-up of the latest Intel generation CPU [3] vs. the previous generation

GRAPHICAL PROCESSING UNIT-BASED PARTICLE-IN-CELL SIMULATIONS*

Viktor K. Decyk, Department of Physics and Astronomy, Tajendra V. Singh and Scott A. Friedman, Institute for Digital Research and Education, UCLA, Los Angeles, CA 90095, U. S. A.

Abstract

New emerging multi-core technologies can achieve high performance, but algorithms often need to be redesigned to make effective use of these processors. We will describe a new approach to Particle-in-Cell (PIC) codes and discuss its application to Graphical Processing Units.

INTRODUCTION

High Performance Computing (HPC) has been dominated for the last 15 years by distributed memory parallel computers and the Message-Passing Interface (MPI) programming paradigm. The computational nodes have been relatively simple, with only a few processing cores. This computational model appears to be reaching a limit, with several hundred thousand simple cores in the IBM Blue Gene. The future computational paradigm will likely consist of much more complex nodes, such as Graphical Processing Units (GPUs) or Cell Processors, which can have hundreds of processing cores, with different and still evolving programming paradigms, such as NVIDIA's CUDA. One anticipates that the next generation HPC computers, unlike Blue Gene, will consist of a relatively small number (<1,000) nodes, each of which will contain hundreds of cores. High performance on the node will in most cases require new algorithms. Between nodes, however, it is likely that MPI will continue to be effective.

Particle-in-Cell (PIC) codes [1-2] are one of the most important codes in plasma physics and other sciences, and use substantial computer time at some of the largest supercomputer centers in the world. Such codes integrate the trajectories of many charged particles, each interacting via electromagnetic fields they themselves produce. In anticipation of future requirements, we have been developing algorithms for PIC codes on this new class of multi-core nodes. As much as possible, we would like these new algorithms to be general enough that they would run well on most of the new emerging architectures. We decided to start with NVIDIA GPUs, because they are powerful, inexpensive, and widely available.

These GPUs consist of 12-30 multiprocessors, each of which has 8 processor cores. The control logic performs the same operation on 32 cores at a time. There is a large (up to 4 GBytes) global memory, which has very high aggregate bandwidth (up to 140 GBytes/sec), far higher than the memory bandwidth of a traditional processor. The memory latency (400-600 clocks) is quite high, however. To hide this latency, the NVIDIA GPUs support thousands of threads simultaneously, and can switch threads in one clock period. To use this architecture, there are two challenges to any algorithm. The first is that the high global memory bandwidth is achieved only when adjacent threads read adjacent locations in memory (stride 1 access, or in the vocabulary of NVIDIA, data coalescing). This is due to the fact that memory is read 64 bytes at a time, and if all 64 bytes are used, memory bandwidth is maximized. The second is that there is no cache. However, each multiprocessor has a small (16 KB), fast (4 clocks) memory which can be shared by threads running on that multiprocessor. It is best to read and write global memory only once (with stride 1 access), storing the data that has to be read more than once or does not have stride 1 access, in small pieces. From this we concluded that ordered, streaming algorithms are optimal for this and similar architectures.

PIC codes codes have 3 major components. The first is a deposit step, where particles contribute charge or current field elements to grid points located near the particle's position. The deposit generally involves a scatter operation. The second is a field solver, where some subset of Maxwell's equation is solved to obtain values of electric and/or magnetic field points on a grid from the charge or current grid points. The third is a particle push step, where particles interpolate electric or magnetic fields at a particle's position by interpolating from nearby field elements. The push generally involves a gather operation. Normally, most of the time is spent in the deposit and push steps, since there are usually many more particles than grids. PIC codes typically have low computational intensity. That is, the number of floating point operations (FLOPs) compared to the number of memory accesses is small, around 2 or 3, so that optimizing memory operations is very important. Parallel algorithms for distributed memory parallel computers have been available for many years [3], and such codes have effectively used 1,000-100,000 processors.

PIC codes can implement a streaming algorithm by keeping particles constantly sorted by grid. This minimizes global memory access, since all the particles at the same grid point read the same field elements: the field elements need to be read only once for the entire group (and can be stored in registers). Cache is not needed, since gather/scatter operations are no longer required. Most importantly, it is possible to store particles so that the deposit and push procedures all have optimal stride 1 memory access. The challenge is whether one can sort the particles in an optimal way.

In this paper, we will discuss an implementation of a streaming algorithm for a simple 2D electrostatic

*Work supported by Northrop Grumman, UCLA IDRE, and USDOE (SciDAC)

VIZSCHEMA – A STANDARD APPROACH FOR VISUALIZATION OF COMPUTATIONAL ACCELERATOR PHYSICS DATA*

S. Shasharina#, J. Cary, M. Durant, S. Kruger, S. Veitzer, Tech-X Corporation, Boulder, CO, 80303, U.S.A.

Abstract

Even if common, self-described data formats are used, data organization (e.g. the structure and names of groups, datasets and attributes) differs between applications. This makes development of uniform visualization tools problematic and comparison of simulation results difficult. VizSchema is an effort to standardize metadata of HDF5 format so that the entities needed to visualize the data can be identified and interpreted by visualization tools. This approach allowed us to develop a standard powerful visualization tool, based on VisIt, for visualization of large data of various kinds (fields, particles, meshes) allowing 3D visualization of large-scale data from the COMPASS suite for SRF cavities and laser-plasma acceleration.

INTRODUCTION

Visualization is extremely valuable in providing better understanding of scientific data generated by simulations and guiding researchers in designing more meaningful experiments. Scientific models need to be compared with each other and validated against experiments. Consequently, most computational scientists rely on visualization tools. However, visualization and data comparison is often made difficult by the fact that various simulations use very different data formats and visualization tools.

Self-describing data formats are increasingly being used for storage of data generated by simulations. Such formats allow the code to store and access data within a file by name. The file storage system then takes care of developing an index for the data. In addition, the data can be decorated with attributes describing the units, dimensions, and other metadata for a particular variable. The self-describing formats now in use also help to deal with binary incompatibilities. Because different machine architectures use different binary representations for numbers, a binary file written by one processor may not be readable by another processor. Self-describing data file formats and interfaces ensure that the data is written in a universal binary format on all processors, and that software reading the data translates it to the appropriate architecture-specific format.

The Hierarchical Data Format (current version is HDF5) [1] and the NetCDF [2] format are in common use in the fusion, accelerator and climate modeling communities. HDF5 allows one to create a multi-tiered data structure inside of a file, so that one can create nested structures of groups and datasets.

Examples of HDF5 use include plasma physics codes such as VORPAL [3], a 3D plasma simulation code developed under development and Tech-X, and SYNERGIA [4], a multi-particle accelerator simulation tool developed at Fermilab. Both codes are actively used in the COMPASS SciDAC project [5]. Many other communities (earth sciences, fusion simulations) also use HDF5.

In spite of the fact that all these codes use self-describing data format, their files are organized very differently. They often do not share the node structure, do not agree on attributes, use different names for physically similar variables and store data in different structures. In other words, self-describing formats, though powerful, do not impose universally interpretable data structures.

For example, VORPAL put particles data in one dataset with all spatial information coming first: x = data[0,:], y = data[1,:], z = data[2.:], followed by momenta: p_x = data[3,:], p_y = data[4,:], p_z = data[5:,:], while SYNERGIA intermixes momenta and spatial information: p_x = data[0,:], x = data [1,:] etc.

How one can guess from looking at the data what is what? How does one recognize that a particular dataset represents a mesh and what kind of mesh is it? How does one indicate that a dataset is mapped to a particular mesh? Which data ordering is used (is it grouped by components or position indices)? Using some standards and common metadata within these formats could resolve this problem.

Visualization tools used by different teams are also very non-uniform. For a long time, scientific community used IDL [6] and AVS/Express [7]. Lately, many teams are moving towards the freely available, open source, high-quality visualization tools such as VisIt [8].

In this paper we present our efforts to develop such a standard for computational applications dealing with field and particles data. Our approach is based on first identifying the entities of interest to visualization, relationships between these entities and then defining intuitive and minimalistic ways to express them using metadata and common constructs used in self-described data formats: *groups*, *datasets*, and *attributes*. We call this data model VizSchema.

It is then used to implement a VisIt plugin (called Vs) which reads visualization entities from HDF5 files into memory and creates VisIt data structures thus providing a data importing mechanism from VizSchema compliant HDF5 files into VisIt.

In what follows we describe the VizSchema data model, Vs plugin, give examples of visualization and discuss future directions.

*Work supported by DOE grant DE-FC02-07ER54907.
#sveta@txcorp.com

THE OBJECT ORIENTED PARALLEL ACCELERATOR LIBRARY (OPAL), DESIGN, IMPLEMENTATION AND APPLICATION

A. Adelmann*, Ch. Kraus, Y. Ineichen, PSI, Villigen Switzerland
S. Russell, LANL, Los Alamos, USA,
Y. Bi, J.J Yang, CIAE, Beijing, China

Abstract

OPAL (Object Oriented Parallel Accelerator Library) is a tool for charged-particle optic calculations in accelerator structures and beam lines including 3D space charge, short range wake-fields and 1D coherent synchrotron radiation and particle matter interaction. Built from first principles as a parallel application, OPAL admits simulations of any scale, from the laptop to the largest High Performance Computing (HPC) clusters available today. Simulations, in particular HPC simulations, form the third pillar of science, complementing theory and experiment. OPAL has a fast FFT based direct solver and an iterative solver, able to handle efficiently exact boundary conditions on complex geometries. We present timings of OPAL-T using the FFT based space charge solver with up to several thousands of cores.

OPAL IN A NUTSHELL

OPAL is a tool for charged-particle optics in accelerator structures and beam lines. Using the MAD language with extensions, OPAL is derived from MAD9P and is based on the CLASSIC class library, which was started in 1995 by an international collaboration. The Independent Parallel Particle Layer (IP^2L) is the framework which provides parallel particles and fields using data parallel ansatz, together with Trilinos for linear solvers and preconditioners. Parallel input/output is provided by H5Part/Block a special purpose API on top of HDF5. For some special numerical algorithms we use the Gnu Scientific Library (GSL).

OPAL is built from the ground up as a parallel application exemplifying the fact that HPC (High Performance Computing) is the third leg of science, complementing theory and experiment. HPC is now made possible through the increasingly sophisticated mathematical models and evolving computer power available on the desktop and in super computer centres. OPAL runs on your laptop as well as on the largest HPC clusters available today.

The state-of-the-art software design philosophy based on design patterns, makes it easy to add new features into OPAL, in the form of new C++ classes. Figure 1 presents a more detailed view into the complex architecture of OPAL.

OPAL comes in the following flavors:

- OPAL-T
- OPAL-CYCL

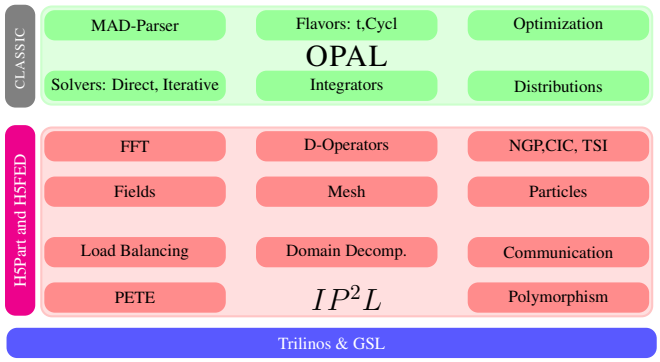

Figure 1: The OPAL software structure

- OPAL-MAP (not yet fully released)
- OPAL-ENVELOPE (not yet fully released)

OPAL-T tracks particles with time as the independent variable and can be used to model beam lines, dc guns, photo guns and complete XFEL's excluding the undulator. Collective effects such as space charge (3D solver), coherent synchrotron radiation (1D solver) and longitudinal and transverse wake fields are considered. When comparing simulation results to measured data, collimators (at the moment without secondary effects) and pepper pot elements are important devices. OPAL-CYCL is another flavor which tracks particles with 3D space charge including neighboring turns in cyclotrons, with time as the independent variable. Both flavors can be used in sequence, hence full start-to-end cyclotron simulations are possible. OPAL-MAP tracks particles with 3D space charge using split operator techniques. OPAL-ENVELOPE is based on the 3D-envelope equation (à la HOMDYN) and can be used to design XFEL's

Documentation and quality assurance are given our highest attention since we are convinced that adequate documentation is a key factor in the usefulness of a code like OPAL to study present and future particle accelerators. Using tools such as a source code version control system (subversion), and source code documentation (Doxygen) together with an extensive user manual we are committed to provide users as well as co-developers with state-of-the-art documentation for OPAL. Rigorous quality control is realized by means of daily build and regression tests.

* andreas.adelmann@psi.ch

RECENT PROGRESS AND PLANS FOR THE CODE elegant *

M. Borland †, V. Sajaev, H. Shang, R. Soliday, Y. Wang, A. Xiao, ANL, Argonne, IL 60439, USA
W. Guo, BNL, Upton, NY, 11973, USA

Abstract

elegant is an open-source accelerator code that has been in use and development for approximately two decades. In that time, it has evolved from a graduate student project with a narrow purpose to a general code for the design and modeling of linacs and storage rings. elegant continues to evolve, thanks in no small part to suggestions from users. elegant has seen extensive application to modeling of linacs, particularly for applications related to free-electron lasers and energy recovery linacs. Recent developments have emphasized both linac and storage-ring-related enhancements, along with parallelization. In this paper, we briefly review the features of elegant and its program suite. We then describe some of the recent progress made in the ongoing development of elegant. We also discuss several noteworthy applications and directions for future work.

INTRODUCTION

The program elegant [1] is now widely used in the accelerator community and is available as source code or in binary form for many operating systems. It started more than two decades ago as a graduate student project when the lead author concluded that it was easier to write a new code than to modify existing codes to include needed features. Since then, it has undergone almost continuous incremental improvement, with releases at approximately six-month intervals. The original structure and philosophy of the code are well suited to this process.

A basic elegant run has two inputs: a command input file and a lattice definition file. The command input file contains a series of namelist-like structures defining a series of commands to set up and execute a run. The lattice input file defines the lattice using a format that is very similar to that popularized by the program MAD [2].

One of the design goals of elegant was to make adding a new element no harder than writing code to implement the physics of the element. Toward this end, a set of data structures was defined that allows the developer to describe the properties and parameters of any new element, as well as the properties of those parameters. This element dictionary has made incremental improvement of the code relatively painless. (It is also used to automatically generate the manual pages for all elements.)

* Work supported by the U.S. Department of Energy, Office of Science, Office of Basic Energy Sciences, under Contract No. DE-AC02-06CH11357.

† borland@aps.anl.gov

elegant attempts to implement as many features as possible using a lumped-element concept. For example, one may impart charge to a beam or change the Twiss parameters of a beam using a lumped element. This has the advantage of allowing elegant to vary or optimize such properties just as it could for a property of a quadrupole or any property of another traditional beamline element. Similarly, many local diagnostic outputs are obtained by inserting one of several diagnostic elements into the beamline.

elegant was the first accelerator code to make thorough use of self-describing data for input and output, starting originally with the Access With Ease (AWE) protocol [3] and transitioning in 1993 to the Self-Describing Data Sets (SDDS) protocol [4]. This feature is as important as the element dictionary in allowing incremental improvement and delivering new results to users in a consistent, usable fashion. With SDDS we can add new data to the output without disrupting users and applications that use the output files. We can also make use of general-purpose pre- and post-processing tools that are not elegant-specific.

In what follows, we discuss recent improvements in elegant and some of the programs distributed with it. We'll begin by discussing improvements of a general nature, followed by a discussion of new features that are specific to ring modeling. Next, we'll summarize the status of on-going parallelization of the code, then turn to a discussion of recent changes to related programs. Finally, we will briefly review some recent applications of elegant and plans for future development. This paper covers changes starting with version 16.0 and ending with version 22.1.

GENERAL IMPROVEMENTS

Although elegant ("ELEctron Generation ANd Tracking") was written for electron tracking, repeated requests were made to allow tracking of other particles. The new change_particle command allows to user to choose different particles by name or specify the charge and mass of the particle of interest.

Optimization is an important feature of elegant and perhaps one of its strengths, compared to other codes. elegant's optimizer uses a single penalty function that is the sum of many terms, each of which is specified as an expression by the user. Essentially anything the program computes, including intermediate and final results of tracking, can be used in an optimization term. New features in optimization include the ability to define optimization terms from templates, so that many similar optimization terms may be added without much effort. We've also added

UPDATE ON MAD-X AND FUTURE PLANS

F. Schmidt (MAD-X custodian*), CERN, Geneva, Switzerland

Abstract

After a intense and hectic code development during the LHC design phase the MAD-X [1] program (Methodical Accelerator Design – Version X) is going through a period of code consolidation. To this end the development on the core has been frozen and most efforts are concerned with a solid debugging in view of a trustworthy production version for the LHC commissioning. On the other hand, the demand on further code development from the LHC pre-accelerators and CLIC are dealt with PTC [2] related parts of the code where the implementation is in full swing. Having reached a mature state of the code the question arises what kind of future can be envisaged for MAD-X.

INTRODUCTION

During the year 2000 the MAD-X project had been started and a first version had been released in June 2002 [1]. Since then all parts of the code have been adapted frequently to deal with constantly changing requirements needed for the LHC design. Since some time now we have shifted our focus to the upcoming LHC commissioning. Since MAD-X will be playing a relevant role in the LHC operation.

Module	Description	Keeper
MAD-X C Core	Maintenance & Debug	H. Grote
APERTURE [3]	Modeling LHC Aperture	J.B. Jeanneret
C6T [4]	SixTrack Converter	F. Schmidt
CORORBIT	Orbit Correction	W. Herr
DYNAP	Tracking Postproc.	F. Zimmermann
EMIT	Emittance, Radiation	R. Tomas
ERROR	Error Assignment	W. Herr
IBS	Intra-Beam Scattering	F. Zimmermann
MAKETHIN	Thin lens Converter	H. Burkhardt
MATCH	Matching Procedures	E. Laface
PLOT	Mad-X Plotting	R. de Maria (interim)
PTC [2]	PTC proper	É Forest KEK
PTC_NORMAL	Normal Form Coeff.	F. Schmidt
PTC_TRACK	Thick lens Lattice Track	V. Kapin ITEP (RU)
PTC_TWISS	Ripken Optics Para.	J.L. Nougaret
SODD [5]	Resonance Comp.	F. Schmidt
SURVEY	Machine Survey	F. Tekker
SXF [6]	Stand. eXchange Format	N. Malitsky BNL
TOUSCHEK	Touschek Effect	C. Milardi IFNL/LNF F. Zimmermann
TWISS	Classical Optics Para.	–
THINTRACK	Thin lens Lattice Track	Y. Sun

Table 1: Module Keepers, People in RED are collaborators from outside CERN, corresponding laboratories in BLUE.

* MAD-X Module keepers see Tab.1

During the years 2008/2009 we have been working on a consolidation of the code such that we can provide a trustworthy MAD-X production version for the LHC commissioning. In particular, since we are presently developing an on-line model [7] of LHC that is based on MAD-X.

On the other hand, there are new demands from other applications notably from the LHC upgrade program, the studies on the LHC pre-accelerators and the CLIC project. Presently, these demands concentrate on better performing modules based on PTC. These developments have been continued and they are not interfering with the consolidation effort for the LHC commissioning.

In this report the key features of the MAD-X are reviewed followed by the most relevant recent MAD-X highlights. The consolidation phase was used to further professionalize the code maintenance which is dealt with in some detail in the next chapter. Besides several outdated features of MAD-X, due to the fact that it is a successor to MAD8, we had to use shortcuts to allow for a gluing of MAD-X with PTC. These shortcuts cannot easily be undone and pose limitations for a further development of the code as a whole. In particular since we will need MAD-X proper in its present state for the LHC commissioning effort. This report closes with a discussion of how one could modernize the code and achieve a better integration of PTC with MAD-X.

KEY FEATURES

The status of MAD-X can best be understood by looking at the design goals of MAD-X followed by a description of what PTC is and how it is connected to MAD-X. From the start we have decided to distribute the work of the code development and maintenance to a large group of module keepers (see Tab. 1) with a code custodian orchestrating their efforts. The job of the custodian is to direct the development of the code and to guarantee its integrity with the goal to provide a code that can handle all requirements for the LHC design and the commissioning alike.

Design Goals

The task at the time was to provide a code in a very short period to allow the design work for the LHC. No grand scheme could be attempted instead we made use of most of the well debugged MAD8 source code (Fortran77) including the traditional MAD8 strengths like sequence editing, matching, plotting, closed-orbit and error routines. However, MAD8 also included out-dated techniques and some feature were flawed if not plain wrong. Those features had to be eliminated: e.g. thicklens non-symplectic tracking

HIGH-FIDELITY INJECTOR MODELING WITH PARALLEL FINITE ELEMENT 3D ELECTROMAGNETIC PIC CODE PIC3P *

A. Candel†, A. Kabel, L. Lee, Z. Li, C. Ng, G. Schussman and K. Ko,
SLAC, Menlo Park, CA 94025, U.S.A.

Abstract

SLAC's Advanced Computations Department (ACD) has developed the parallel Finite Element 3D electromagnetic code suite ACE3P for modeling of complex accelerator structures. The Particle-In-Cell module Pic3P was designed for simulations of beam-cavity interactions dominated by space charge effects. Pic3P solves the complete set of Maxwell-Lorentz equations self-consistently and includes space-charge, retardation and boundary effects from first principles. In addition to using conformal, unstructured meshes in combination with higher-order Finite Element methods, Pic3P also uses causal moving window techniques and dynamic load balancing for highly efficient use of computational resources. Operating on workstations and on leadership-class supercomputing facilities, Pic3P allows large-scale modeling of photoinjectors with unprecedented accuracy, aiding the design and operation of next-generation accelerator facilities. Applications include the LCLS RF gun.

THE PARALLEL CODE PIC3P

In Pic3P, the full set of Maxwell's equations is solved numerically in time domain using parallel higher-order Finite Element methods. Electron macro-particles are pushed self-consistently in space charge, wake- and external drive fields.

Finite Element Time-Domain Field Solver

Ampère's and Faraday's laws are combined and integrated over time to yield the inhomogeneous vector wave equation for the time integral of the electric field **E**:

$$\left(\varepsilon\frac{\partial^2}{\partial t^2}+\sigma\frac{\partial}{\partial t}+\nabla\times\mu^{-1}\nabla\times\right)\int^t\mathbf{E}(\mathbf{x},\tau)\,\mathrm{d}\tau=-\mathbf{J}(\mathbf{x},t), \tag{1}$$

with permittivity ε and permeability μ. The effective conductivity σ provides a simple model for Ohmic losses.

The computational domain is discretized into curved tetrahedral elements and $\int^t\mathbf{E}\,\mathrm{d}\tau$ in Equation (1) is expanded into a set of hierarchical Whitney vector basis functions $\mathbf{N}_i(\mathbf{x})$ up to order p within each element:

$$\int^t\mathbf{E}(\mathbf{x},\tau)\,\mathrm{d}\tau=\sum_{i=1}^{N_p}e_i(t)\cdot\mathbf{N}_i(\mathbf{x}). \tag{2}$$

For typical simulation runs with second-order elements (curved and using second-order basis functions), $N_2 = 20$. Up to $N_6 = 216$ different basis functions can be used in each element. Tangential continuity between neighboring elements reduces the global number of degrees of freedom, in contrast to discontinuous Galerkin methods.

Substituting Equation (2) into Equation (1), multiplying by a test function and integrating over the computational domain results in a system of linear equations (second-order in time) for the coefficients e_i. Numerical integration is performed with the unconditionally stable implicit Newmark-Beta scheme [1]. More detailed information about the employed methods has been published earlier [2].

Higher-Order Particle-Field Coupling

Electron macro particles are specified by position **x**, momentum **p**, rest mass m and charge q. The total current density **J** in Equation (1) is then approximated as

$$\mathbf{J}(\mathbf{x},t)=\sum_i q_i\cdot\delta(\mathbf{x}-\mathbf{x}_i(t))\cdot\mathbf{v}_i(t), \tag{3}$$

for delta-particles with $\mathbf{v}=\frac{\mathbf{p}}{\gamma m}$, $\gamma^2=1+|\frac{\mathbf{p}}{mc}|^2$. The classical relativistic collision-less Newton-Lorentz equations of motion are integrated using the standard Boris pusher [3].

Starting with consistent initial conditions and fulfilling the discrete versions of Equation (1) and the continuity equation

$$\frac{\partial\rho}{\partial t}+\nabla\cdot\mathbf{J}=\mathbf{0} \tag{4}$$

simultaneously during time integration leads to numerical charge conservation.

The use of higher-order Finite Elements not only significantly improves field accuracy and dispersive properties [4], but also leads to intrinsic higher-order accurate particle-field coupling. For delta-particles, the numerical current deposition involves the (exact) evaluation of line integrals over vector basis functions along the elemental particle trajectory segments for a given time step, using Gaussian quadrature [5].

* Work supported by the U. S. DOE ASCR, BES, and HEP Divisions under contract No. DE-AC002-76SF00515.
† candel@slac.stanford.edu

BEAM DYNAMICS IN THE LOW ENERGY PART OF THE LOW EMITTANCE GUN (LEG)

M. Dehler, S. G. Wipf, Paul Scherrer Institut, Switzerland

Abstract

One option for the electron source of the SwissFEL is the Low Emittance Gun (LEG), which is currently under development at PSI. It consists of a pulsed DC gun operating at 500 keV and has the option of using either a photo cathode or a field emitter array. The gun is followed by a pulsed in-vacuum solenoid and a two-frequency cavity, not only used to accelerate the beam but also to create a highly linear energy correlation required for ballistic bunching. All components are rotationally symmetric, so a full particle-in-cell simulation of the setup using 2 1/2 D MAFIA, including space charge, wake fields and beam loading effects, shows the base line performance. Given the relatively low beam energy and high brightness of the beam, there were concerns with respect to the sensitivity to mechanical misalignments in the structure. So we investigated these using the 3D in-house code CAPONE and calculated tolerances, which are well within acceptable limits.

INTRODUCTION

To realize compact X-ray free electron lasers, electron sources with a high brilliance and ultra low emittance are required. The SwissFEL project at PSI is based on the development of such concepts, allowing a substantial reduction in size and cost of such a facility. In order to reach the Angstrom wavelength range, peak currents of 1.5 kA, a relative energy spread of 10^{-4} and normalized transverse slice emittances in the order of 300 nm rad are crucial in the standard operation mode.

Several options are under discussion for the electron source. One consists of an S-band RF gun with a photo cathode[1] running at gradients of 100 MV/m, which will be tested in the 250 MeV injector facility currently under construction. The other, examined here, employs a pulsed diode at an accelerating gradient of 125 MV/m gradient over a four millimeter gap[2], where a prototype is under commissioning at PSI. The baseline scenario assumes a photo-cathode, but cathodes using field emitter arrays may be promising candidates[4, 5].

Even after the high gradient acceleration in the diode, the electron beam is still fragile at energies of 500 keV. A low initial beam current of 5.5 A with an overall charge of 200 pC is beneficial in that respect, but requires a large bunch compression ratio of 270 to obtain a peak current sufficient for lasing. Therefore after the diode, the electron beam is accelerated off-crest in a two-frequency cavity. The fundamental mode at 1.5 GHz is combined with a higher harmonic at 4.5 GHz to introduce a highly linear energy chirp to do ballistic bunching in the following drift delivering a peak current of 20 A to the linac. The beam current and phase space at the end of the drift are compatible with those expected from the S-band RF gun option, so that we can use the same linac design for both options. Fig. 1 shows the layout. A pulsed solenoid (not shown in the figure) between diode and two-frequency cavity corrects the residual divergence of the beam after the gun.

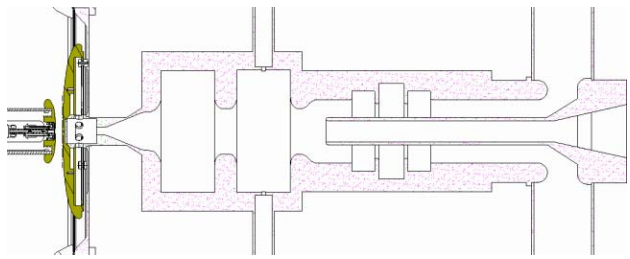

Figure 1: Pulsed DC gun with dual frequency cavity (solenoid not visible)

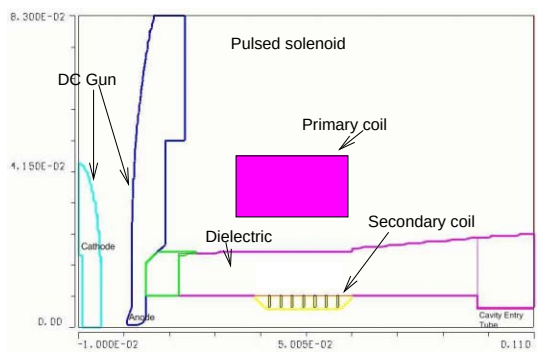

Figure 2: Diode and pulsed solenoid

The simulations have been performed in two steps. Since all elements are rotationally symmetric, the base line performance assuming perfect alignment and ideal beam properties is obtained from a $2\frac{1}{2}$D particle in cell simulation using MAFIA TS2[6]. The influence of misalignment, beam offsets etc. was obtained with the in-house code CAPONE[7] and is described in a separate section.

BASE LINE PERFORMANCE

As was mentioned above, the assembly is rotational symmetric, so it was modeled in two dimensional cylindrical coordinates. The setup consists of the following, the cath-

THE XAL INFRASTRUCTURE FOR HIGH LEVEL CONTROL ROOM APPLICATIONS

A. Shishlo#, C. K. Allen, J. Galambos, T. Pelaia , ORNL, Oak Ridge, TN 37831, U.S.A.
C. P. Chu, SLAC, Menlo Park CA.

Abstract

XAL is a Java programming framework for building high-level control applications related to accelerator physics. The structure, details of implementation, and interaction between components, auxiliary XAL packages, and the latest modifications are discussed. A general overview of XAL applications created for the SNS project is presented.

INTRODUCTION

The development of XAL [1] was started in 2001 at the SNS project as a framework for high level accelerator physics applications. The Java programming language was chosen because it addresses the need for a GUI interface, database services, plotting, and numerical simulations. When XAL development first began there was a lack of free mathematical and plotting packages, but the situation has since improved. EPICS has been chosen as a communication protocol. Today the XAL framework consists of the following parts:

- A hardware representation of the machine for connectivity and control.
- A beam simulation model termed the "online model" for model reference and comparison to the hardware operation.
- An application framework to provide a common “look and feel” and functionality for all XAL applications.
- Services that run continuously in the background (24/7), and which can communicate with several XAL applications simultaneously.
- A set of auxiliary mathematics, graphics, and plotting packages.
- The channel access communication library.

In this paper we present descriptions of these parts of XAL and an overview of applications implemented on the base of this framework for the SNS project.

ACCELERATOR MODEL

An accelerator model represents a structural view of an accelerator. According to this model the accelerator consists of ordered accelerator sequences which usually represent accelerator beam lines, and they can have other ordered sub-sequences or nodes corresponding to physical devices. An instance of such a structure is shown on Fig. 1. The lowest level of the accelerator model hierarchy is represented by such components as magnets, BPMs, wire scanners, RF gaps, position markers etc. Usually accelerator nodes correspond to real physical devices, but it is not necessarily a one-to-one mapping.. For instance, at SNS there are single devices consisting of a quadrupole + dipole windings + BPM strip-lines. We consider these functionalities as three separate accelerator nodes (quad + dipole corrector + BPM), all at the same position.

XAL uses an XML file called an “optics_source” as a natural way to initialize this accelerator hierarchy. This XML file includes all information about sequences, components, positions, parameters, and necessary EPICS’s PV names for device signals.

There are two ways to prepare such files. First, it can be done manually from scratch or by modification of an existing file if you are interested in only a relatively small accelerator model for testing XAL features. Second, you can prepare an application that will generate the file for you by using a relational database. Of course, this application will be specific for each accelerator, because accelerator database structures are usually different.

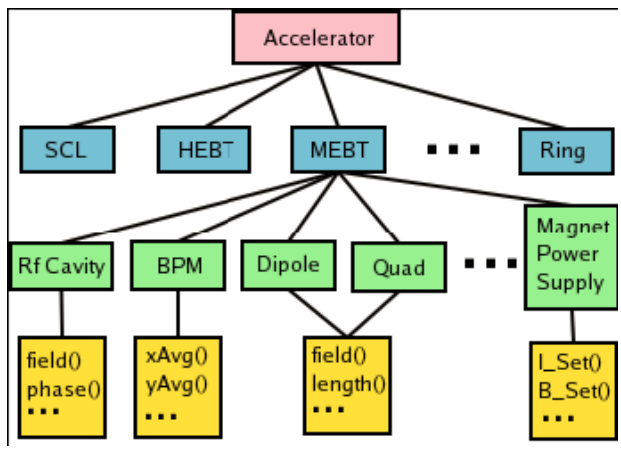

Figure 1: An example of the XAL accelerator model structure.

In the beginning of XAL development, the optics XML file was the only source for the accelerator model initialization, but later several new XML files were added to provide the model with the necessary information. First, there was an XML file with hardware node status information. This is a small file describing availability of certain diagnostics nodes, because they frequently go from the“online” to the “offline” state, and the model should know about a validity of the diagnostic signals. The second new XML file maps an accelerator node type with a particular implementation of this type in the model. This file was introduced to generalize XAL and to use it for different accelerators where the similar devices (i.e. BPM in SNS or J-PARC) can have different functionality. The third one includes information about signals from

#shishlo@ornl.gov

IMPROVEMENT PLANS FOR THE RHIC/AGS ON-LINE MODEL ENVIRONMENTS *

K.A. Brown†, L. Ahrens, J. Beebe-Wang, J. Morris, S. Nemesure,
G. Robert-Demolaize, T. Satogata, V. Schoefer, S. Tepikian
C-AD Dept., BNL, Upton, NY

Abstract

The on-line models for Relativistic Heavy Ion Collider (RHIC) and the RHIC pre-injectors (the AGS and the AGS Booster) can be thought of as containing our best collective knowledge of these accelerators. As we improve these on-line models we are building the framework to have a sophisticated model-based controls system. Currently the RHIC on-line model is an integral part of the controls system, providing the interface for tune control, chromaticity control, and non-linear chromaticity control. What we discuss in this paper is our vision of the future of the on-line model environment for RHIC and the RHIC pre-injectors. Although these on-line models are primarily used as Courant-Snyder parameter calculators using live machine settings, we envision expanding these environments to encompass many other problem domains.

INTRODUCTION

The Collider Accelerator Department (C-AD) at Brookhaven National Laboratory (BNL) operates a series of accelerators that serve the purpose of providing beams to the RHIC experiments. These accelerators include the AGS, which first operated with beams in 1960 and the two RHIC rings, that began beam operations in 2000.

RHIC consists of two super-conducting accelerators, 2.4 miles in circumference, with counter-rotating beams. It has six interaction regions where the two beams can be put into collisions with zero crossing angle. We currently operate with collisions in two of these regions. RHIC can be operated in many different modes and with many different types of beams [1]. For example, RHIC is able to run with two different ion beams in the two rings simultaneously (e.g., gold and deuteron beams in collision) [2]. RHIC can accelerate gold ions up to 100 GeV/nucleon and polarized proton beams up to 250 GeV/c (for more on RHIC performance see [3, 4]).

To deliver polarized protons to RHIC, the beam accelerates as H^- ions through the 200 MeV LINAC is stripped to H^+ and brought up to 2.16 GeV/c in the Booster synchrotron. The beam is then transferred into the AGS and accelerates to 23.8 GeV/c. Finally the beam is transferred to the two RHIC rings, ending with polarized protons up to 250 GeV. For ion operations the process starts at the Tandem Van de Graff. A gold beam, for example, is stripped of some of the outer shell electrons at the Tandem and is brought through a long transport line to the Booster. From the Booster the gold ions are transferred to the AGS and stripped to Au^{77+} in the transfer line. The final two electrons are stripped off in the AGS to RHIC transfer line.

ACCELERATOR CONTROLS SYSTEM

We have two ways to view accelerator controls interfaces. One can take an engineering view in which we think in terms of power supply configurations and in physical units of current and voltage. This paradigm had worked well for decades, before large scale computing was able to take over the more computationally involved process of working in terms of beam parameters, such as betatron tune, chromaticity, and other Courant-Snyder parameters [5].

What is important is that we develop controls that allow the best mapping between how we think of the accelerator and how we control it. This also allows more of the information that describes the various subsystems to be captured into the controls systems. For example, if you have a transport model of a beam line in the controls, the system will contain not only the transfer functions for control units (e.g., some 0 to 10 volt reference to a power supply, derived from a 16 bit digital to analog conversion module) but also transfer functions from current to field, gradient, and even normalized strengths. This then captures not only the power supply information, but also the magnet information. The controls system now begins to hold the best collective knowledge of the accelerators. It could even contain the best collective knowledge of the beam dynamics.

The controls systems at C-AD span multiple generations of technologies. The controls for RHIC represent the largest systems, in terms of total number of control points (over 220,000 settings and over 160,000 measurements) [6]. From the point of view of the online models, there are then multiple interfaces that need to be defined to collect live parameters of the accelerators.

Generally speaking, all of the controls systems are hierarchical with multiple physical and software layers. At the lowest level we speak of a front end computer (FEC) that directly interfaces to some piece of hardware (a power supply or an instrumentation module). The front end systems interface to the console layers of the system through high speed Ethernet employing fiber-optic network connections. In this respect one can think of the controls system as a widely distributed computer system where computational work is performed in parallel. This is somewhat

* Work performed under Contract Number DE-AC02-98CH10886 with the auspices of the US Department of Energy.
† kbrown@bnl.gov

BEAM-BEAM SIMULATIONS FOR KEKB AND SUPER-B FACTORIES

K. Ohmi, KEK, Tsukuba, Japan

Abstract

Recent progress of KEKB and nano beam scheme adopted in KEKB upgrade are discussed. For the present KEKB, chromatic x-y coupling, which was the key parameter to improve luminosity, is focussed. Beam-beam simulations with weak-strong and strong-strong models for nano beam scheme are presented. A weak-strong simulation was done in the presencee of the longitudinal microwave instability. Finally status of beam simulations in KEK supercomputers is presented.

INTRODUCTION

Crab cavity has been installed into KEKB to boostup the luminosity performance. Basically the crab cavity should give us potential to increase the beam-beam parameter more than 0.1. Actually various errors disturb to achieve the high beam-beam performace. For example linear x-y coupling at IP induces an emittance growth with couple to the beam-beam nonlinear interaction. Fast turn by turn fluctuation of the beam position also inducd an emittance growth with couple to the interaction. To achieve the high beam-beam parameter, errors should be removed as possible as we could. Tuning of colliders is just the work to remove errors. Tolerance for errors are estimated in simulations, but it is hard to know how much errors exist, how to correct the errors and how the errors were corrected in an accelerator.

Recently KEKB achieved the new luminosity record. The luminosity record increases 20%, from 1.76 to 2.1 $\times$ 10^{34} cm^{-2}s^{-1} in June 2009. It is twice of the design luminosity, 1×10^{34} cm^{-2}s^{-1}. Tuning of chromatic x-y coupling improved the luminosity remakably.

For KEKB upgrade, we turn to the strategy to boost-up the luminosity. Higher beam-beam parameter is hard to achieve against various errors. Increasing currnt is also problem for the operation cost. Nano-beam scheme, in which low emittance and low beta beams collide with a large crossing angle, is alternative way.

We discuss simulations of the crab crossing of the present KEKB and nano-beam scheme of the KEKB upgrade in Sec II and III, respectvely. In Sec. IV, the computer environment of KEK is reviewed.

RECENT PROGRESS OF KEKB

Chromatic x-y coupling

The existence of the chromatic x-y coupling was known by a measurement of the synchro-beta sideband in the beam size on the x-y tune space [1]. Simulations including the chromatic coupling has been performed using a symplectic integration method of the chromaticity [2]. Hamiltonian which expresses generalized chromaticity is given by

$$\begin{aligned} &H_I(x,\bar{p}_x,y,\bar{p}_y,\bar{\delta}) \qquad (1)\\ &= \sum_{n=1}(a_n x^2 + 2b_n x\bar{p}_x + c_n\bar{p}_x^2 + 2d_n xy + 2e_n x\bar{p}_y \\ &+2f_n y\bar{p}_x + 2g_n\bar{p}_x\bar{p}_y + u_n y^2 + 2v_n y\bar{p}_y + w_n\bar{p}_y^2)\bar{\delta}^n/2. \end{aligned}$$

The coefficients $10 \times n$ are related to n-th order chromaticity of 10 Twiss parameters, $\alpha_{x,y}, \beta_{x,y}, \nu_{x,y}$ and $r_i, i = 1, 4$. Transfer map using H as a generating function guarantees the 6D symplectic condition.

Alternative way is the direct map for the betatron variables $\boldsymbol{x} = (x, p_x, y, p_y)^t$ and z as

$$\boldsymbol{x}(s+L) = M_4(\delta)\boldsymbol{x}(s). \qquad (2)$$

$$z(s+L) = z(s) + \boldsymbol{x}^t M_4^t(\delta) S_4 \partial_\delta M_4(\delta)\boldsymbol{x}/2 \qquad (3)$$

where $M_4(\delta)$, which is the revolution matrix at the interaction point, which contains 10 Twiss parameters and their chromaticity. The transformation for z guarantees the 6-D symplectic condition.

Twiss parameters at the interaction point is measured by turn by turn position monitors located at the both side of the interaction point [3, 4]. Their chromaticity is given by scanning RF frequcncy in the range of $\pm 200 \sim 300$ Hz.

Figure 1 shows the measured x-y coupling parameters as functions the momentum deviation. The parameters are fitted by polynomial of the momentum deviation, as follows,

$$\begin{aligned} r_1(\delta(\%)) &= 0.00848 - 0.00435\delta + 0.00909\delta^2 + 0.151\delta^3 \\ r_2(\delta(\%)) &= 0.0137 + 0.00696\delta + 0.0222\delta^2 - 0.320\delta^3 \\ r_3(\delta(\%)) &= 0.189 - 0.304\delta + 2.45\delta^2 - 1.24\delta^3 \qquad (4)\\ r_4(\delta(\%)) &= 0.0277 - 0.942\delta + -0.512\delta^2 - 0.301\delta^3 \end{aligned}$$

The coefficients, which are chromaticity, varies run by run, and differ from prediction of the optics design code like SAD. Therefore the accelerator model based on the measured chromaticity is important.

Using these transformation, synchro-beta resonances and their effects on the beam-beam interaction have been

RECENT ADVANCES OF BEAM-BEAM SIMULATION IN BEPCII*

Y. Zhang†, IHEP, Beijing, China

Abstract

The luminosity of BEPCII (the upgrade project of Beijing electron-positron collider) have reached 3.0×10^{32} cm^{-2}s^{-1}@1.89GeV in May 2009. In this paper we'll compare the beam-beam simulation results with the real machine. In the case the single bunch current is lower than 8mA, the simulation coincides well with the real. Some phenomenon related to synchro-betatron resonances during machine tuning and simulation is shown . The tune is close to half integer help us increase luminosity, however the detector background increases at the same time. It is believed that the beam-beam dynamic effect result in the drop of the dynamic aperture. We also study the possible luminosity contribution from the crab waist scheme in BEPCII.

INTRODUCTION

BEPCII is an upgrade project from BEPC. It is a double ring machine. Following the success of KEKB, the crossing scheme was adopted in BEPCII, where two beams collide with a horizontal crossing angle 2×11mrad. The design luminosity of BEPCII is 1.0×10^{33}cm^{-2}s^{-1} at 1.89GeV, about 100 times higher than BEPC. The construction started in January 2004 and completed in June 2008 when the detector is positioned. The luminosity was only achieved 1.0×10^{32}cm^{-2}s^{-1}, since the two profile monitors in the positron ring excite very strong longitudinal instability [1]. When the two monitors were removed, 2.0×10^{32}cm^{-2}s^{-1} was achieved. In May 2009, we decided to move the horizontal tune more closer to half integer, which help us achieve 3.0×10^{32}cm^{-2}s^{-1}, and the project was reviewed by the governement in July 2009. Table 1 shows the main design and achieved parameters in BEPCII.

The beam-beam code used in our simulation is a Particle-in-Cell code [2]: (1) the transport map in the arc is linear approximation which is same as Hirta's BBC code where the synchrotron radaiation and quantum excitation is included, (2) the beam-beam force is calculated by solving Poisson equation using FFT, (3) finite bunch length effect is included by longitudinal slices, and the interpolation scheme is used to improve the convergence of slice number [3], (4) the finite horizontal crossing angle is included by Lorentz Boost [4].

In the following, we'll compare the simulated beam-beam limit with the achieved in the real machine. According to the simulation, the synchro-betatron resonances would be excited in some tune region, and similar phenomenon appears in the tune scan of real machine. We'll also show that the dynamic effect reduce the aperture in the near half-integer region. We also study the possible luminosity contribution of the crab-waist scheme in our machine. At last a summary and discussion is presented.

Table 1: Parameters of BEPCII (Design and Achieved)

	Design	**Achieved**
E [GeV]	1.89	1.89
C [m]	237.53	
N_b	93	70
I_b [mA]	9.8	8
$\mathcal{L}$ [$\times 10^{32} cm^{-2} s^{-1}$]	10	3.0
ξ_y	0.04	0.025
θ_c [mrad]	2×11	
β_x^*/β_y^* [m]	1 / 0.015	
ϵ_x/ϵ_y [nm]	144 / 2.2	
σ_z [cm]	1.5	
σ_e	5.16×10^{-4}	
ν_x/ν_y	6.53 / 7.58	6.51 / 5.58
ν_s	0.034	0.032
τ_x/τ_y [turn]	31553 / 31553	
τ_s [turn]	15777	

BEAM-BEAM LIMIT

The beam-beam parameter is defined as

$$\xi_u = \frac{N r_e}{2\pi\gamma} \frac{\beta_u^0}{\sigma_u(\sigma_x + \sigma_y)} \quad (1)$$

where N is the particle number per bunch, r_e the classical electron radius, γ the relativistic factor and it should be noted that β^0 is unperturbed beta function and σ is perturbed beam size. If we do not consider the luminosity loss caused by finited bunch length and crossing angle, the bunch luminosity can be expressed as

$$L = \frac{N^2 f_0}{4\pi\sigma_x\sigma_y} \quad (2)$$

where f_0 is the revolution frequency, and it should be noted that σ is perturbed beam size. For flat beams $\sigma_y \ll \sigma_x$, the achieved beam-beam parameter can be expressed with bunch luminosity as

$$\xi_y = \frac{2 r_e \beta_y^0}{N\gamma} \frac{L}{f_0} \quad (3)$$

* Work supported by National Natural Sciences Foundation of China (10725525 and 10805051)

† zhangy@ihep.ac.cn

MODELING OF ULTRA-COLD AND CRYSTALLINE ION BEAMS*

H. Okamoto#, H. Sugimoto, Hiroshima University, Hiroshima, Japan
Y. Yuri, Takasaki Advanced Radiation Research Institute, JAEA, Gumma, Japan
M. Ikegami, Keihanna Research Laboratory, Shimadzu Corporation, Kyoto, Japan
J. Wei, Tsinghua University, Beijing, China

Abstract

An ultimate goal in accelerator physics is to produce a "zero-emittance" beam, which is equivalent to making the beam temperature the absolute zero in the center-of-mass frame. At this limit, if somehow reached, the beam is Coulomb crystallized. Schiffer and co-workers first applied the molecular dynamics (MD) technique to study the fundamental features of various Coulomb crystals. Their pioneering work was later generalized by Wei et al. who explicitly incorporated discrete alternating-gradient (AG) lattice structures into MD simulations. This paper summarizes recent numerical efforts made to clarify the dynamic behavior of ultra-cold and crystalline ion beams. The MD modeling of beam crystallization in a storage ring is reviewed, including how one can approach the ultra-low emittance limit. Several possible methods are described of cooling an ion beam three-dimensionally with radiation pressure (the Doppler laser cooling).

INTRODUCTION

Mutual Coulomb interactions among stored particles play a substantial role in beam dynamics especially when those particles are densely distributed in phase space [1,2]. The volume occupied by the particles in six-dimensional phase space is called "emittance" that can directly be linked to the beam "temperature" measured in the center-of-mass frame. In theory, the emittance of a beam converges to zero (except for quantum noises) at the ultra-low temperature limit [3]. It can thus be said that space-charge-induced phenomena become more prominent as the emittance or temperature goes down.

The emittance is approximately conserved if the rate of Coulomb collisions between individual particles is low [4]. That is basically due to the Hamiltonian nature of lattice elements (magnets, cavities, etc.) that only produce conservative forces. In practice, however, we almost always prefer a beam with a lower emittance. To meet this general requirement, we must introduce dissipative interactions into the system to "cool" the beam. Needless to say, the ultimate goal of cooling is to make the beam temperature the absolute zero.

Many questions arise, however: is it really possible in principle to establish a zero-emittance state? Can such an ultimate state, if it exists, be stable? How does the beam look like at that limit? These questions have been answered since the mid 1980's [5-13]. Schiffer and co-workers first carried out systematic theoretical researches on strongly-coupled non-neutral plasmas by employing the MD technique [5-9], but their work was based on the smooth approximation that may eliminate possible realistic effects in cooler storage rings. This fact motivated the later, more sophisticated MD work by Wei et al. who took discrete lattice structures into account [10-13]. Their MD simulations actually revealed essential differences between ultra-cold states in a uniform channel and those in an AG channel. Through all these continuous efforts, it is now strongly believed that stable zero-emittance beams can exist, at least, in theory.

The purpose of this paper is to give a brief review of computer modelling of ion beams in the ultra-low temperature regime. After showing the primary conditions to form and maintain a crystalline ion beam in a storage ring, we outline the MD method employed generally for crystalline-beam studies. We then proceed to the description of several cooling models including the Doppler laser cooling [14,15] that is currently the only solution toward beam crystallization. Although the Doppler limit is actually very close to the absolute zero, the powerful laser cooling force only operates in the longitudinal direction of beam motion [16,17]. It is thus necessary to somehow make it work three-dimensionally. For this purpose, we here consider the *resonant coupling method* (RCM) that can easily be implemented in a real storage ring [18,19]. Finally, a unique storage-ring lattice free from momentum dispersion [20,21] is described which can resolve the problem of "tapered cooling" [12,22].

CRYSTALLINE BEAMS

Schiffer, Hasse and others numerically demonstrated that a system of many identical charged particles confined by a time-independent harmonic potential exhibits a spatially ordered configuration at the low-temperature limit [5-9]. This phenomenon is referred to as "Coulomb crystallization". In this unique state of matter, the Coulomb repulsion among particles just balances with the external focusing potential. Suppose a coasting ion beam, for instance. If the line density is sufficiently low, all ions are aligned along the design beam orbit at equal intervals (string crystal). By increasing the line density, we can convert this one-dimensional (1D) configuration into a two-dimensional (2D) (zigzag crystal). The zigzag crystal is eventually transformed to a three-dimensional (3D) figure (shell crystal) if we put more ions in the beam. The threshold line density from a particular crystalline structure to another can be estimated from the Hasse-Schiffer theory [8]. Similar structural transitions occur even for bunched beams. Figure 1 shows a typical multi-shell Coulomb crystal predicted by a MD simulation.

*Work supported in part by Grants-in-Aid for Scientific Research.
#okamoto@sci.hiroshima-u.ac.jp

DEVELOPING THE PHYSICS DESIGN FOR NDCX-II, A UNIQUE PULSE-COMPRESSING ION ACCELERATOR*

A. Friedman, J. J. Barnard, R. H. Cohen, D. P. Grote, S. M. Lund, W. M. Sharp, LLNL, USA
A. Faltens, E. Henestroza, J-Y. Jung, J. W. Kwan, E. P. Lee, M. A. Leitner, B. G. Logan, J.-L. Vay, W. L. Waldron, LBNL, USA
R. C. Davidson, M. Dorf, E. P. Gilson, I. Kaganovich, PPPL, USA

Abstract

The Heavy Ion Fusion Science Virtual National Laboratory (a collaboration of LBNL, LLNL, and PPPL) is using intense ion beams to heat thin foils to the "warm dense matter" regime at $\lesssim 1$ eV, and is developing capabilities for studying target physics relevant to ion-driven inertial fusion energy. The need for rapid target heating led to the development of plasma-neutralized pulse compression, with current amplification factors exceeding 50 now routine on the Neutralized Drift Compression Experiment (NDCX). Construction of an improved platform, NDCX-II, has begun at LBNL with planned completion in 2012. Using refurbished induction cells from the Advanced Test Accelerator at LLNL, NDCX-II will compress a ~500 ns pulse of Li^+ ions to ~1 ns while accelerating it to 3-4 MeV over ~15 m. Strong space charge forces are incorporated into the machine design at a fundamental level. We are using analysis, an interactive 1D PIC code (ASP) with optimizing capabilities and centroid tracking, and multi-dimensional Warp-code PIC simulations, to develop the NDCX-II accelerator. This paper describes the computational models employed, and the resulting physics design for the accelerator.

INTRODUCTION

The Heavy Ion Fusion Science Virtual National Laboratory (HIFS-VNL) is a collaboration of Lawrence Berkeley National Laboratory, Lawrence Livermore National Laboratory, and the Princeton Plasma Physics Laboratory. The VNL is using intense ion beams to enable the study of matter in the poorly-understood "warm dense matter" (WDM) regime at $\lesssim$1 eV, and is developing capabilities for experimental studies of inertial-fusion target physics relevant to ion-driven inertial fusion energy. For an overview, see [1].

The need for rapid target heating motivated the development of ion beam compression in the presence of a neutralizing plasma (which serves to minimize the beam space-charge forces that otherwise would inhibit compression to a compact volume). Bunching factors exceeding 50 have been achieved on the Neutralized Drift Compression Experiment (NDCX) at LBNL. Funding for an improved research platform, NDCX-II, has been approved (via the American Recovery and Reinvestment Act of 2009) and construction is beginning at LBNL, with planned completion in 2012. This will be the first ion induction accelerator specifically designed to heat targets with short pulses. Using refurbished induction cells, Blumlein voltage sources, and transmission lines from the decommissioned Advanced Test Accelerator (ATA) at LLNL, NDCX-II will compress a ~1 m, ~500 ns pulse of Li^+ ions to ~1 cm, ~1 ns while accelerating it to 3-4 MeV over ~15 m. This is accomplished in two stages: the induction accelerator itself, which shortens the pulse to ~0.2 m, 20 ns (~5x increased speed and ~5x decreased length); and a downstream neutralized drift compression line, which enables the final compression (spatial and temporal) through a factor of ~20 or more. The layout is shown in Fig. 1.

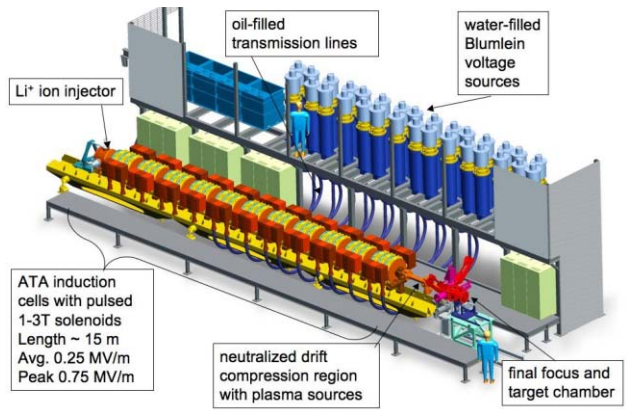

Figure 1: CAD rendering of a design concept for NDCX-II.

The ferrite in each ATA cell offers 0.014 V-s of flux swing, while the Blumleins can source as much as 250 kV with a FWHM of 70 ns. Passive pulse-shaping elements can be inserted into the "compensation boxes" attached to each cell, offering some flexibility in the accelerating waveforms. It is possible to generate longer pulses (and necessary to do so at the front end of the machine), as well as pulses with waveforms optimized to confine the beam-ends, but the need to minimize costs motivates keeping the voltage of any new power supplies to 100 kV or less. The NDCX-II lattice period is unchanged from that of the ATA, at 0.28 m; the accelerating gaps (across which the driving inductive electric field appears) are 2.8 cm long. Because ions do not rapidly reach high speeds, transverse confinement of the beam against its own space charge requires that the existing DC solenoids be replaced by much stronger pulsed solenoids with fields approaching 3 T.

For three reasons, it will be necessary to rebuild the radially innermost parts of the ATA cells. Firstly, a major

* This work was performed under the auspices of the USDOE by LLNL under Contract DE-AC52-07NA27344, by LBNL under Contract DE-AC02-05CH11231, and by PPPL under Contract DE-AC02-76CH03073.

SELF FIELD OF SHEET BUNCH: A SEARCH FOR IMPROVED METHODS

G. Bassi, University of Liverpool and Cockcroft Institute, Liverpool, UK *
J. A. Ellison, K. Heinemann, University of New Mexico, Albuquerque, NM, USA †

ABSTRACT

We consider a sheet bunch represented by a random sample of $\mathcal{N}$ simulation particles moving in a 4D phase space. The mean field (='self field') of the bunch is computed from Maxwell's equations in the lab frame with a smoothed charge/current density. The particles are tracked in the beam frame, thus requiring a transformation of densities from lab to beam frame. We seek improvements in speed and practicality in two directions: (a) choice of integration variables and quadrature rules for the field calculation; and (b) finding smooth densities from scattered data. For item (a) we compare our singularity-free formula with the retarded time as integration variable, which we currently use, with a formula based on Frenet-Serret coordinates. The latter suggests good approximations in different regions of the retardation distance which could save both time and storage. For item (b) we discuss Fourier vs. kernel density estimation and mention quasi vs. pseudo-random sampling.

INTRODUCTION

In this paper we discuss current and future approaches to numerically integrating the Vlasov-Maxwell system for a sheet bunch. More information on our current work can be found in [1]-[3]. We first present the mathematical problem in the lab frame. We write the field as an integral of the time history of the source. Then the initial value problem (IVP) for the Vlasov equation defines the $u = ct$ evolution of the phase space density, f_L. The coefficients of the Vlasov equation depend on the Maxwell self field and thus contain integrals over the time history of f_L.

It is both physically and computationally advantageous to determine the so-called beam frame phase space density, f_B. We define the beam frame phase space variables in terms of the lab frame. The independent variable in the lab frame (LF) is u and the independent variable in the beam frame (BF) is arc length s along a suitably defined reference orbit. The lab to beam phase space variable transformation gives the relation between f_B and f_L and f_B satisfies a BF Vlasov equation. Our goal is an efficient computation of the s-evolution of f_B given its value f_{B0} at say $s = 0$. However, this problem is not well posed; solutions are not unique. The root of this is a causality issue; at s, certain coefficients of the BF Vlasov equation need information about f_B outside the interval $[0, s]$. This problem, which is pertinent to the BF and absent in the LF, is easily resolved to what we believe is a good approximation.

We want to numerically integrate the 4D BF Vlasov equation and we do this in terms of a random sample of $\mathcal{N}$ points which simulate the 4D phase space density. We work in a high performance computing (HPC) environment. Even so, we do not have a fast enough algorithm to take $\mathcal{N}$ large enough to obtain an accurate estimate of the 4D density. Furthermore, there are probably more efficient ways to obtain the 4D density, e.g., the method of local characteristics. However, the self field calculation only needs the BF spatial density, ρ_B, and a 2D current density type function, which we denote by τ_B. We believe our sample of 4D points is large enough to accurately estimate these 2D quantities and this makes a simulation approach feasible. We randomly generate an initial sample of BF phase space points from f_{B0}, and move this sample according to the BF equations of motion. Having resolved the causality issue, the self field can be computed at arc length s from the history of $g_B = (\rho_B, \tau_B)$. The calculation of g_B requires a density estimation procedure from our scattered data which we discuss. To move the points from s to $s + \delta s$ we freeze the self field at s and move the points according to the equations of motion. Important to our approach is the discovery of an s-independent grid on which to represent the spatial density and a parallel implementation of our algorithm.

STATEMENT OF PROBLEM FOR SHEET BUNCH IN LAB FRAME

We consider particle motion in the $Y = 0$ plane in a right handed coordinate system, (Z, X, Y), under an external magnetic field $\mathbf{B}_{ext}(Z, X, Y) = B_{ext}(Z)\mathbf{e}_Y$. The equations of motion without self field are

$$\dot{\mathbf{R}} = \frac{\mathbf{P}}{m\gamma(\mathbf{P})c}, \ \dot{\mathbf{P}} = qB_{ext}(Z)\frac{1}{m\gamma(\mathbf{P})c}\begin{pmatrix} P_X \\ -P_Z \end{pmatrix}, \quad (1)$$

where $\mathbf{R} = (Z, X)^T$, $\mathbf{P} = (P_Z, P_X)^T$, $\dot{} = d/du$, m is the electron rest mass, q is the electron charge and γ is the Lorentz factor. The associated 4D phase space density, $f_L(\mathbf{R}, \mathbf{P}; u)$, evolves according to the Liouville equation $\partial_u f_L + \dot{\mathbf{R}} \cdot \partial_{\mathbf{R}} f_L + \dot{\mathbf{P}} \cdot \partial_{\mathbf{P}} f_L = 0$, where f_L is normalized so that its integral over a phase space region represents the fraction of the beam in that region. All densities in this paper are normalized in this way.

We are interested in the evolution of f_L when coupled to the self field and we begin with the coupled Vlasov-Maxwell initial boundary problem in 3D with a shielding boundary condition and initial data at $u = u_i$ where u_i will be specified further below. In general, the self field will push the particles out of the $Y = 0$ plane unless the bunch is a 'sheet bunch' and the self

* gabriele.bassi@stfc.ac.uk
† Work supported by US DOE grant DE-FG02-99ER41104

SIMULATION OF MICROWAVE INSTABILITY IN LER OF KEKB AND SUPERKEKB

D. Zhou*, K. Ohmi, K. Oide, Y. Suetsugu, K. Shibata, KEK, 1-1 Oho, Tsukuba 305-0801, Japan

Abstract

Microwave instability in the LER of KEKB may be one obstacle to achieving high luminosity as expected by beam-beam simulations. To understand the single-bunch beam dynamics of KEKB LER, we constructed a numerical impedance models by calculating ultra-short wake potentials of various vacuum components, resistive wall and coherent synchrotron radiation. The geometrical wakes were calculated by 3D electromagnetic code GdfidL. And CSR impedance were estimated by a dedicated code. Similar work was also done for LER of SuperKEKB. Using these impedance models we simulated the microwave instability at LER of KEKB and SuperKEKB by solving Vlasov-Fokker-Planck (VFP) equation in the longitudinal phase space. The results of impedance calculation and simulations were presented in this paper.

INTRODUCTION

KEKB [1] has been operated for more than 10 years since its first commissioning from Dec. 1, 1998. In June 2009, the peak luminosity reached $2.11 \times 10^{34}\mathrm{cm}^{-2}\mathrm{s}^{-1}$ with stored beam currents of 1.64/1.12A (LER/HER) due to crab crossing and off-momentum optics corrections. One of the merits of KEKB [2] which contributed to such high luminosity is squeezing the vertical beta function at interaction point (IP) to 0.59 cm. Correspondingly, the natural bunch length is around 4.6 mm. And at normal operating bunch current of 1.0 mA at LER, the measured bunch length is around 7 mm.

Since the beam-beam simulations showed that the crab crossing should boost the luminosity by a factor of 2 [3], the present achieved luminosity is still far from expectations. Besides chromatic coupling induced by lattice nonlinearity [4], microwave instability in the LER may be another potential obstacle for KEKB to achieving higher luminosity by way of increasing beam currents.

Recently, Y. Cai et al. studied the microwave instability in the LER of KEKB using a broadband resonator impedance model [5]. In that work, it was demonstrated that the model described the longitudinal beam dynamics very well when comparing with experimental observations. As predicted by Cai's model, the threshold of microwave instability at LER of KEKB is 0.5 mA, which is well lower than the present operating current of 1.0 mA. In this paper, we introduce the studies on microwave instability in the LER of KEKB and SuperKEKB using numerically calculated impedance models.

* dmzhou@post.kek.jp

QUASI GREEN'S FUNCTION OF WAKE POTENTIAL

To study the longitudinal single-bunch instabilities, we first calculate the ultra-short wake potentials of various vacuum components. GdfidL installed on a cluster with 256 GB memory is available at KEK. As trade-off between the capability of the cluster and the interested frequency range, 0.5 mm bunch length was chosen for most vacuum components of KEKB LER.

Fig. 1 shows the total geometrical wake potentials of LER of KEKB and SuperKEKB. The length of driving gaussian bunch used in GdfidL is 0.5 mm. Due to significant improvements in the vacuum components, the impedance of SuperKEKB rings will be well suppressed. Coherent synchrotron radiation (CSR) is another important impedance source at LER of KEKB and SuperKEKB. The bending radius of normal dipoles at KEKB LER and wigglers are 15.87 m and 16.3 m, respectively. For SuperKEKB LER, only half of the wigglers will remain. Such magnets will produce CSR as bunch length get short to a few minimeter. Thus a dedicated code was developed by K. Oide in 2008 to calculate the CSR impedance in LER of SuperKEKB. In this code, the paraxial approximation was adopted [6]. Electronic fields due to CSR were calculated in the frequency domain and then wake potential was obtained by Fourier transformation. The calculated CSR wake potentials of 0.5 mm bunch are shown in Fig. 2. Interference between adjacent magnets caused modulations at the tail parts of the CSR wake potentials.

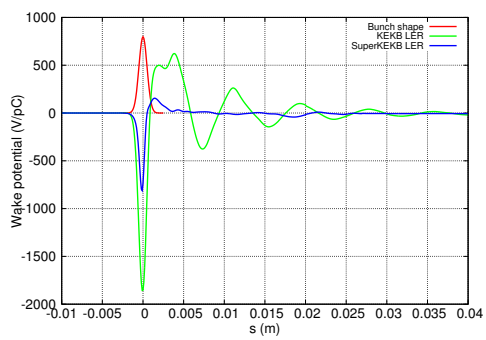

Figure 1: Calculated geometrical wake potentials of 0.5 mm bunch for LER of KEKB and SuperKEKB.

STUDY OF BEAM-SCATTERING EFFECTS FOR A PROPOSED APS ERL UPGRADE *

A. Xiao †, M. Borland, X. Dong, ANL, Argonne, IL 60439, USA

Abstract

Beam-scattering effects, including intra-beam scattering (IBS) and Touschek scattering, may become an issue for linac-based 4^{th}-generation light sources, such as X-ray free-electron lasers (FELs) and energy recovery linacs (ERLs), as the electron density inside the bunch is very high. In this paper, we describe simulation tools for modeling beam-scattering effects that were recently developed at the Advanced Photon Source (APS). We also demonstrate their application to a possible ERL-based APS upgrade. The beam loss issue due to the Touschek scattering effect is addressed through momentum aperture optimization. The consequences of IBS for brightness, FEL gain, and other figures of merit are also discussed. Calculations are performed using a particle distribution generated by an optimized high-brightness injector simulation.

INTRODUCTION

The Coulomb scattering between particles inside a beam has been widely studied for circular accelerators. They were largely ignored for linacs in the past, since significant effects are not expected for one-pass, low-repetition-rate systems with relatively large beam size. The scattering rate is quite low, and there is not enough time for the beam to develop any noticeable diffusion. The situation has dramatically changed since linac-based 4^{th}-generation light sources are on the horizon. To provide users with synchrotron radiation with unprecedented high brightness, the required linac beam must have extremely low emittance with significant charge and a high repetition rate. To ensure that the machine can be run safely with acceptable beam losses and that the beam quality will be not harmed by IBS, we developed a series of simulation capabilities in `elegant` [1]. They provide the ability to simulate beam-scattering effects for an arbitrarily distributed linac beam with energy variation.

Beam-scattering effects are traditionally separated into two categories, Touschek effect and IBS, based on whether the scattered particles are lost immediately after the scattering event or not, respectively. In the case of IBS, we only see diffusion that leads to increased emittance in 6-D phase space; whereas in Touschek, a single scattering event may result in loss of the scattered particles. Different theoretical approaches are used to calculate the beam size diffusion rate and beam loss rate. In developing our simulation tools, we followed the same path: the widely used Bjorken-Mtingwa's [2] formula is chosen for calculating the emittance growth rate due to the IBS effect, while a combination of Piwinski's formula and Monte Carlo simulation is used for determination beam loss rates and positions.

Both the Bjorken-Mtingwa formula and Piwinski's formula were developed for stored beam, which has constant energy, and both assume a Gaussian bunch. These assumptions are generally invalid for a linac beam. In previous papers [3, 4, 5, 6], we discussed the beam loss issue for a one-pass transport system (Gaussian beam, constant beam energy), and the IBS for a arbitrarily distributed accelerating beam. In this paper, we describe newly developed methods that give us the ability to simulate the beam loss for an arbitrarily distributed linac beam, and summarize the already existing IBS tools. We also give an example application to a possible ERL-based APS upgrade design [7] using a particle distribution generated by an optimized high-brightness injector simulation [8].

A PROPOSED APS ERL UPGRADE

The APS has an eye on building an ERL for a future upgrade. Figure 1 shows the layout of one proposed design. The existing APS ring is used as part of the new machine. Since the radiation shielding of the APS already exists, there is concern about beam loss rate from the high-average-current ERL beam. Also, because of energy recovery, we will find that a small energy deviation generated at high energy may exceed the energy aperture at the end of deceleration, resulting in beam loss. Therefore, a detailed simulation tool that can determine the beam loss rate and the beam loss position precisely is needed.

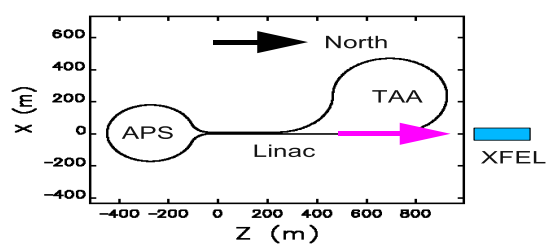

Figure 1: Layout of a proposed APS ERL upgrade.

In general, a linac beam departs from the normally assumed Gaussian distribution that holds for a stored beam,

* Work supported by the U.S. Department of Energy, Office of Science, Office of Basic Energy Sciences, under Contract No. DE-AC02-06CH11357.

† xiaoam@aps.anl.gov

THE SIMULATION OF THE ELECTRON CLOUD INSTABILITY IN BEPCII AND CSNS/RCS*

Y. D. Liu#, N. Wang
Institute of High Energy Physics, CAS, P.O. Box 918, 100049, Beijing, China

Abstract

Electron Cloud Instability (ECI) may take place in any positively charged particle circular accelerator especially in positron and proton storage rings. This instability has been confirmed to be a serious restriction to the beam stabilities. The physical model on the formation of electron cloud in various kinds of magnetic fields was introduced in the first section of the paper. The transverse and longitudinal wake field model to present the interaction between electron cloud and beam were introduced in another section of the paper. As an example, in positron storage in BEPCII and RCS of CSNS, the densities of electron cloud and beam instabilities caused by the accumulated electrons were simulated.

INTRODUCTION

The electron cloud accumulated in the vacuum chamber is usually associated with the transverse coupled bunch instability, bunch blow up and bunch lengthening. Experimental studies and numerical simulation have been developed for these phenomena [1]. Now BEPC has been upgraded to a two-ring collider, namely BEPCII, with electron and positron beams circulating in each separate ring. In its commissioning operation, ECI is much weaker because of many restraining methods used in positron ring. The effects of these restraining methods have been validated. In this paper, the simulation to electron cloud in different restraining conditions was introduced.

CSNS is a proton accelerator facility with consists of a linac and a rapid cycling synchrotron (RCS). Two bunches with a population of $1.88\text{x}10^{13}$ will be accumulated and accelerated in the RCS ring, and the electron-proton instabilities might happen in such high intensity proton ring. The ECI in CSNS/RCS is investigated in the last section. The main parameters of the BEPCII and CSNS/RCS ring are summarized in Table 1 and Table 2, respectively [2].

FORMATION OF ELECTRON CLOUD IN BEPCII AND CSNS/RCS

Electrons sourced from the (1) photoelectrons arising from the synchrotron radiation hitting the wall of the vacuum chamber, and (2) secondary emission from electrons hitting the walls, are attracted by the beam electric field and accumulate around the positron beam. Photoelectrons are produced in the chamber and antechamber by the photons hitting the wall with yield rate Y~0.1 and reflectivity R~0.1. If there is photon absorber, the Y and R become as small as Y~0.02, R~0.1.

Table 1: Parameters of the BEPCII

Parameters	Value
Beam energy E(GeV)	1.89
Bunch population $N_b(10^{10})$	4.84
Bunch spacing L_{sep}(m)	2.4
Bunch number n	93
Average bunch length σ_z(m)	0.015
Average bunch sizes $\sigma_{x,y}$(mm)	1.18,0.15
Chamber half dimensions $h_{x,y}$(mm)	60,27
Synchrotron tune Q_s	0.033
Tune $Q_{x,y}$	6.53,7.58
Circumference C(km)	0.237
Average beta function $<\beta>$(m)	10

Table 2: Parameters of the CSNS/RCS

Parameters	Symbol, unit	Value
Inj./Ext. Energy	Ein/Eext, GeV	0.08/1.6
Circumference	C, m	248
Bunch population	N_p, $\times 10^{12}$	9.4
Harmonic number	H	2
Repetition freq.	f_0, H_z	25
Betatron tune	ν_x/ν_y	5.86/5.78
Beam pipe radii	a/b, cm	10
Proton loss rate	P_{loss}, turn^{-1}	1.33×10^{-4}
Proton e– yield	Y_p, e–/p/loss	100
Ionization e–	Y_i, e–/p/loss	1.31×10^{-5}

The percentage of photoelectron escaping out of the antechamber depends on the width of antechamber. In the simulation the beam field is presented by B-E formula and the numerical solver of Poisson-Superfish in the central region of $(10\sigma_x,10\sigma_y)$ and out of this region, respectively. In the simulation we assume that secondary electrons yield (SEY) with and without TiN coating in the chamber is 1.06 and 1.8, respectively.

Simulation results show that the EC density can be reduced by about: 5x if the antechamber is adopted, 6x if the TiN is coated only, 3x if the photon absorber is made in the wall of the chamber only, and 5x if the electrode is installed in the beam chamber. In BEPCII, the antechamber, the photon absorber, and the TiN coating approaches have been adopted. With these three effects taken into account in the simulation, the electron density will be decreased about 80 times, i.e., from $1.1\text{x}10^{13}$ m^{-3} in the case without any restraining method to $1.3\text{x}10^{11}$m^{-3},

*Work supported by National Natural Science Foundation of China (10605032)
#liuyd@mail.ihep.ac.cn

MODELING LASER STRIPPING WITH THE PYTHON ORBIT CODE

T. Gorlov, A. Shishlo, ORNL, Oak Ridge, Tennessee, 37831, U.S.A.

Abstract

Laser assisted hydrogen stripping has become a widely discussed alternative to the existing stripper foil approach. A simulation tool for this new approach is presented. The application is implemented in the form of an extension module to the Python ORBIT parallel code that is under development at the SNS. The physical model in the application utilizes quantum theory to calculate the evolution and ionization of hydrogen atoms and ions affected by the superposition of electromagnetic and laser fields. The algorithm, structure, benchmark cases, and results of simulations are discussed for several existing and future accelerators.

INTRODUCTION

One of the serious problems with operating the SNS facility in Oak Ridge involves the injection system of the accumulator ring. The current system uses a thin carbon foil to convert H^- beam from the linac to protons at the ring injection point. The planned upgrade of SNS involves a power increase of the injected beam that will lead to excessive heating and to rapid failure of the stripper foil. For this reason SNS is developing alternative injection processes for higher powers.

There are two such investigations at SNS. The first involves the development of better stripper foils [1] and the second is the replacement of the stripper foil by a laser-assisted stripping (LS) process [2]. Moreover, LS is an attractive method for other projects using conversion-injection of H^- beam. This paper presents a computational model for the three step LS developed at the SNS [3-5], and that can also be applied to other projects.

Basically, the theoretical description of LS requires the self-consistent application of quantum mechanics, laser physics, and accelerator physics. The central problem is the excitation-ionization of a hydrogen beam in a superposition of electromagnetic and laser fields $H^0+\gamma\rightarrow H^{0*}\rightarrow p+e^-$. Success of the ionization process for each particle of the beam can be predicted with probability P using quantum mechanics. The problem of LS injection is conditioned by the requirements of the total LS efficiency $\overline{P}$ and output emittance parameters of the proton beam. By solving the problem one can determine the requirements on the input hydrogen beam and the laser beam parameters for successful injection.

The LS is a new scientific field [3-5] with no established computational component. The proof-of-principle (POP) of LS has been successfully demonstrated at the SNS [3]. To computationally support the experiment a simple quantum model [4] of adiabatic rapid passage (ARP) was applied. The model considers a two level hydrogen atom and linear frequency growth in time of the laser field in the atom's rest frame. The model consists of a system of two linear differential equations that can be solved by any Math package. Many physical phenomena taking place in a real experiment and significantly affecting the final LS efficiency are not included in the model. Nevertheless the model yields a good estimation of LS efficiency and can be used both as an initial stage for LS calculation and for benchmarking more detailed models. It should be noted that the purpose of the POP experiments was to demonstrate feasibility of the LS idea founded on the basic principles of quantum mechanics. The expectation of the model was successfully met experimentally.

For the next experiments planned in the SNS project it is necessary to demonstrate the feasibility of LS injection for the detailed SNS requirements. Experimental LS involves many different phenomena that should be included in the calculation. These include: the Stark effect and splitting of the hydrogen atom energy levels; spontaneous decay; electric field ionization; and possible circulation of the external electromagnetic field. Computing the LS for the next experiments is necessary for determining the simplest technical equipment and for optimizing the LS efficiency over the numerous parameters in the LS scheme.

A short description of the LS physical model, taking into account all the listed phenomena, can be found in [3]. A computer model of LS presented in this paper has been realized in form of an extension module in the PyORBIT parallel code developed at the SNS [6]. The choice of the implementation is conditioned by the general direction of development of accelerator codes at the SNS. The main advantages of the chosen direction are: rapid and pure object oriented prototyping of applications at the Python level; the widespread use and detailed documentation of Python; high performance execution of the classes at the C++ level; simple writing of extension modules; and parallel computing with PyORBIT based on MPI library. Moreover the present PyORBIT already contains templates for developing extension modules. If the developer has a unique physical problem requiring different classes than those in PyORBIT, he can create new extension modules to solve the problem.

This paper is organized as follows. Section 2 gives a short overview of the physical model of the LS and formulates the mathematical problem for computing the LS. The purpose of the section is to show the amount and kinds of computations required for solving the problem of LS. Section 3 describes the organization of the LS code and classes for getting the most efficient computations. Section 4 presents benchmarks and tests of the LS code. Section 5 outlines the scope of problems that can be solved by the code. Section 6 summarizes the paper summarizing and suggests some problems to be treated in the future.

USING GEANT4-BASED TOOLS TO SIMULATE A PROTON EXTRACTION AND TRANSFER LINE

F.W. Jones, R. Baartman, and Y.-N. Rao
TRIUMF*, 4004 Westbrook Mall, Vancouver V6T 2A3, Canada

Abstract

The simulation toolkit GEANT4 has been used to create high-level tools for specific user groups, such as SPENVIS in space physics and GATE in medical imaging. In Accelerator Physics, comparable efforts are being devoted to develop general-purpose programs for simulating beam lines and accelerators, allowing access to Geant4's facilities for 3D geometry, tracking, and interactions in matter without the need for specialised programming techniques. In this study we investigate the use of two high-level tools based on Geant4, BDSIM and G4BEAMLINE, to model a 65-meter beam line supplying protons from the TRIUMF cyclotron to the ISAC Rare Isotope Beam facility. We outline some features of the codes and comment on their different approaches to defining the beam line geometry. Due to its ability to model some important aspects such as rectangular dipoles and magnetic fringe fields, G4beamline was utilized for the simulations presented here, for validation of the model and the investigation of beam losses.

INTRODUCTION

In using simulation tools to investigate particle losses in accelerators and beam lines, the effects of particle interactions in matter, and in particular the secondary particles arising from electromagnetic and hadronic interactions, are very important for safety issues, loss monitoring and diagnostics, and radiation damage and activation of hardware.

The Geant4 simulation toolkit[1] offers a versatile way to track particles in an accelerator or beam line geometry, with realistic fields. For interactions in matter it offers a wide range of physics processes and models and a host of other facilities for studying losses with tracking of all relevant secondaries. The choice of physics models allows tuning of the simulation to the particular energy range and particles of interest.

Tapping into the power of Geant4 generally requires facility in C++, as the user must supply C++ code to define and implement the geometry, to specify the sampling of track information in sensitive detectors, and to instantiate the necessary "manager" objects to initialize and coordinate the simulation. Although C++ skills are part of the culture of high energy particle physics, they are not always as easy to find in other fields, and this has prompted the development of higher-level tools built from Geant4.

Accelerator physicists can benefit from two such tools, BDSIM and G4Beamline. In the following we will describe some of the capabilities of these tools and our development of a prototype model of a TRIUMF beam line in each code. A limitation in BDSIM (being addressed by the code authors at the time of writing) prevented us from advancing to a full simulation, but in G4Beamline we proceeded to refine the model and to validate its tracking and optical properties against measured beam profiles. The validated model enabled us to perform simulations aimed at estimating the influence of multiple scattering in the cyclotron extraction foil on losses in the beam line, of which some first results will be presented.

GEANT4, BDSIM, AND G4BEAMLINE

GEANT4

Geant4 provides a software toolkit for tracking and simulation, in a 3D geometry, of particle interactions in matter. It is object-oriented and scalable to very large and diverse applications. A key characteristic of its design is to allow the user to plug in new or modified simulation components without the need for any modification of the Geant4 code itself.

The code is written in C++ and is implemented as a collection of class libraries in various categories. For a given application, the user provides code for a main program and auxiliary classes which instantiate the components of the simulation: geometry, particles, physics processes, data collection objects (sensitive detectors), and so on. The main program also invokes the "glue", or manager, classes from the toolkit which initialize and coordinate the simulation run. For each instance of an application, the main program and user-written classes are compiled and linked together with the Geant4 libraries to make an executable.

This approach follows the principle that for a simulation code *the most powerful and general input language is the language the code is written in*. For Geant4 any input system less complex than C++ code may limit the expression of complex problems. A somewhat gentler principle is that *a scripting language for object-oriented simulation should itself be object-oriented*.

On the other hand, simpler and easier input methods can be devised for problems with a specialized and well-defined scope, particularly if the scale of the problem is relatively small. For accelerators and beam lines, BDSIM and G4Beamline provide the needed functionality using input methods similar to basic scripting or shell languages.

*TRIUMF receives federal funding via a contribution agreement through the National Research Council of Canada

END TO END SIMULATIONS OF THE GSI LINEAR ACCELERATOR FACILITY

G.. Clemente, W. Barth, L. Groening, A. Orzhekhovskaya, S. Yaramishev, GSI, Darmstadt, Germany
U. Ratzinger, R. Tiede, J.W. Goethe University, Frankfurt a.M., Germany.
A. Kolomites, S Minaev, ITEP, Moscow, Russia

Abstract

During the last year several numerical investigations have been started at GSI in order to improve the performance of the linear accelerator facility. The main activities regard the upgrade of the high current UNILAC accelerator including the severe upgrade of the HSI injector, the HITRAP decelerator and, in the frame of the future FAIR project, the development of the new dedicated proton linac. End to end beam dynamics simulations are a powerful tool concerning the machine design, commissioning and optimization. Particle distributions, generated from beam emittance measurements, are transferred through the whole chain of accelerating structures and beam transport lines. Detailed calculations of space charge effects as well as external and measured mapping of the electromagnetic fields are used to provide the most reliable results. The paper presents a general overview of all activities performed at GSI concerning the linear accelerator complex.

INTRODUCTION

The scientific program at FAIR requires a sever upgrade of the existing GSI linear accelerator complex in terms of beam brilliance and absolute beam current. To fulfill the experimental heavy ion requirements the UNILAC must provide up to 3.3 x 10^{11} U^{28+}particles within macropulses of 100 µs long [1]. At the final energy of 11.4 MeV/u the beam will be injected into the SIS18 with a repetition rate up to 4 Hz.

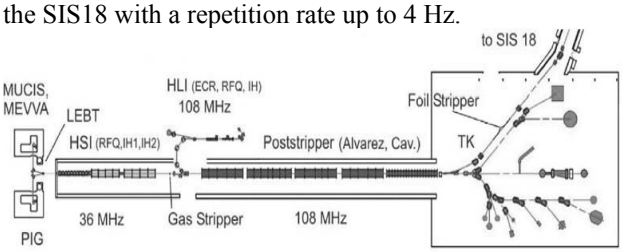

Fig.1: The present linear accelerator complex at GSI.

On the other side, FAIR will provide up to 7 x 10^{10} p-bar/h which, taking into account the antiproton production and cooling rate implies a primary proton beam of 2 10^{16} p/h. This intensity is far beyond the capabilities of the existing UNILAC and, for that reason, a new dedicated proton injector has to be built [2].

In parallel, activities on linear accelerators at GSI are not only focused on the FAIR project. Recently, in the frame of the atomic physics HITRAP project [3], a 4.00 Mev/u Ni^{28+} beam coming from the ESR was decelerated to 6 keV/u making available high charged and cooled beams for trapping experiments.

UNILAC UPGRADE

The next upgrade activities are mainly focused on the low energy front end which represented a bottleneck concerning operation with higher brilliance. The High Current Injector [4] consists of a 36 MHz IH-RFQ from 2.2 keV/u to 120 keV/u and a short 11 cell adapter RFQ called Super Lens. The following acceleration step is performed by two IH-DTL's which deliver a 1.4 MeV/u beam. After the stripping in a supersonic gas jet, uranium beams with charge state of 28+ are delivered to the Alvarez-DTL and accelerated to 11.4 MeV/u with minor losses.

Upgrades of the HSI

The first upgrade of the HSI-RFQ was performed in 2004 after five years of continuous operation. New electrodes were produced increasing the quality of surfaces and thus reducing the RF power consumptions from 650 kW to 380 kW. Additionally, the RFQ Input Radial Matcher (IRM) was redesigned to improve the beam transmission through the whole front-end system.

DYNAMION calculations were performed using particles distributions generated by measured emittances and predicted an intensity gain of up to 15% for high current uranium beam (15 mA). Those simulations were later on perfectly confirmed by measurements [5].

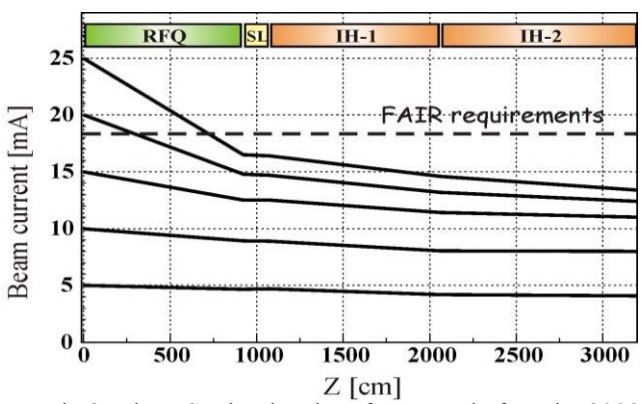

Fig.2: The HSI simulated performance before the 2009 upgrade for different input current in comparison with the requirements for FAIR.

APERTURE AND BEAM-TUBE MODELS FOR ACCELERATOR MAGNETS*

H. De Gersem†, Katholieke Universiteit Leuven, Belgium
S. Koch, T. Weiland, Technische Universität Darmstadt, Germany

Abstract

Standard 2D magnetodynamic finite-element models for accelerator magnets are accomplished by dedicated models for the aperture and for the beam-tube end parts. The resulting hybrid and coupled models necessitate the application of specialized algebraic solution techniques in order to preserve the computational efficiency, i.e., matrix-free iterative solvers combined with fast Fourier transforms and Schwarz-type preconditioners.

INTRODUCTION

3D finite-element (FE) models of accelerator magnets may become prohibitive when transient phenomena at small temporal and spatial scale should be resolved, i.e., eddy current effects in windings, beam tube and yoke or filamentary and coupling effects in superconductive cables. Simulation times of several hours have been reported. As a consequence, such calculations are only feasible at later stages of the design process, when geometry, materials and operating conditions are more or less fixed. At an earlier design stage, parameter variations and optimization steps are carried out, almost exclusively on the basis of semi-analytical formulae. It makes sense to support this design phase by FE models that succeed in attaining lower but acceptable accuracies within substantially smaller simulation times, compared to transient 3D simulation [3]. Efforts in the direction of this goal consider 2D FE models where extensions are implemented that deal with typical 3D effects and model some small-scale effects in a problem specific way. In this paper, two extensions for 2D and 3D FE models are proposed. The high-resolution aperture model and the beam-tube end model developed here, both significantly increase the modeling power for superconductive magnets and succeed in keeping the computation time for transient 2D FE simulation as low as a few minutes.

APERTURE MODEL

Domain Decomposition and Mixed Formulation

The magnet geometry is divided in two parts: an outer domain Ω_1 including the windings and yoke and a cylindrical inner domain Ω_2 in the magnet aperture (Fig. 1). The interface is denoted by $\Gamma_{12} = \Omega_1 \cap \Omega_2$. A mixed magneto-quasistatic (MQS) formulation is applied:

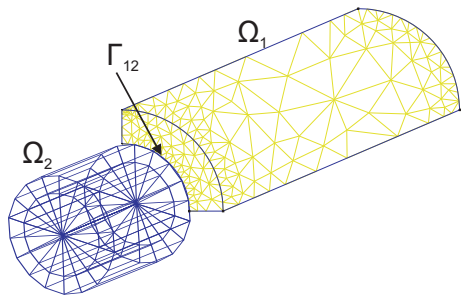

Figure 1: Magnet model: FE mesh for the outer part and tensor-product grid for the aperture.

$$\nabla \times \left(\nu \nabla \times \vec{A}\right) + \sigma \frac{\partial \vec{A}}{\partial t} = \vec{J}_\mathrm{s} \quad \text{in } \Omega_1 \; ; \qquad (1)$$

$$-\nabla \cdot (\mu \nabla \psi) = 0 \quad \text{in } \Omega_2 \; , \qquad (2)$$

where $\vec{A}$ is the magnetic vector potential, ψ the magnetic scalar potential, $\vec{J}_\mathrm{s}$ the applied current density, μ the permeability, $\nu = 1/\mu$ the reluctivity and σ the conductivity. The normal continuity of the magnetic flux density $\vec{B} = \nabla \times \vec{A} = -\mu \nabla \psi$ and the tangential continuity of the magnetic field strength $\vec{H} = \nu \nabla \times \vec{A} = -\nabla \psi$ are enforced at the interface Γ_{12}. The domains are equipped with different formulations that are dual with respect to each other. The MQS formulation in terms of $\vec{A}$ is capable of considering the eddy current phenomena in the yoke, beam tube and windings, at the expense of being a vectorial partial differential equation (PDE). On the contrary, the MQS formulation in terms of ψ is static but is a scalar formulation. Such so-called *mixed* formulations have been frequently used for MQS simulation in the eighties, especially because of the relatively small number of degrees of freedom which was beneficial for the direct and Krylov-type solvers used at that time [11]. A drawback of a mixed formulation is the fact that the computed magnetic energy and power loss do not converge monotonically with respect to the mesh size as is the case for the non-mixed formulations. The motivation for choosing a mixed formulation will become clear below.

Discretization and System Properties

$\vec{A}$ is discretized in Ω_1 by the standard lowest-order edge elements $\vec{w}_j$, whereas ψ is discretized in Ω_2 by standard

* This work was supported by the Helmholtzzentrum für Schwerionenforschung GmbH (GSI), Darmstadt and by the Katholieke Universiteit Leuven under grant STRT1/09/041.

† herbert.degersem@kuleuven-kortrijk.be

A FAST AND UNIVERSAL VLASOV SOLVER FOR BEAM DYNAMICS SIMULATUONS IN 3D*

Sylvain Franke**, Wolfgang Ackermann, Thomas Weiland,
Technische Universität Darmstadt, Institut für Theorie Elektromagnetischer Felder,
Schlossgartenstraße 8, 64289 Darmstadt, Germany

Abstract

The Vlasov equation can describe the evolution of a particle density under the effects of electromagnetic fields and thus it is possible to describe the evolution of a charged particle beam within an accelerator beam line. The Vlasov equation forms a partial differential equation in a 6D phase space witch renders it very expensive if it is solved via classical methods. A more efficient approach consists in representing the particle distribution function by a discrete set of characteristic moments. For each moment a time evolution equation can be stated. These ordinary differential equations can then be integrated efficiently by means of numerical methods if all acting forces together with a proper initial condition are given. The beam dynamics simulation tool V-Code has been implemented at TEMF on the basis of the moment approach. In this paper the numerical model, main features and designated use cases of the V-Code will be presented.

INTRODUCTION

The distribution of particles in the 6-dimensional (6D) phase space can be described by a density distribution function $f(\vec{r},\vec{p},\tau)$ with space coordinates $\vec{r}=(x,y,z)$, normalized momentum $\vec{p}=(p_x,p_y,p_z)$ and equivalent time $\tau = c\cdot t$. Their evolution in the phase space can then be expressed by the Vlasov equation

$$\frac{\partial f}{\partial \tau}+\frac{\partial f}{\partial \vec{r}}\cdot\frac{\vec{p}}{\gamma}+\frac{\partial f}{\partial \vec{p}}\cdot\frac{\vec{F}}{m_0c^2}=0 \qquad (1)$$

where γ represents the relativistic factor, $\vec{F}$ the applied forces, m_0 the particles rest mass and c the speed of light in free space.
Equation (1) is applicable for any forces $\vec{F}$ with slow variation in space [2]. Coulomb forces within an charged particle beam as well as forces from external electromagnetic fields meet this condition. Thus, the Vlasov equation is applicable for beam dynamics simulations of charged particle beams in accelerators.
It is very expensive to solve such a partial differential equation via classic numerical methods for a time varying 6D density distribution function.

* Work supported by DFG through SFB 634.
** franke@temf.tu-darmstadt.de

MOMENT APPROACH

A more efficient approach is to consider a discrete set of characteristic moments of the particle distribution function instead of the function itself [3]. Following this approach the problem can be reduced to a set of ordinary differential equations which can be evaluated by means of standard time integration methods.

Moment Definition

The classical raw moments $<\mu>$ are obtained from the distribution function f by a weighted integration over the whole phase space Ω

$$<\mu> = \int_\Omega \mu\ f(\vec{r},\vec{p},\tau)\ \mathrm{d}\Omega. \qquad (2)$$

Here, the normalized density distribution function to ensure

$$1 \stackrel{!}{=} <1> = \int_\Omega f(\vec{r})\ \mathrm{d}\Omega \qquad (3)$$

has to be applied for proper algebraic relations.

A numerically advantageous choice of moments witch ultimately allows the determination of the overall position and the overall momentum of a particle distribution is given by the first order raw moments

$$\mu \in \{x, y, z, p_x, p_y, p_z\} \qquad (4)$$

in Cartesian coordinates.

By choosing the higher order moments in a centralized notation

$$\mu \in \{(x-<x>)^{l_1}\cdot\ \ldots\ \cdot(p_z-<p_z>)^{l_6},\ \ldots\} \qquad (5)$$

one automatically obtains a translatory invariant description of the shape of the particle distribution function.
For example, a subset of the second order moments

$$\begin{aligned}{\sigma_x}^2 &= <(x-<x>)^2>\\ {\sigma_y}^2 &= <(y-<y>)^2>\\ {\sigma_z}^2 &= <(z-<z>)^2>\end{aligned}$$

then identify the important variances of the underlying particle distribution.

DISCRETIZING TRANSIENT CURRENT DENSITIES IN THE MAXWELL EQUATIONS*

Mark L. Stowell, Daniel A. White,†
Lawrence Livermore National Laboratory, P.O. Box 808, Livermore CA, 94551, USA

Abstract

We will briefly discuss a technique for applying transient volumetric current sources in full-wave, time-domain electromagnetic simulations which avoids the need for divergence cleaning. The method involves both "edge-elements" and "face-elements" in conjunction with a particle-in-cell scheme to track the charge density. Results from a realistic, 6.7 million element, 3D simulation are shown. While the authors may have a finite element bias the technique should be applicable to finite difference methods as well.

INTRODUCTION

The Maxwell Equations

The Maxwell Equations with a current density source term can be written

$$\begin{aligned} \frac{\partial}{\partial t}\vec{D} &= \nabla \times \vec{H} - \vec{J} \\ \frac{\partial}{\partial t}\vec{B} &= -\nabla \times \vec{E} \end{aligned}$$

where

$$\vec{D} = \epsilon \vec{E} \text{ and } \vec{B} = \mu \vec{H}$$

These equations are commonly discretized using "edge-elements", or discrete 1-forms, for the electric field and "face-elements", or discrete 2-forms, for the magnetic flux density. This scheme requires that $\vec{J}$ also be approximated with edge-elements, which works quite well in many situations. However, this scheme does have certain drawbacks.

One difficulty with 1-form current densities is that they can spread through material interfaces into non-physical regions. For example, consider a vacuum region abutting a weak conductor which contains a constant current density. What value for $\vec{J}$ should be applied to the edges which are shared between these two regions? If the constant $\vec{J}$ value is used, then the conducting region will contain the correct value but the vacuum region will also contain a non-zero current density. If a value of zero is applied on these edges, then the vacuum region will correctly have zero current but the conductor will contain less current density than desired.

Another difficulty, and the one we will focus on, arises if the current density is transient and the primary interest is to determine how a cavity will resonate after a current pulse passes through it. The problem here is that the continuity equation for the electric charge,

$$\frac{\partial \rho}{\partial t} + \nabla \cdot \vec{J} = 0,$$

is only weakly satisfied. Therefore, current densities can, and often do, leave behind non-physical charge densities after they pass through the computational mesh. These charge densities can, in turn, produce a non-physical, static, electric field which not only adds unexpected, mesh dependent, features to field plots but can also reduce the accuracy of the meaningful portion of the solution.

Integrating the charge continuity equation over time we obtain

$$\rho(t_b) - \rho(t_a) = -\int_{t_a}^{t_b} \nabla \cdot \vec{J} dt.$$

Assuming t_a and t_b are chosen such that $\vec{J}$ is everywhere equal to zero before t_a and after t_b with no charges being left behind anywhere within the problem domain we would have $\rho(t_a) = \rho(t_b) = 0$ and so

$$\int_{t_a}^{t_b} \nabla \cdot \vec{J} dt = 0.$$

This is the constraint that we hope to satisfy. The accuracy with which this can be accomplished will hinge on our ability to accurately represent the divergence of the vector flux density $\vec{J}$.

Discrete Differential Forms

Differential Forms provide a general mathematical formalism to describe not only Div, Grad, and Curl but also integral relationships like the fundamental theorem of calculus, Kelvin-Stokes theorem, and the Divergence theorem. For example these three theorems can each be described by the generalized Stokes' theorem:

$$\int_{\Omega} d\omega = \oint_{\partial\Omega} \omega \qquad (1)$$

Where "ω" is a differential form and "d" is the exterior derivative appropriate for that form type. Specifically, if ω is a 1-form (a standard vector field), this expression states that

$$\int_{\Sigma} \nabla \times \omega \cdot \vec{n}\, dA = \oint_{\partial\Sigma} \omega \cdot d\vec{r} \qquad (2)$$

which is the classical Kelvin-Stokes theorem. Another important characteristic of differential forms is that for any k-form, ω, its exterior derivative, $d\omega$, is a (k+1)-form.

* This work performed under the auspices of the U.S. Department of Energy by Lawrence Livermore National Laboratory under Contract DE-AC52-07NA27344, UCRL LLNL-CONF-420323.

† stowell1@llnl.gov, white37@llnl.gov

SIMULATION AND COMMISSIONING OF J-PARC LINAC USING THE IMPACT CODE

M. Ikegami, KEK, Tsukuba, Ibaraki 305-0801, Japan
H. Sako, T. Morishita, JAEA, Tokai, Naka, Ibaraki 319-1195, Japan
G. Shen, BNL, Upton, NY 11973-5000, USA

Abstract

The IMPACT code has been utilized for the beam commissioning of J-PARC linac. The activity is presented by reviewing two illustrative topics, where the experimental data is analyzed to realize a finer tuning. One is the RF set-point tuning for a DTL tank, where we have a significant discrepancy between the experimental result and prediction from a simple numerical model. The other is the beam profile measurement, where significant beam quality deterioration is found to develop in a characteristic way. In both cases, the IMPACT code has helped us to deepen our insight into the beam behavior.

INTRODUCTION

The beam commissioning of J-PARC linac was started in November 2006, and its initial stage was completed in October 2007 by achieving the linac beam power of 1.2 kW [1]. This beam power corresponds to 20 kW from the succeeding 3-GeV RCS (Rapid Cycling Synchrotron), and it is sufficient for the initial beam commissioning of the downstream facilities. Since then, J-PARC linac has been operated to provide a stable beam for the commissioning of downstream RCS, MR (Main Ring), and their beam lines to the experimental targets. After succeeding in delivering the first beams to all the experimental targets in May 2009, we are now in the next stage where we seek the operation with higher beam power.

J-PARC is a high-power frontier machine aiming at 1-MW beam power from RCS (133 kW from linac) in the final phase. Accordingly, it is of essential importance to reduce the uncontrolled beam loss, and hence, to avoid excess radio-activation of the accelerator components so as to maintain its hands-on maintenance capability. This is the case even in the early stages of the beam commissioning, and we need to reduce the integrated beam loss during the beam tuning. Therefore, it is required to realize a more sophisticated and efficient tuning rather than a traditional trial-and-error tuning. To this end, a simple and fast on-line numerical model plays an essential role in the beam commissioning of J-PARC linac.

On the other hand, the beams in a high-intensity linac are subject to strong space-charge forces. It often invokes collective and nonlinear phenomena, such as emittance growth and halo formation, being accompanied with the various operational errors. As these phenomena often lead to undesirable beam losses, we need to realize a precise tuning in beam-power ramp-up. Even a very small fraction of beam loss can cause serious radio-activation in a high-intensity operation. Therefore, more thorough and fine-grained understanding of the beam behavior and the space-charge-driven phenomena is required in ramping up the beam intensity. To this end, we need a precise and detailed simulation of the beam behavior with a time-consuming PIC (Particle-In-Cell) tracking.

In the beam commissioning, we fully utilize two numerical models which complement each other. One is an on-line envelope model, and the other is an off-line PIC model.

As an on-line model, we have adopted XAL originally developed for SNS [2]. XAL is a JAVA-based high-level software development framework dedicated to accelerator beam commissioning, and it includes an envelope model to be utilized as an on-line model. This model is capable of calculating the evolution of rms beam widths and a beam center orbit swiftly. However, it can not simulate the space-charge-driven emittance growth and halo development. This model has been used for various beam tuning in J-PARC linac directly connected with high-level software [3].

As an off-line model, we have mainly adopted the IMPACT code developed at LBNL [4]. IMPACT is a fully three-dimensional PIC code optimized for parallel computing, which is suitable for the detailed simulation for the space-charge-driven phenomena including emittance growth, halo formation, and resulting beam loss. We use IMPACT for the beam simulation from the RFQ (Radio Frequency Quadrupole linac) exit to the injection point to RCS. The initial distribution for the IMPACT simulation is generated with the PARMTEQM code [5].

In this paper, we show some examples of the studies

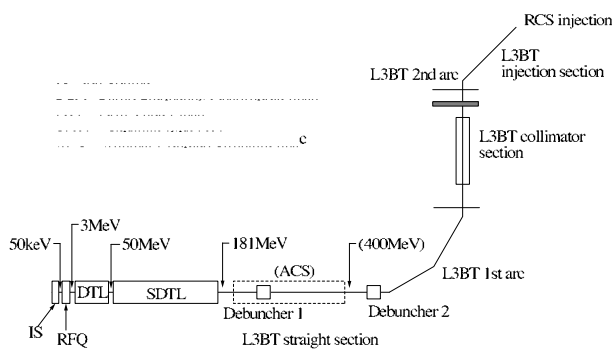

Figure 1: Schematic layout of J-PARC linac.

PHYSICS PROBLEM STUDY FOR A 100 MEV, 500 MICROAMP H⁻ BEAM COMPACT CYCLOTRON *

Technology Division of BRIF, CIAE (written by Tianjue Zhang[1;#], Jianjun Yang[1,2;†], and Hongjuan Yao[1])

[1.] China Institute of Atomic Energy, Beijing 102413, China
[2.] Department of Engineering Physics, Tsinghua University, Beijing 100084, China

Abstract

A high intensity compact cyclotron, CYCIAE-100, is selected as the driving accelerator for Beijing Radioactive Ion-beam Facility (BRIF). At present the physics design of this machine has been accomplished. This paper gives a brief review of the general design of this machine. For further intensity upgrade of this compact machine in the future, it is crucial to carry out in-depth study on the self fields effects including the contributions of single bunch space charge and the interaction of many radially neighboring bunches. In order to include the neighboring bunch effects fully self-consistently in compact cyclotrons, a new physical model is established for the first time and implemented in the parallel PIC code OPAL-CYCL. After that, the impact of the single bunch space charge and neighboring bunches on the beam dynamics in CYCIAE-100 for different intensity levels are studied by the simulations using the new model.

INTRODUCTION

Since 2004 a new exotic beam project, Beijing Radioactive Ion-beam Facility (BRIF), has been started at CIAE. As a driving accelerator for BRIF[1], CYCIAE-100 adopts a compact structure with 4 straight sectors. The H^- ions produced by the multi-cusp ion source are accelerated, and the high intensity proton beams are extracted through dual stripping. The extracted beam is 200–500μA featured with energy of 75–100 MeV, which is continuously adjustable. Figure 1 shows the overall structure of CYCIAE-100 and Table 1 lists its key parameters. From the view of beam dynamics, the physics problem of this machine is composed of several aspects, including axial injection, central region, acceleration, stripping extraction and beam lines, which have been described in several papers published formerly[2]–[5]. The basic physics design and current construction status of machine will be briefly reviewed in the following section.

Table 1: Key Parameters of CYCIAE-100

Item	value
ion source type	multi-cusp
injection current	> 5 mA
number of poles	4
angle of poles	~47°
radius of poles	2000 mm
outer diameter of yoke	6160 mm
height of magnet	2820 mm
total iron weight	~415 t
field range	0.15–1.35 T
gap between hills	50–60 mm
injection energy	40 keV
rf frequency	44.32 MHz
Dee Voltage	60–120kV
number of cavities	2
harmonic number	4
extraction type	multi-turn stripping

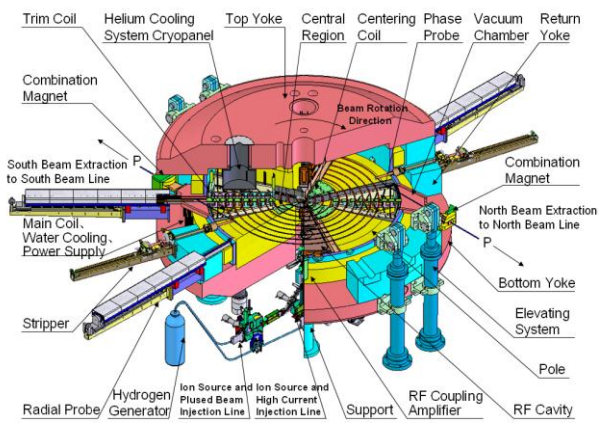

Figure 1: Sketch of the major parts of CYCIAE-100.

Beam loss is the key factor which limits the beam current of a high intensity cyclotron. Space charge effects, being one of the most significant collective effects, play an important role in high intensity cyclotron. Space charge may cause massive beam loss at the low- and middle-energy accelerator. In CYCIAE-100, the injection energy is only 40keV and the maximal energy is 100MeV (γ=1.106), and therefore, space charge can be remarkable under high current conditions. In addition, a common

*Work supported by the NSFC, under contract 10775185
#tjzhang@ciae.ac.cn
†yangjianjun00@mails.tsinghua.edu.cn

SPACE CHARGE SIMULATIONS FOR ISIS

BG Pine, DJ Adams, B Jones, CM Warsop, RE Williamson
Rutherford Appleton Laboratory (STFC), Oxfordshire, UK.

Abstract

The ISIS Facility at the Rutherford Appleton Laboratory in the UK produces intense neutron and muon beams for condensed matter research. It is based on a 50 Hz proton synchrotron which accelerates ~3E13 protons per pulse (ppp) from 70 to 800 MeV, corresponding to beam powers of ~0.2 MW. Studies are under way for major upgrades in the Megawatt regime. Underpinning this programme of operations and upgrades is a study of the high intensity effects that impose limitations on beam power.

The behaviour of the beam in the 50 Hz rapid cycling synchrotron (RCS) is largely characterised by high space charge levels and the effects of fast ramping acceleration. High intensity effects are of particular importance as they drive beam loss, but are not fully understood with only limited analytical models available. This paper reviews several methods by which these effects are explored numerically on ISIS, and compares them where possible with experimental or analytical results. In particular we outline development of a new space charge code Set, which is designed to address key issues on ISIS and similar RCS machines.

INTRODUCTION

ISIS high intensity operation is restricted by beam loss, as irradiation of equipment limits access for essential maintenance. Understanding beam loss is therefore of vital importance, however due to the complex interactions between the beam particles and their environment such understanding is challenging both analytically and numerically.

The ISIS Synchrotron Group is actively studying high intensity effects of the beam in a number of different ways, both to improve performance of the accelerator and also to enable the design of upgrades which can achieve significantly higher beam intensities. Aspects of this work are reported here, including closely related profile monitor simulations, injection painting, beam dynamics, half integer studies and developments of codes.

PROFILE MONITOR

ISIS profile monitors are important for studies of injection painting, space charge, beam halo, betatron motion and instabilities, as well as suffering space charge effects of their own. The profile monitors on ISIS use ions, liberated from the residual gas by passage of the beam, to reconstruct transverse beam distributions. A (near) uniform electric field, perpendicular to the direction of the beam, accelerates ions to a suitable detector. The number of ions detected is assumed to be proportional to the local beam intensity. This process suffers from two major sources of error: 1) irregularity in the electric field used to drive the ions to the detector; 2) broadening effects produced by the space charge field of the beam, which at high intensities can dominate the measured profile width. Fortunately correction schemes for both of these phenomena have been found, and are discussed below.

Drift field effects

A model of an ISIS profile monitor (see Figure 1) was constructed in CST Studio Suite [1]. Figure 2 displays the potential produced by the electrodes in both transverse and longitudinal cross-sections. As can be seen the required linear field is not achieved perfectly – both transverse and longitudinal sections show deviation from the ideal behaviour.

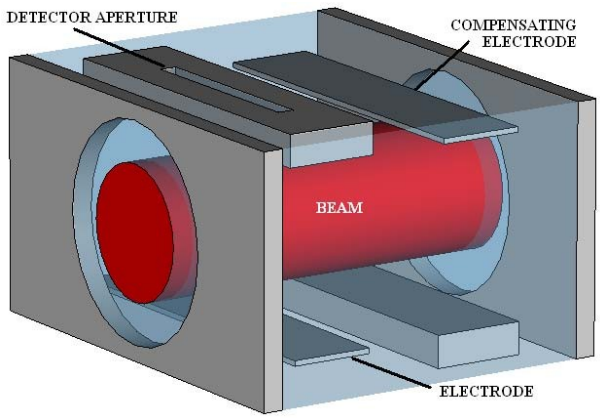

Figure 1: Residual Gas Profile Monitor.

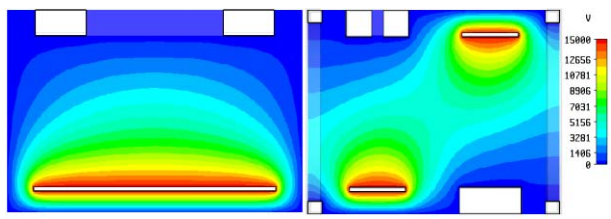

Figure 2: Electrostatic potentials: transverse - left, longitudinal - right.

In order to study these effects in more detail, potentials were calculated then extracted from the CST model, and used as the field source in a specially developed 2D particle tracker. Realistic beam distributions (parabolic, elliptic) were used as the source of particles. The results showed that a simple scaling correction was effective for reasonably well centred and behaved beam distributions [2]. 3D simulations [3] showed considerably more complex behaviour, as particles may oscillate along longitudinal field saddle points between the two electrodes in the monitor body. On investigation however this more complex behaviour could be accounted for by a

AN INTEGRATED BEAM OPTICS-NUCLEAR PROCESSES FRAMEWORK IN COSY INFINITY AND ITS APPLICATIONS TO FRIB*

B. Erdelyi#, Northern Illinois University, DeKalb, IL 60115. and ANL, Argonne, IL 60439
L. Bandura, NSCL, Michigan State University, East Lansing, MI 48824

Abstract

When faced with the challenge of the design optimization of a charged particle beam system involving beam-material interactions, a framework is needed that seamlessly integrates the following tasks: 1) high order accurate and efficient beam optics, 2) a suite of codes that model the atomic and nuclear interactions between the beam and matter, and 3) the option to run many different optimization strategies at the code language level with a variety of user-defined objectives. To this end, we developed a framework in COSY Infinity with these characteristics and which can be run in two modes: map mode and a hybrid map-Monte Carlo mode. The code, its applications to the FRIB, and plans involving large-scale computing will be presented.

INTRODUCTION

The next generation of nuclear physics research will require advanced exotic beam facilities based on heavy ion driver accelerators. There are many next-generation facilities that are currently under commissioning, construction, or envisioned [1-5]. Included amongst these is the future Facility for Rare Isotope Beams (FRIB) at the National Superconducting Cyclotron Lab at Michigan State University. These facilities are capable of producing exotic beams composed of rare nuclei in large quantities. The exotic isotopes are produced via projectile fragmentation and fission in targets. High-performance fragment separators, a key component of all rare isotope facilities, consist of superconducting magnets that are used for the capture, selection, and transport of rare isotopes. Large aperture magnets are necessary in order to accept rare isotope beams with large emittances resulting from their production mechanism.

The beam optics code COSY INFINITY uses powerful differential algebraic (DA) techniques for computing the dynamics of the beam in the fragment separator through high order transfer maps [6]. However, until now it has lacked the ability to calculate the beam-material interactions occurring in the target and energy absorbers. Here, a hybrid map-Monte Carlo code has been developed and integrated into COSY in order to calculate these interactions. The code tracks the fragmentation and fission of the beam in target and absorber material while computing energy loss and energy and angular straggling as well as charge state evolution. This is accomplished by implementing auxiliary codes such as ATIMA [7] and GLOBAL [8]. EPAX [9] is utilized to return cross sections of fragmentation products. The special case of fission has been treated by using the code MCNPX [10] to accurately predict the cross sections and dynamics of exotic beams produced by a ^{238}U beam incident on a Li or C target. The extensions to the code have made it possible to simultaneously compute high order optics and beam-material interactions in one cohesive framework.

The hybrid map-Monte Carlo code can calculate important quantities that describe the performance of the fragment separator. These include the transmission and the separation purity. In a map-only approach, calculations such as these are not possible. Experimental planning and optimization is possible with the hybrid map-Monte Carlo code, as various fragment separator settings can be readily adjusted. Here we present a description of the code, examples of calculations with it, and its application to the separation of rare isotopes.

IMPLEMENTATION

A solely map-based approach is not sufficient to model the evolution of an exotic beam in the fragment separator. It is impossible to take into account fragmentation and fission of the beam in matter in such an approach. There are also many other effects that are nondeterministic. Stochastic effects such as energy and angular straggling in matter and charge exchange demand a Monte Carlo method. To compute the extent of the stochastic effects, the most up-to-date programs such as ATIMA for calculating energy loss and energy and angular straggling have been integrated into COSY as simple procedures.

To get an accurate view of the evolution of the beam, any material that the beam passes through must be divided up into "slices." There are a couple of reasons to do this. One reason is that some of the rarer isotopes would not be produced at all if the whole target or wedge material thicknesses were used. By the same argument, each slice cannot be too thick as it won't account for multiple fragmentations or fissions. Having slices that are too thin increases the run time of the program. Also, the data acquired from MCNPX assumes a very thin thickness (0.1068 g/cm^2), so any deviation from this thickness per slice will give increasingly inaccurate results. The approximation for the cross sections and dynamics will be worse. A target thickness on this order will not be used for a FRIB, so for the most accurate approximations, more than one slice per target is used. The target thicknesses would typically be about 30%-40% of the range of the primary beam in the target material. Convergence tests have been performed to determine how many slices are necessary for a normal target thickness. This value is approximately one slice per 10% of the

*This work was supported by the U.S. Department of Energy, Office of Nuclear Physics, under Contract No. DE-AC02-06CH11357
#erdelyi@anl.gov

THE STUDY ON THE SPACE CHARGE EFFECTS OF RCS/CSNS

S. Xu, S. Fang, S. Wang,* Institute of High Energy Physics (IHEP), Beijing, 100049, China

Abstract

The China Spallation Neutron Source (CSNS) is an accelerator-based facility. It operates at a 25 Hz repetition rate with an initial design beam power of 100 kW and is upgradeable to 500 kW. The accelerator of CSNS consists of a low energy linac and a Rapid Cycling Synchrotron (RCS). The RCS is a key component of CSNS. In this kind of high intensity RCS, the beam is space charge dominated, and the space charge effects are the main source of beam loss. Many simulation works were done for the study of space charge effects for CSNS/RCS by using the codes ORBIT and SIMPSONS. Various conditions are considered in the simulations, including the effects of different lattice structure, different tunes, the combine effect of sextupole field and space charge, different painting beam distribution, etc. The beam loss and emittance growth are compared for different conditions.

INTRODUCTION

The China Spallation Neutron Source (CSNS) is based on a high power accelerator, which consists of a 80 MeV linac, a 1.6 GeV rapid cycling synchrotron and beam transport lines [1]. The accelerator complex is designed to deliver a beam power of 100 kW at a 25 Hz repetition rate, with an upgrade capability of up to 500 kW by raising the linac output energy and increasing the intensity. The RCS is a key component of CSNS. It accumulates a beam injected at 80 MeV, accelerates the beam to a design energy of 1.6 GeV, and extracts the high energy beam to the target. Due to the high beam density and high repetition rate, the rate of beam loss must be controlled to a very low level. In this kind of high power RCS, especially at the low energy end, the beam is space charge dominated, and the space charge effects are the main source of beam loss. The space charge effects limit the maximum beam density, as well as beam power. Many simulations were done to study space charge effects in CSNS/RCS by using the codes ORBIT and SIMPSONS. Various conditions, which may influence the space charge effects and beam loss, are considered, including the effects of different lattice structure, different tune, the combine effect of sextupole field and space charge, different painting beam distribution, etc. The beam loss and emittance growth are compared for different conditions. The simulation results are the foundation of physics design and the choice of design parameters. To control the uncontrolled beam loss, the transverse and momentum beam collimation systems are designed. With the beam collimation, the uncontrolled beam loss can be compressed to less than 1W/m.

* wangs@ihep.ac.cn

The present lattice of the CSNS/RCS is a triplet based fourfold structure, as shown in Fig. 1. Table 1 shows the main parameters of the lattice.

Table 1: Main Parameters of the Lattice

Circumference (m)	228
Superperiod	4
Number of dipoles	24
Number of long drift	12
Total Length of long drift (m)	75
Betatron tunes (h/v)	4.82/4.80
Chromaticity (h/v)	-4.3/-8.2
Momentum compaction	0.041
RF harmonics	2
RF Freq. (MHz)	1.0241~2.3723
Trans. acceptance (μπm.rad)	540
RF Voltage (kV)	165

SPACE CHARGE EFFECTS DURING INJECTION

Painting Schemes

Two painting schemes—correlated and anti-correlated painting—are both available in the injection of CSNS/RCS. For correlated painting, both the emittance ε_x and ε_y are painted from small to large during injection. It produces a rectangular transverse beam profile without space charge effects. For anti-correlated painting, the emittance is painted from small to large in one direction, and from large to small in the other direction (vertical direction here). It produces an elliptical transverse beam profile without space charge effects. In the case of disregarding space charge effects, the painting beam density is uniform. Figs. 2 and 3 show simulation results of painting with and without space charge effects. The upper left and right graphs show the particles distribution in (x, x') and (y, y') phase space respectively. The lower graphs show the distribution in (x, y) space and the emittance evolution during painting.

OPTIMIZATION ALGORITHMS FOR ACCELERATOR PHYSICS PROBLEMS*

B. Mustapha# and P. N. Ostroumov
Physics Division, Argonne National Laboratory, IL 60439, U.S.A.

Abstract

Optimization tools are needed in every step of an accelerator project, from the design to commissioning to operations. However, different phases have different optimization needs that may require different optimization algorithms. For example, a global optimizer is more appropriate in the design phase to map the whole parameter space whereas a local optimizer with a shorter path to solution is more adequate during operations to find the next best operating point. Different optimization algorithms are being used in accelerator physics, we mention in particular standard algorithms such as least square minimization and evolutionary algorithms such as genetic optimization. Over the years, we have developed several optimization tools for beam tracking codes to include 3D fields and SC effects. Including particle tracking in the optimization process calls for parallel computing. We will review the different algorithms and their implementation and present few highlight applications.

OPTIMIZATIONS IN ACCELERATOR PHYSICS

Optimizations are heavily used in the design phase of an accelerator project, but they are much less used to support the commissioning and operations once the machine is built. During the design phase, optimizations are used in the design of the different beam line elements: magnets, rf cavities, etc. They are also used for the lattice optimization to find the appropriate sequence of elements and drift spaces. Once the lattice is defined more optimizations are used to determine the appropriate element settings for optimal beam dynamics and beam quality. This is often iterated with the lattice design. Once the accelerator is built, more effort is dedicated to hardware problems than to developing a realistic model of the machine. We believe that using the appropriate optimization tools during the commissioning should help better understand the machine's behaviour and expedite the delivery of the first beam. Fits to reproduce the experimental data using a model should significantly improve the predictability of the model to use for real-time machine operations. Often, simplified models (1D, single particle) are used to support daily machine operations [1]. Simple models have the advantage of being fast and able to describe the overall behaviour of the machine while detailed 3D models are slow and still cannot reproduce the details seen in the data [2]. We believe that a significant effort should be dedicated to developing more realistic 3D models before being able to use them to support real-time machine operations. Once such models are fully developed large scale parallel computing could be used for fast turn-around simulations and optimizations.

* This work was supported by the U.S. Department of Energy, Office of Nuclear Physics, under Contract No. DE-AC02-06CH11357.
# Corresponding author: brahim@anl.gov

ELEMENTS OF AN OPTIMIZATION PROBLEM

The first important step is the proper definition of the optimization problem. An optimization problem has one or more objectives which are the important quantities or qualities characteristics of the problem that you would like to optimize. These objectives depend on the parameters of the problem which are the variables affecting the outcome or the solution to the problem. It is usually a good practice to choose the parameters to which the solution is more sensitive. These parameters could be subject to constraints and or correlations which define the limits of the parameter space. The simplest case is where the parameters are independent with lower and upper bounds. If the parameters are correlated, it is usually recommended to reduce them into a set of independent parameters. The last and most important element of an optimization problem is the choice of the appropriate optimization algorithm. Depending on the nature of the problem, the most appropriate algorithm could be a local optimizer, a global one, a standard or an evolutionary.

LOCAL VERSUS GLOBAL OPTIMIZATION ALGORITHMS

It is usually not hard to find a local minimum of an objective function. What is hard is to prove that the minimum found is a good one and it is even harder to prove that a minimum is an absolute or a global one. A local optimizer usually starts with a first guess then finds a direction that minimizes the objective function and moves one step in that direction. The procedure is repeated iteratively until no more progress could be made. A local algorithm is usually fast because it explores the parameter space along a single path defined by the minimization direction adjusted at every step. In contrast, a global optimizer should explore the entire parameter space and eventually find all local minima before finding a global one. It should also prove that the minimum found is a global one which makes it much slower than a local optimizer. Luckily, not all problems or applications require global optimizations. A global optimizer is more appropriate to use in the design phase of an accelerator project to map the whole parameter space and make sure not to miss the best set of design parameters. Such a global optimizer should also find all feasible solutions to

APPLICATION OF MULTIOBJECTIVE GENETIC ALGORITHM IN ACCELERATOR PHYSICS*

L. Yang†, NSLS-II, Upton, NY 11973, USA
D. Robin, F. Sannibale, C. Steier, W. Wan, ALS, Berkeley, CA 94720, USA

Abstract

The optimization of an accelerator system is important in both design and upgrade stage, and many of them are Multiobjective problems, i.e. searching for a balance between several quantities. A full understanding of this balance could provide the decision maker more information on the final choice. In this paper we present the application of an optimization algorithm called Multiobjective Genetic Algorithm (MOGA) in two problems. One is the lattice of a synchrotron light source (take ALS as an example) and the other is a VHF gun.

INTRODUCTION

The optimization of an accelerator system is obviously an important problem in both design and upgrade stage. Depending on different system, storage ring or LINAC, collider or light source, this could be minimizing the emittance, optimizing beta functions and bunch length. For a optimization algorithm, the challenges come from the convergence of solutions, constraints on variables and objective functions, conflicting objective functions. In this paper we will introduce an algorithm called multiobjective genetic algorithm (MOGA), show the applications on two problems, one is the lattice optimization for the Advanced Light Source (ALS), a problem with strong constraints in both variable space and objective space. The other is VHF Gun, in which a single simulation cost a couple of hours, therefore in order to get result in a reasonable amount of time, the convergence speed becomes very important.

GENETIC ALGORITHM AND MULTIOBJECTIVE OPTIMIZATION

Genetic algorithm (GA) is a search technique in optimization, it was developed in 1970s [8, 7, 4] and now as a class of evolutionary algorithms (EA). The outline of Genetic Algorithm (GA) usually has four steps, first a set of numbers in parameter space are chosen, i.e. the initial population, then they are paired to produce new candidate, we call them parents and children. This is called crossover. The third step is mutation, where children are given a random change according to certain strategy. The last step mimics the nature select process, where the objective functions are evaluated for each child, and the children are sorted according to their corresponding objective functions. This is a complete generation, and some good children candidate are allowed to continue the evolution.

In the early development, the multiobjective optimization problems (MOP) was converted to a single objective optimization problem by weighted sum method. Later, the truly multiobjective optimization with nondominated sorting was developed based on GA [5]. The detailed mathematical definition of dominance can be found in ref. [4, 2, 10]. It extends the comparison between two scalars to two vectors.

MOGA has been introduced into photoinjector design [2] and accelerator lattice optimization [6, 10]. The comparison of MOGA and GLASS is also shown in [9].

Algorithm 1 Multi-Objective Genetic Algorithms

```
Initialize population (first generation, random)
repeat
    select parents to generate children (crossover)
    mutation(children)
    evaluate(children)
    merge(parents, children).
    non-dominated sort(rank)
    select half of (parents, children)
until reach a generation with the desired convergence to the PO set
```

The structure of our MOGA implementation is shown in algorithm. 1. The first population is initialized with uniformly distributed random numbers, as we will see in storage ring lattice optimizations, most of these random populations at first did not give physical solutions due to transverse stable condition.

Two parents are chosen from the population, and used to generate two children. The newly generated values follows certain probability density function (PDF) as shown in Fig. 1. Following Ref. [4] we are using polynomial PDF with one parameter η to control the shape. This form is convenient to include the boundaries without artificial cuts when the new values are outside of it.

The "new born" children are applied with an operation of mutation, this mimics the effect from nature environment. We also choose a polynomial PDF to describe it. Fig. 2 shows the probability of the old value $x = -1$ will be mutated to. It has equal probability to go less or greater than -1.

After the new generation is produced, we then evaluate the objective functions, which are the lattice functions in our case. The results are ranked based on their objective functions and the violation to the constraints. Here we also follow Dr. Deb's approach [5], where Nondomi-

* Work supported by the Director, Office of Science, U. S. Department of Energy under Contract No. DE-AC02-05CH11231.

† lyyang@bnl.gov

APPLICATION OF DIRECT METHODS OF OPTIMIZING STORAGE RING DYNAMIC AND MOMENTUM APERTURES

M. Borland †, L. Emery, V. Sajaev, A. Xiao, ANL, Argonne, IL 60439, USA
W. Guo, BNL, Upton, NY, 11973, USA

Abstract

Optimization of dynamic and momentum apertures is one of the most challenging problems in storage ring design. For storage-ring-based x-ray sources, large dynamic aperture is important in obtaining high injection efficiency, which leads to efficient operation and protects components from radiation damage. X-ray sources require large momentum aperture to obtain sufficiently long Touschek lifetimes with low-emittance beams. We have developed effective methods of optimizing dynamic and momentum apertures that rely directly on tracking using a moderately sized Linux cluster. After reviewing the method, we describe examples of its application to APS operations, upgrades, and next-generation storage rings.

INTRODUCTION

One of the most desirable characteristics of storage-ring-based x-ray light sources is low emittance. To achieve this, lattice designers use strong focusing to obtain large horizontal phase advance per cell, leading to large chromatic aberrations and thus strong chromaticity correcting sextupoles in order to obtain adequate momentum aperture (MA). In addition, low emittance means small dispersion, requiring yet stronger chromatic sextupoles. This leads to small dynamic aperture (DA), making it more difficult to accumulate beam. In extreme cases, the dynamic aperture may be so small that sufficient lifetime is not achieved.

Ring designers commonly add extra families of sextupoles to correct the effect of the chromatic sextupoles [1]. The challenge is to adjust the sextupoles to simultaneously maximize both DA and MA. Perhaps the most common approach is to minimize many resonance and tune variation driving terms [2]. However, one must carefully choose the weights for these terms, based on experience and, ultimately, tracking. Further, we commonly want non-zero linear chromaticity to suppress instabilities, which challenges the assumptions of the perturbative approach, since then one does not want the higher-order chromaticities to be minimized, but rather one needs to use them to reduce the chromatic tune spread.

In this paper, we discuss further a tracking-based optimization method [3] that has proven very successful and is a considerable improvement over previous attempts discussed in [4] and, in part, in [3]. Following an explanation of the method, we discuss application to the Advanced Photon Source (APS) storage ring and the NSLS-II ring.

Although our method could use any tracking code, the ability to create fully scripted simulations is essential, since matching and tracking must run without human intervention. Thus, we use the tracking program `elegant` [5, 6], as well as the SDDS Toolkit [7] and `geneticOptimizer` [8].

OPTIMIZATION METHOD

In this method we use many computers simultaneously to evaluate the DA and MA for various lattice tunings (e.g., tunes and sextupole settings). DA and MA computation includes radiation damping, synchrotron oscillations, and physical apertures. After completion of a sufficient number of evaluations, a genetic algorithm is used to "breed" more candidate configurations based on the best configurations seen so far. The process continues until a sufficiently good solution is obtained or until the results stop improving.

Dynamic Aperture

For the DA, we've found that the area of the stable region is a good parameter to use, with some limitations and conditions. We first determine the DA by performing line scans outward from the origin. (Scanning outward is used instead of scanning inward in order to avoid being fooled by stable islands.) Once the stable boundary is found, we analyze the boundary points to clip off any regions that "stick out" in a manner that indicates a poorly behaved boundary. An example is shown in Figure 1: The region that sticks out on the right side is probably related to a stable island and is not considered a useful contribution to the DA. Finally, having found the clipped DA boundary, we compute its area and its contribution to the penalty function. Because the area computation ignores contributions from useless regions, the optimized results are unlikely to display such regions.

The contribution to the penalty function is computed by comparing the area A to the desired area A_d using a weighting factor ΔA

$$P(A) = \begin{cases} (A - A_d)^2/\Delta A^2 & A < A_d \\ 0 & A \geq A_d \end{cases} . \qquad (1)$$

For APS we typically want an aperture $-13\text{mm} \leq x \leq 7\text{mm}$ and $|y| \leq 1.5\text{mm}$, giving $A_d = 30\mu\text{m}^2$.

In some cases, the DA area may be misleading, for example, a solution with large vertical aperture but small hori-

*Work supported by the U.S. Department of Energy, Office of Science, Office of Basic Energy Sciences, under Contract No. DE-AC02-06CH11357.

† borland@aps.anl.gov

RadTrack: A USER-FRIENDLY, MODULAR CODE TO CALCULATE THE EMISSION PROCESSES FROM HIGH-BRIGHTNESS ELECTRON BEAMS*

M. Ruelas, G. Andonian, RadiaBeam Technologies, LLC, Marina Del Rey, CA, USA
S. Reiche, Paul Scherrer Institute, Switzerland

Abstract

One of the most important goals of simulations is to accurately model beam parameters and compare results to those obtained from real laboratory diagnostics. Many codes are specialized to either model beam dynamics or emitted radiation. For meaningful physical results, the output of these codes are stitched together in start-to-end fashion. This procedure, which is often employed by simulation experts, is cumbersome, and has wide room for error in data entry or file parsing. This paper describes the development and deployment of RadTrack: a user-friendly code, with start-to-end support of typical accelerator and radiation codes to accurately model laboratory diagnostics.

INTRODUCTION

The code RadTrack was developed to accurately model observable beam parameters in a real laboratory environment. The code emphasizes modularity to address a comprehensive set of problems and an easily navigable user-interface to attract a wide user base. The graphical user-interface is built on a visualization canvas that easily generates and displays important information. The interface is intuitive for seamless management of start-to-end simulations, which incorporate several codes of varying I/O context. The interface allows for simple parallelization for complex, memory demanding calculations. RadTrack was developed as a code that can calculate beam dynamics and emitted radiation processes in a transparent, intuitive manner accessible to most accelerator scientists and students.

RADTRACK CORE

The code RadTrack was first developed as an extension to the radiation code QUINDI [1] to calculate the radiative effects of bending beam trajectories. The code QUINDI was developed for a specific problem and its results have been benchmarked to experiments at the Brookhaven National Laboratory Accelerator Test Facility [2]. RadTrack builds upon the code in a number of ways, while also incorporating other desirable features.

The RadTrack core code is broken down into a number of modular steps. The particle trajectories are calculated using Q-Tracker, an extension to the code QUINDI. Q-Tracker is a simple particle tracker, with trajectories determined by the Lorentz force law, which outputs the 6-dimensional phase space used by RadTrack. The radiation field solver is a modified version of the existing code QUINDI. The radiation emission is calculated using the Lienerd-Wiechert potentials [3]:

$$\vec{E}\left(r,t\right)=\frac{e}{\sqrt{4\pi\epsilon_0}}\left[\frac{\vec{n}-\vec{\beta}}{\gamma^2\left(1-\vec{\beta}\cdot\vec{n}\right)^3R^2}\right]_{\text{ret}}+\left[\frac{\vec{n}\times\left[\left(\vec{n}-\vec{\beta}\right)\times\dot{\vec{\beta}}\right]}{c\left(1-\vec{\beta}\cdot\vec{n}\right)^3R}\right]_{\text{ret}}$$

where $\vec{n}$ is the unit vector pointing from the radiation point to an observation point and R is the distance to the observation point. The magnetic field is derived from

$$\vec{B}\left(r,t\right)=\left[\vec{n}\times\vec{E}\left(r,t\right)\right]_{\text{ret}}$$

The fields in the above relations are calculated at the retarded time $t'=t+R(t)/c$.

The RadTrack modular approach separates the functions of particle trajectory calculation and radiation field solving. Figure 1 displays the modular philosophy employed by the code where individual functions are separated to allow for in-depth, comprehensive problem analysis. This is advantageous for implementation of the start-to-end function, where multiple outputs of codes are parsed as inputs into subsequent codes. For example, the user may use particle trajectories from other codes, like TREDI [4], in conjunction with the radiation solver QUINDI or the trajectories from Q-Tracker with another radiation code. Efforts

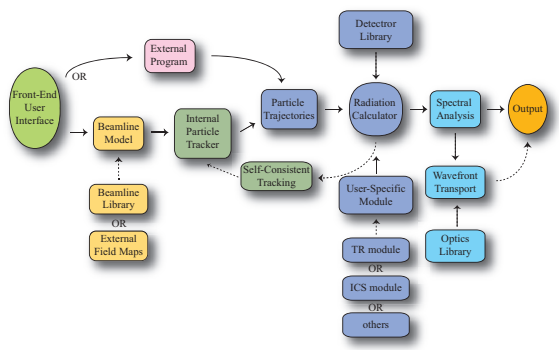

Figure 1: Flow diagram of the RadTrack code design. The ultimate goal is to simulate real laboratory diagnostic observables using the computation tools available to the user (acceleration, radiation, transport, etc.).

* Work supported by DOE Grant No. DE-FG02-08ER85018

TOMOGRAPHIC RECONSTRUCTION OF A BEAM PHASE SPACE FROM LIMITED PROJECTION DATA*

G. Asova†, S. Khodyachykh‡, M. Krasilnikov, F. Stephan, DESY, 15738 Zeuthen, Germany
I. Tsakov, INRNE BAS, Sofia, Bulgaria

Abstract

The production of electron beams suitable for the successful operation of the European XFEL is studied at the Photo-Injector Test Facility at DESY, Zeuthen site (PITZ). The PITZ beamline is equipped with three dedicated stations for transverse emittance measurements and in the forthcoming shutdown period a section for transverse phase-space tomography diagnostics will be installed. The module contains four observation screens and therefore only four projections can be used in order to reconstruct an underlying phase-space density distribution.

This work presents the performance of a number of reconstruction algorithms on limited projection sets using numerical data applied to the PITZ operating conditions. Different concepts for comparison between an original phantom and the reconstructed distribution are presented.

INTRODUCTION

The PITZ facility is dedicated to the development and optimization of electron sources subsequently to be used in FELs like the FLASH and the future European XFEL. Such goals require detailed knowledge of the electron beam properties according to which the PITZ beamline is equipped with extensive diagnostics components. A key element for the performance of a FEL is the small transverse emittance, wherefrom the transverse phase space is a central point in the electron source characterization at PITZ. Currently, the transverse phase space is being reconstructed using single slit scan technique [1] and a new module for transverse phase space tomography diagnostics will be installed in the forthcoming 2009-upgrade.

The module consists of four screen stations as each two surround a FODO cell. Correspondingly, four projections are to be used for tomographic reconstruction. The design has been discussed in [2] and expectations towards its performance with nominal beam parameters of 1 nC bunch charge, 32 MeV/c momentum and normalized transverse emittance of 1 mm mrad can be found in [3]. The setup will also be used in a combination with a transverse deflecting cavity structure to study the longitudinal phase space of individual pulses within the bunch train. In any case the choice of proper reconstruction algorithm is of great importance.

* This work has partially been supported by the European Community, contract No. RII3-CT-2004-506008 and 011935.

† galina.asova@desy.de
‡ Presently at Siemens AG, Rudolstadt, Germany.

This work focuses on the performance of a few reconstruction algorithms with respect to their applicability to limited input projection data. The methods discussed are Filtered Backprojection (FBP), Constrainted Additive Algebraic Reconstruction Technique (caART) and Maximum Entropy (MENT). Several approaches to quantify the quality of the reconstruction conclude the contribution.

TRANSVERSE PHASE-SPACE TOMOGRAPHY OF AN ELECTRON BEAM

Tomography deals with the reconstruction of an n-dimensional object knowing an infinite number of its $(n-1)$-dimensional projections calculated at different view angles in $[0, \pi]$. A great number of scientific and practical areas are using the tomography ideas - medical imaging is interested in innocuous cross sectioning of the human body, archaeology needs non-destructive material inspection.

The object of interest in the transverse beam dynamics is an underlying density distribution $\rho(x, x', y, y')$ at a given position along the beamline. The density distribution cannot be obtained instantly but its spatial components are directly measurable by means of screens, wire scanners, etc. Meeting an observation screen, for instance, the four-dimensional phase space is projected onto a spatial distribution (x, y). A number of projections of the spatial distribution, taken at different angles, are needed for the reconstruction and, therefore, one needs to vary the orientation of the phase space on the screen. The last is equivalent to rotation of the beam in the phase space and is achievable by altering the focusing conditions using magnets. Let the system be linear such that M denotes a valid 2×2 transformation matrix from the position of reconstruction z_i to the position of observation z_f and $p(x_f)$ is a projection onto the horizontal axis at z_f. The condition on the linearity should be interpreted so that the matrices M describe well the transport between the two longitudinal positions. The projection can be written as a function of the initial phase-space coordinates as the Radon transform

$$p(x_f) = \iint \rho(x_i, x_i')\, \delta(x_f - M_{11}x_i - M_{12}x_i')\, dx_i dx_i'. \quad (1)$$

The problem to be solved is, having a number of $p(x_f)$ with different matrices M, to find a unique inversion of the Radon transform. Disregarding any intrinsic measurement errors, the singularity of the solution depends on the number of projections, the equidistant steps between each

PARTICLE-IN-CELL SIMULATION OF ELECTRON-HELIUM PLASMA IN CYCLOTRON GAS STOPPER*

Y.K. Batygin#, G. Bollen, C. Campbell, F. Marti, D.J. Morrissey, G. Pang, S. Schwarz, NSCL, Michigan State University, East Lansing, MI 48824, USA

Abstract

The cyclotron gas stopper is a newly proposed device to stop energetic rare isotope ions from projectile fragmentation reactions in a helium-filled chamber [1, 2]. The radioactive ions are slowed down by collisions with a buffer gas inside a cyclotron-type magnet and are extracted via interactions with a Radio Frequency (RF) field applied to a sequence of concentric electrodes (RF carpet). The present study focuses on a detailed understanding of space charge effects in the ion extraction region. The space charge is generated by the ionized helium gas created by the stopping of the ions and eventually limits the beam rate. Particle-in-cell simulations of a two-component (electron-helium) plasma interacting via Coulomb forces were performed in the space charge field created by the stopping beam.

INTRODUCTION

The cyclotron gas stopper is a device for the deceleration of radioactive ions created by the projectile fragmentation (see Fig. 1). Fast ions (~100 MeV/u) are injected into a helium-filled chamber inside a vertical magnetic field where they immediately enter a solid degrader so that they can be captured by the magnetic field. The fast ions lose the remainder of their kinetic energy in collisions with the helium buffer gas. This process ionizes the helium atoms. An electric field parallel to the magnetic field is used to remove electrons and move positively charged ions to the RF-carpet. At high incoming particle rates, the amount of ionization becomes so large that the stopped ions cannot be completely removed. As a result, a neutralized plasma accumulates in the center of the stopping chamber and additional fast ions are not or are only slowly extracted because they come to rest in the plasma-shielded region. This present work analyzed the overall process of charge migration to provide estimates of ion stopping efficiency as a function of incoming particle rate.

NUMERICAL METHOD

Present simulations are based on a preceding detailed numerical study of rare isotope production, transport, and stopping in a gas-filled magnetic field [1]. The program LISE++ [3] was used to calculate the transmission, yields, and ion-optical properties of the projectile fragment beam. A C++ version of the ATIMA code [4] was used to calculate the energy lost by the incoming beam in the solid degrader. The Stopping and Range Tables from the SRIM package [5] were used to calculate the energy loss in the helium gas. The CycStop code [6] combined this input to calculate the fast ion stopping

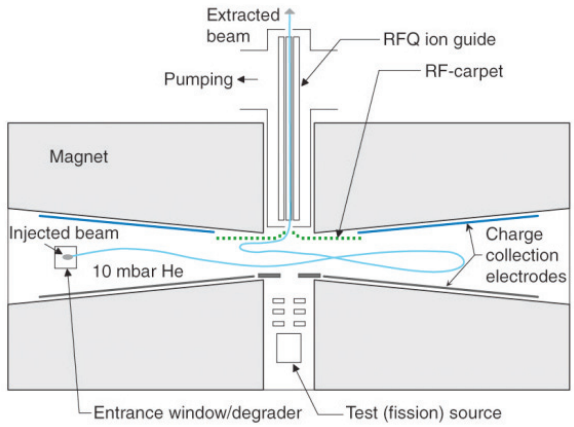

Figure 1: Schematic layout of cyclotron gas stopper [1]. The fast projectile fragments are incident horizontally at the left and after stopping are moved to the center for axial extraction.

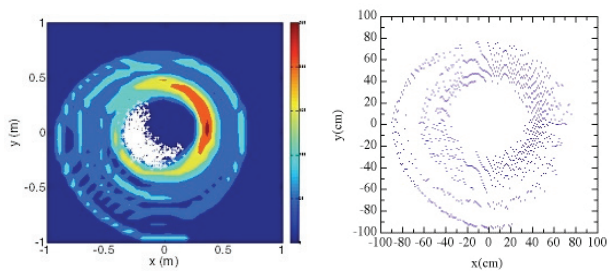

Figure 2: (Left) Top view of the energy loss density in color and the positions of the stopped ions in white, and (right) the distribution of e^-/He^+ ion-pairs created by the stopping of a ^{79}Br beam from the CycStop code [6].

distribution, the losses, and the spatial deposition of energy in the helium. The energy distributions were the input for the space charge phenomena in the present work (see Fig. 2).

The calculation of space charge effects in e^-/He^+ plasma were performed with a modified version of the BEAMPATH code [7]. The simulations were performed by simultaneous tracking of He^+ and electrons in the field created by their own space charge forces, $\vec{E}_{sc}$, and applied external electric field, $\vec{E}_o$, with a velocity $\vec{v}$ given by

$$\vec{v} = k(\vec{E}_o + \vec{E}_{sc}), \quad (1)$$

*Work supported by the US Department of Energy under Contract No DE-FG02-06ER41413
#batygin@nscl.msu.edu

INCORPORATING PARTIAL SIBERIAN SNAKES INTO THE AGS ONLINE MODEL*

V. Schoefer†, L.Ahrens, K.Brown, A. Luccio, W. MacKay, T. Roser
BNL, Upton, NY 11973, USA

Abstract

In order to preserve polarization during polarized proton operation for RHIC, two partial Siberian Snakes are employed in the AGS, where a large number of strong spin depolarizing resonances must be crossed. These snakes cause a significant distortion to the injection lattice of the AGS and must be included in the online model. In this report, we discuss the problem of modeling snakes as optical elements, particularly as MAD-X elements, and present results comparing measurement to the AGS online model.

OVERVIEW

Polarized proton beam in the RHIC complex is created in the OPPIS source and accelerated though a 200 MeV Linac. The beam is then accelerated in the Booster and subsequently injected into the Alternating Gradient Synchrotron (AGS) at a a Gγ = 4.5, and accelerated to a Gγ of 45.5 Here G is the anomalous g-factor magnetic moment of the proton (G = 1.7928) and γ is the relativistic Lorentz factor.

In order to preserve polarization of the beam during acceleration through intrinsic and imperfection depolarizing resonances, the AGS lattice has been outfitted with two partial Siberian snakes. The snakes magnets are helical dipoles which, to provide sufficient spin rotation in the limited physical space available in the AGS lattice, have a "double pitch" structure [1]. That is, the far upstream and downstream regions of each snake are helices of one pitch and the central regions are of different, slower, pitches. One snake is superconducting and the other is normal conducting and they are called the 'cold' and 'warm' snakes respectively.

The central helical field of the cold snake can be run as high as 2.5 T, but it typically operated at 2.1 T. These field strengths correspond to rotations of the proton spin vector of 10 % (or 18 degree) and 15% (or 27 degree), respectively, around the longitudinal axis. The warm snake is operated with a central helical field of 1.53T, which corresponds to a spin rotation of 5% (9 degrees) about the longitudinal axis. Both snakes are run with constant current throughout the AGS acceleration cycle.

Each of the two snakes is strongly focusing in both planes and they represent a significant perturbation to the AGS optics. Both snakes require external magnetic elements to provide matching to the typical AGS lattice and each therefore has four quadrupoles near it used to compensate for perturbations to the linear optics [2].

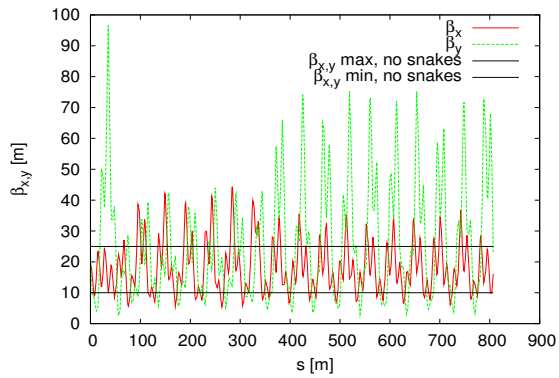

Figure 1: Modeled AGS β functions at injection energy with both snakes included and using operational currents in the compensation quadrupoles. Black lines show the maximum and minimum beta functions in a lattice without snakes. The compensation quadrupole currents that are ultimately determined to be optimal are often far from the modeled fit.

The beam orbit inside the helical dipoles is itself a helix. At injection energy, this helix has a radius of approximately 2 cm and ideally beam is delivered into the snake displaced horizontally by that amount, with no vertical displacement. As the beam rigidity increases, the radius of the helix decreases like γ^{-1}.

The cold snake also has a significant off-axis longitudinal magnetic field component. A 1 meter long superconducting solenoid has been included in the design of the snake to compensate for that effect. However, since the beam's offset from the central axis is a function of energy and the solenoid can only be operated DC, the coupling contribution from the cold snake's longitudinal field can only be completely cancelled at a single beam rigidity.

Accurate modeling of the snakes is critical to polarized proton operation because avoidance of intrinsic and imperfection depolarizing resonances simultaneous requires tight control of the vertical closed orbit and a vertical betatron tune near an integer value (9 in the case of the AGS). This is a region of configuration space that tends to be both physically and numerically sensitive.

* Work performed under Contract Number DE-AC02-98CH10886 with the auspices of the US Department of Energy
† schoefer@bnl.gov

A FAST POINT TO POINT INTERACTION MODEL FOR CHARGED PARTICLE BUNCHES BY MEANS OF NONEQUISPACED FAST FOURIER TRANSFORM (NFFT)

T. Flisgen*, G. Pöplau, U. van Rienen, Rostock University, 18059 Rostock, Germany

Abstract

Demanding applications such as heavy ion fusion, high energy colliders and free electron lasers require the study of beam phenomena like space-charge induced instabilities, emittance growth and halo formation. Numerical simulations for instance with GPT (General Particle Tracer, Pulsar Physics) calculate the mutual Coulomb interactions of the tracked particles [5]. The direct summation of the forces is rather costly and scales with $\mathcal{O}(N^2)$. In this paper we investigate a new approach for the efficient calculation of particle-particle interactions: the fast summation by Nonequispaced Fast Fourier Transform (NFFT) [3, 4], whereas the NFFT is a generalization of the well known Fast Fourier Transformation (FFT). We describe the algorithm and discuss the performance and accuracy of this method for several particle distributions.

INTRODUCTION

The design of particle accelerators requires a sophisticated understanding of the dynamic behaviour of the particle bunch. Therefore several algorithms have been developed to determine the trajectories of the particles in the six-dimensional phase space.

Assuming the energy spread of the charged particles to be small, the space-charge forces may be computed in the bunch's rest frame by superposing the electrostatic field of each particle. The electric field at the position of the j-th particle $\boldsymbol{r}_j \in \mathbb{R}^3$ in the rest frame is given by

$$\boldsymbol{E}(\boldsymbol{r}_j) = \frac{1}{4\pi\varepsilon_0} \sum_{\substack{\ell=1 \\ j\neq\ell}}^{N} q_\ell \frac{\boldsymbol{r}_j - \boldsymbol{r}_\ell}{\|\boldsymbol{r}_j - \boldsymbol{r}_\ell\|^3}, \quad j = 1, \ldots, N, \quad (1)$$

where N denotes the number of particles, q_ℓ the charge of the ℓ-th particle, ε_0 the permittivity of vacuum and $\|\cdot\|$ the Euclidean norm. Since $(N-1)$ interactions have to be taken into account for each of the N particles, the direct evaluation of the sum in Eq. (1) reaches a disadvantageous numerical complexity of $\mathcal{O}(N^2)$. Note that the evaluation of the electric field strength has to be performed in each discrete time step of the tracking to determine the forces acting on the particles.

FAST SUMMATION USING THE NFFT

The presented method calculates the electric fields of the bunch approximately using the Nonequispaced Fast Fourier Transform [3, 4]. The algorithm overcomes the quadratic runtime behaviour of the direct field evaluation and scales with $\mathcal{O}(N \log N)$.

Splitting of Potential Function

To describe the NFFT-based fast field calculation, the potential of a charged particle is separated into a short-range and a long-range effect:

$$\phi(\boldsymbol{r}) = \frac{1}{4\pi\varepsilon_0}\frac{q}{r} = \phi_{sr}(\boldsymbol{r}) + \phi_{lr}(\boldsymbol{r}). \quad (2)$$

Note that $\boldsymbol{r} \in \mathbb{R}^3$ denotes the point in the space, where the potential is evaluated and $r = \|\boldsymbol{r}\| \in \mathbb{R}_{\geq 0}$ the distance between the charged particle (here located at the origin) and the point of field estimation.

We demand the short-range effect $\phi_{sr}(\boldsymbol{r})$ to have compact support, such that $\phi_{sr}(\boldsymbol{r}) = 0 \ \forall \ r \geq \varepsilon_I$ and the long-range effect $\phi_{lr}(\boldsymbol{r})$ to be bounded and $(p-1)$ times differentiable. The variable ε_I denotes the near field radius.

To cope with the singularity at $r = 0$ and to ensure the smoothness of the long-range effect, we regularize the potential at $r = \varepsilon_I$ using an ansatz function (see the dashed, the crossed and the dotted curves in Fig. 1).

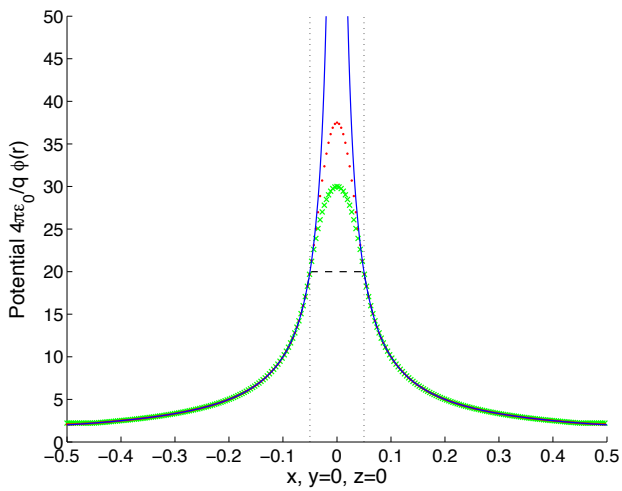

Figure 1: Potential $\phi(\boldsymbol{r})$ (solid) and long-range effect $\phi_{lr}(\boldsymbol{r})$ with $p = 1$ (dashed), $p = 2$ (crossed), $p = 3$ (dotted), where $\varepsilon_I = 1/20$ and $\boldsymbol{r} = (x\ 0\ 0)^T$.

Notice that the potential function is regularized at the boundary $r = l_B = 9/20$ as well to obtain a periodic smooth long-range contribution $\phi_{lr}(\boldsymbol{r})$. The deviation be-

* thomas.flisgen@uni-rostock.de

TRIUMF-VECC ELECTRON LINAC BEAM DYNAMICS OPTIMIZATION

Y. Chao, F. Ames, R. Baartman, I. Bylinskii, S. Dechoudhury, G. Goh, S.R. Koscielniak, R.E. Laxdal, M. Marchetto, L. Merminga, V. Naik, V.A. Verzilov, F. Yan, V. Zvyagintsev
TRIUMF, 4004 Wesbrook Mall, Vancouver, BC, Canada, V6T 2A3

Abstract

The TRIUMF-VECC Electron Linac is a device for gamma-ray induced fission of actinide targets, with applications in nuclear physics and material science. A phased construction and commissioning scheme will eventually lead to a 50 MeV, 10 mA CW linac based on superconducting RF technology. Using this linac to deliver high intensity electron beams for applications such as an energy-recovered light source is a possibility integrated in the design study. The multitude of design and tuning parameters, diverse objectives and constraints require a comprehensive and efficient optimization scheme. For this purpose we adopted the genetic optimization program developed at Cornell University as a prototype. Feature extensions were developed to accommodate specifics of the Electron Linac design, provide framework for more generic and integrated design process, and perform robustness/acceptance analyses. In this report we will discuss the method and its application to the design optimization of the Electron Linac. [4].

OVERVIEW

TRIUMF and VECC of Kolkata, India are signing an MOU to jointly develop Injector Cryo-Modules for an electron linac (E Linac) for radioactive ion beam (RIB) production via photo-fission of ^{238}U. This provides a source of neutron-rich isotopes complementary in character to those produced by proton beams.

The E Linac accelerates 10 mA CW e^- beam (16 pC/bunch) to 50 MeV with 1.3 GHz superconducting RF cavities housed in three cryo-modules. The beam is generated at a 100 keV grid-modulated thermionic gun with a 650 MHz pulse structure. A normal conducting buncher and two 1.3 GHz SRF single cell cavities provide graduated bunching and longitudinal matching into the main accelerating structure. Transverse focusing is provided by solenoids or quadrupoles.

Table 1: Beam parameters for the E Linac

RIB 16 pC per bunch	**100 keV**	**10 MeV**
RMS ε_N transverse (μm)	7.5	12.5
Bunch length (cm)	2.8 (±20°*)	0.6
Energy spread	±1 keV	±40 keV
High brightness 100 pC per bunch	**200 -300 keV**	**50 MeV**
RMS ε_N transverse (μm)	1.0	10.0
Bunch length (mm)	4.0	1.0
Energy spread	±0.5 keV	±50 keV

Coupled to a high brightness photo injector, the E Linac can potentially be used in applications beyond RIB production, such as an X-ray source through Compton scattering. It is therefore interesting and relevant to investigate if, and how, the same configuration can deliver both the 16-pC/bunch RIB beam and a 100-

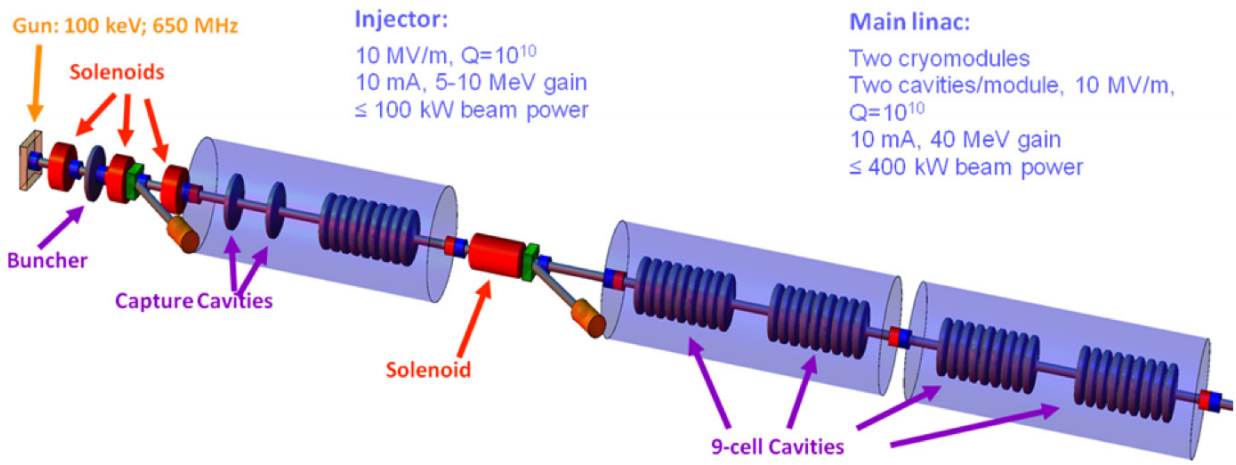

Figure 1: Schematic of the TRIUMF E Linac.

* TRIUMF receives funding via a contribution agreement through the National Research Council of Canada. This work is supported in part by funding from VECC, Kolkata, India.

DESIGN OF 10 GEV LASER WAKEFIELD ACCELERATOR STAGES WITH SHAPED LASER MODES *

E. Cormier-Michel, E. Esarey, C.G.R. Geddes, C.B. Schroeder, W.P. Leemans,
Lawrence Berkeley National Laboratory, Berkeley CA, 94720, USA
D.L. Bruhwiler, B. Cowan, K. Paul,
Tech-X Corporation, Boulder CO, 80303, USA

Abstract

We present particle-in-cell simulations, using the VORPAL framework, of 10 GeV laser plasma wakefield accelerator stages. Scaling of the physical parameters with the plasma density allows us to perform these simulations at reasonable cost and to design high performance stages. In particular we show that, by choosing to operate in the quasi-linear regime, we can use higher order laser modes to tailor the focusing forces. This makes it possible to increase the matched electron beam radius and hence the total charge in the bunch while preserving the low bunch emittance required for applications.

INTRODUCTION

Laser driven wakefield accelerators (LWFAs) are able to produce accelerating gradients thousands of times higher than conventional accelerators, making them suitable to build compact devices. In a LWFA the radiation pressure of the laser pulse induces charge separation, producing a plasma wave (wake) traveling at the group velocity of the laser pulse, close to the speed of light, and hence able to accelerate particles to relativistic velocities (see [1] for a complete review). Energies up to a GeV have been obtained in only a few centimeters [2]. Recently, experiments have shown that it is possible to control the injection and the acceleration of electrons [3, 4], providing a path towards high quality electron beams that can be used for applications, including free electron lasers [5], gamma ray sources [6] and colliders for high energy physics [7]. Light sources need stable electron bunches of the order of a GeV. A multi-TeV collider was designed using staging of several 10 GeV LWFA accelerator modules at a density of $n_0 \sim 10^{17}$ cm^{-3}, each about a meter long [7]. Efficient transfer of the laser energy to the accelerated beam, acceleration of positrons and conservation of a low emittance must be considered for applications. In this paper we present the design of these stages using Particle-In-Cell (PIC) simulations with the VORPAL framework [8]. We show that by using higher order laser modes, in the quasi-linear regime, the focusing forces in the wake can be controlled in order to improve the stage efficiency.

* The author acknowledge the assistance of the VORPAL development team. Work supported by the U.S. Department of Energy, HEP Contract No. DE-AC02-05CH11231, and the COMPASS SciDAC project, and by NA-22, and used computational facilities at NERSC.

RESULTS

The PIC method is a fully self-consistent algorithm which allows non-linear evolution of the plasma wake and of the laser pulse simultaneously. In PIC simulations the smallest dimension, i.e., the laser wavelength ($\lambda \sim 1$ μm), needs to be resolved, whereas the box size increases with the plasma wave wavelength $\lambda_p = (\pi c^2 m/e^2 n_0)^{1/2}$, where n_0 is the plasma density. The acceleration length also increases with higher energy stages, i.e., lower plasma densities, making the simulations more computationally intensive. Simulations of a 1 GeV stage, to model the recent experiments or gamma ray sources, with a density of $n_0 \sim 10^{18}$ cm^{-3}, require of the order of 10^6 processor-hours and $\sim$ TB of storage. This allows only a few runs in three dimensions (3D), and parameter scans for stage optimization can be done in two dimensions (2D) only. Because the size of the box in 3D and the simulation length each scale as $n_0^{-3/2}$, a 10 GeV stage at $n_0 = 10^{17}$ cm^{-3} would require 10^9 processor-hours which is not yet achievable with today's computational facilities. Approximations are then necessary to simulate such stages at the nominal density and reduced models, such as envelope and quasistatic models [9, 10] or calculation in a Lorentz boosted frame [11, 12, 13], can be used.

The approach used here to design high energy modules is to simulate shorter, higher density stages with scaling of the physical parameters with the plasma density [14]. In the scaled simulations the dimensionless parameters $k_p L$, $k_p r_0$ and a_0, where $k_p = 2\pi/\lambda_p$ is the plasma wave number, L and r_0 are the laser length and spot size respectively, and $a_0 = 7.2 \times 10^{-19} \lambda^2[\mu\mathrm{m}] I[\mathrm{W/cm^2}]$ is the normalized laser intensity, are kept constants. PIC simulations in the quasi-linear regime ($a_0 \simeq 1$) at different densities and comparison with a quasi-static code in 2D cylindrical geometry at $n_0 = 10^{17}$ cm^{-3} show that the wake structure stays constant under these conditions [15]. Simulations also show that laser evolution, self-focusing and depletion, and electron beam dephasing scale as predicted by the linear theory, even though this theory is strictly valid in the low intensity limit ($a_0 \ll 1$), thus allowing scaled design of multi-GeV stages. Reduction of wake amplitude due to the presence of a charged beam (beam loading) also scales predictably for a wide range of parameters, allowing prediction of beam charge in unscaled stages [14]. Fig. 1(a) shows the accelerating wake structure at $n_0 = 10^{18}$ cm^{-3}

MULTIPOLE EFFECTS IN THE RF GUN FOR THE PSI INJECTOR

M. Dehler, Paul Scherrer Institut, Switzerland

Abstract

For the 250 MeV test injector at PSI, it is planned to use a 2.6 cell RF gun originally developed for high charge operation in the CLIC test facility CTF-2. First start-to-end simulations assuming perfect field symmetries show, that this gun should be able to generate bunches at 200 pC with an emittance of below 400 nm rad, which would be compatible with the requirements for the SwissFEL. This gun uses double side coupled RF feeds in the last cell as well a asymmetrical tuners in the last two cells, which lead to transverse multipole effects in the field and phase space distribution and may lead to a deteriorated emittance. Since the beam in the last cells is already relativistic at energies between 4 and 6.4 MeV, this effect can be computed in a clean way by looking at the distributions of the integrated beam voltage at the cavity iris and deriving any transverse kicks via the Panovsky-Wenzel theorem. Doing this approach for the various operation modes planned for the SwissFEL shows an emittance dilution well below critical thresholds.

INTRODUCTION

Within the framework of the SwissFEL project at PSI, a 250 MeV test injector facility (see fig. 1 on the next page) is under construction, which will be used to develop test techniques to create and transport high brilliance electron beams suitable for short wave length free electron lasers.

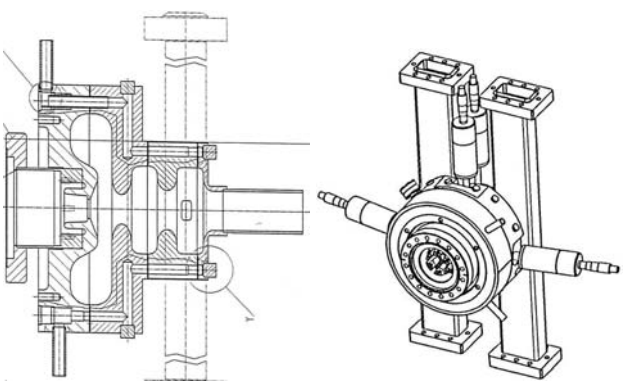

Figure 2: Geometry of the RF gun

Initially it will operate as a stand-alone machine. It must produce the ultra-high brightness electron beam and permit an objective assesment of the technological risks, which are associated with the construction of a low-energy XFEL user facilty. Later it is intended to use it as the injector for the main linac of the future SwissFEL free electron laser facility.

Table 1: Baseline operation modes of the SwissFEL

	High	Small
Bunch charge Q (pC)	200	10
Laserspot σ_r (μm)	270	100
Pulse length FWHM (ps)	9.9	3.7
Acc. gradient (MV/m)	100	100
$\epsilon_{N,slice}$ @ 150 MeV (nm rad)	320	80
$\epsilon_{N,proj}$ @ 150 MeV (nm rad)	330	96

For the electron source itself, two options are forseen. The first uses a pulsed DC gun in combination with a two-frequency cavity; the high initial gradient in the gun is supposed to give a high brilliance beam at a reduced current of 5.5 Amperes, which is compressed ballistically by the subsequent two-frequency RF cavity in combination with a drift to approximately 20 A[1]. The alternative consists in using a more convential S-band RF gun running at 100 MV/m and to generate this 20 A beam current directly at the exit of the gun[2]. Recent results from LCLS[3] make this option look rather promising.

For first tests, it is planned to use a 2.6 cell gun originally developed for high current operation in the CLIC test facility CTF-2. The general geometry of this gun[4] is shown in fig. 2. The specialty compared to other design is the large diameter first half cell, where the TM_{02} resonance is used for the main accelerating mode. The original reason for this choice is, that this resonance is particularly well suited for the operation with extremely high beam charges and currents. For the operation at the modest currents of the SwissFEL (Tab. 1), this feature has no influence.

The structure is rotationally symmetric, with perturbations introduced by tuners, field sensors and the holes of the power couplers. These introduce field asymmetries in the monopole type accelerating mode, the main effect of these being transverse kicks on the beam. Small dipole and quadrupole corrector magnets after the gun can easily compensate the integral average kick over the bunch length. What remains, is the transient, time varying part, which leads to emittance growth. More recent designs[5] avoid these problems by obviating the need for tuners all together through more precise manufacturing and by compensating the field perturbation coming from the power coupler with a more complicated race track geometry of the cells.

AN APPLICATION OF DIFFERENTIAL ALGEBRAIC METHODS AND LIOUVILLE'S THEOREM: UNIFORMIZATION OF GAUSSIAN BEAMS

Bela Erdelyi[†‡] and Shashikant Manikonda[‡]
[†]Department of Physics, Northern Illinois University, DeKalb, IL 60115
[‡]Physics Division, Argonne National Laboratory, Argonne, IL 60439

Abstract

Most charged particle beams under realistic conditions have Gaussian density distributions in phase space, or can be easily made so. However, for several practical applications beams with uniform distributions in physical space are advantageous or even required. Liouville's theorem and the symplectic nature of beam's dynamic evolution pose constraints on the feasible transformational properties of these density distribution functions. Differential Algebraic methods offer an elegant way to investigate the underlying freedom involving these beam manipulations. Here, we explore the theory, necessary and sufficient conditions, and practicality of the uniformization of Gaussian beams from a rather generic point of view.

INTRODUCTION

Several practical applications such as irradiation of targets for isotope production, uniform irradiation of detectors for improved efficiency, irradiation of biological samples and materials for testing require manipulation of beam density distributions. Typically, these applications require uniform spatial distributions at the target location. However, most beams delivered by accelerators to these targets are Gaussian. There are several approaches for uniformization of Gaussian beams. One such method, the so-called nonlinear focusing method, uses higher order multipoles to provide a material-less, elegant, purely optical solution. Prior work done in this direction, using nonlinear focusing methods, can be found in [**?**] and references therein. In this paper we present a new approach based on differential algebraic (DA) techniques to investigate the underlying freedom involving these beam manipulations.

Background

Detailed understanding of the beam dynamics requires the study of the motion of the reference particle as well as the motion of the particle in the relative coordinates. The position and momenta are usually sufficient to describe the motion. Usually the arclength s along the reference orbit is used as the independent variable. At each point on the reference orbit it is possible to define an unique orthogonal coordinate system, denoted by $(\hat{e}_x, \hat{e}_y, \hat{e}_s)$, satisfying a certain set of conditions [**?**, **?**]. In this coordinate system the motion of the particles in the beam can be described using relative coordinates, which are given by

$$\vec{z}(s) = \begin{pmatrix} x, a = \frac{p_x}{p_0}, y, b = \frac{p_y}{p_0}, \\ l = k(t - t_0), \delta = \frac{(E - E_0)}{E_0} \end{pmatrix}$$

where the position (x, y) describe the position of the particle in the local coordinate system, p_0 is a fixed momentum and E_0 and t_0 are the energy and the time of flight of the reference particle, a and b are the momentum slopes, E is the total energy, and k has a dimension of velocity which makes l a length like coordinate. The point $\vec{z} = 0$ corresponds to the reference particle.

Let position s_i, s_f be the initial and final position on the reference orbit. The transfer map or transfer function $\mathcal{M}$ relates initial conditions at s_i to the conditions at s_f via

$$\vec{z}(s_f) = \mathcal{M}(s_i, s_f)(\vec{z}(s_i)). \quad (1)$$

For weakly non-linear systems, like an accelerator system, the map can be expanded as a Taylor series. Implementation of such a map on a computer would require the map to be truncated at a certain order. A detailed discussion of the properties and use of the Taylor transfer maps can be found in [**?**].

Beam Phase Space Density Function

Beam production mechanism usually determines the phase space density function describing the distribution of particles in the beam. Let function $f(\vec{z}_i)$ be the initial phase space density function of the beam. According to Liouville's theorem, as long as the sytem can be considered a Hamiltonian system, the phase space distribution of the beam will stay constant along the trajectories. It also implies that the the volume of phase space occupied by the beam is conserved. Hence, it can be written that

$$f(\vec{z}_i) = g(\vec{z}_f), \quad (2)$$

where g is the final phase space density function at any point s_f along the reference orbit. In terms of the transfer map of the system (1), (2) becomes

$$g(x_f, a_f, y_f, b_f, \delta_f) = f \circ \mathcal{M}(s_i, s_f)^{-1}(x_f, a_f, y_f, b_f, \delta_f) \quad (3)$$

where $(x_f, a_f, y_f, b_f, \delta_f)$ are the initial and final phase space coordinates. The function $g(x_f, a_f, y_f, b_f, \delta_f)$ is the new phase space density function, $\mathcal{M}(s_i, s_f)$ is the transfer map of the system. For most practical application the

COSY EXTENSIONS FOR BEAM-MATERIAL INTERACTIONS*

L. Bandura#, NSCL, Michigan State University, East Lansing, MI 48824
B. Erdelyi, Northern Illinois University, DeKalb, IL 60115. and ANL, Argonne, IL 60439

Abstract

While COSY INFINITY provides powerful DA methods for the simulation of fragment separator beam dynamics, the master version of COSY does not currently take into account beam-material interactions. These interactions are key for accurately simulating the dynamics from heavy ion fragmentation and fission. In order to model the interaction with materials such as the target or absorber, much code development was needed. There were four auxiliary codes implemented in COSY for the simulation of beam-material interactions. These include EPAX for returning the cross sections of isotopes produced by fragmentation and MCNPX for the cross sections of isotopes produced by the fission and fragmentation of a ^{238}U beam. ATIMA is implemented to calculate energy loss and energy and angular straggling. GLOBAL returns the charge state. The extended version can be run in map mode or hybrid map-Monte Carlo mode, providing an integrated beam dynamics-nuclear processes design optimization and simulation framework that is efficient and accurate. The code, its applications, and plans for large-scale computational runs for optimization of separation purity of rare isotopes at FRIB will be presented.

INTRODUCTION

The next generation of nuclear physics research will require advanced exotic beam facilities based on heavy ion driver accelerators. There are many next-generation facilities that are currently under commissioning, construction, or envisioned [1-5]. Included amongst these is the future Facility for Rare Isotope Beams (FRIB) at the National Superconducting Cyclotron Lab at Michigan State University. These facilities are capable of producing exotic beams composed of rare nuclei in large quantities. The exotic isotopes are produced via projectile fragmentation and fission in targets. High-performance fragment separators, a key component of all rare isotope facilities, consist of superconducting magnets that are used for the capture, selection, and transport of rare isotopes. Large aperture magnets are necessary in order to accept rare isotope beams with large emittances resulting from their production mechanism.

The beam optics code COSY INFINITY uses powerful differential algebraic (DA) techniques for computing the dynamics of the beam in the fragment separator through high order transfer maps [6]. However, until now it has lacked the ability to calculate the beam-material interactions occurring in the target and energy absorbers. Here, a hybrid map-Monte Carlo code has been developed and integrated into COSY in order to calculate these interactions. The code tracks the fragmentation and fission of the beam in target and absorber material while computing energy loss and energy and angular straggling as well as charge state evolution. This is accomplished by implementing auxiliary codes such as ATIMA [7] and GLOBAL [8]. EPAX [9] is utilized to return cross sections of fragmentation products. The special case of fission has been treated by using the code MCNPX [10] to accurately predict the cross sections and dynamics of exotic beams produced by a ^{238}U beam incident on a Li or C target. The extensions to the code have made it possible to simultaneously compute high order optics and beam-material interactions in one cohesive framework.

The hybrid map-Monte Carlo code can be used to calculate important quantities that describe the performance of the fragment separator. These include the transmission and the separation purity. In a map-only approach, calculations such as these are not possible. Experimental planning and optimization is possible with the map-Monte Carlo code, as various fragment separator settings can be readily adjusted. Here we present a description of the code and how it is implemented in COSY.

DESCRIPTION OF HYBRID MAP-MONTE CARLO CODE

While COSY INFINITY possesses a powerful DA framework for accurate simulation of beam dynamics in electromagnetic fields, the master version does not allow for the simulation of beam-material interactions. This ability is necessary, however, in order to model the dynamics of fission and fragmentation products. In order to track heavy ions through target and absorber material, much code development to COSY was needed.

New additions made to the code include the implementation of auxiliary codes to determine how many of each type of isotope are produced from the fragmentation and fission of an energetic heavy ion beam.of a given nuclear mass A and nuclear charge Z incident on a specified target of a given thickness. Also, the dynamics of these new particles need to be determined. It is necessary to model the cross sections and dynamics of fragmentation and fission separately due to the auxiliary codes available.

Fragmentation Cross Sections

In the case of any primary beam that has nuclear charge Z<92, the secondary particles of interest are fragmentation products. The cross sections of these

*This work was supported by the U.S. Department of Energy, Office of Nuclear Physics, under Contract No. DE-AC02-06CH11357
#bandura@anl.gov

OPTIMIZING SRF GUN CAVITY PROFILES IN A GENETIC ALGORITHM FRAMEWORK*

A.S. Hofler#, P. Evtushenko, F. Marhauser, Thomas Jefferson National Accelerator Facility, Newport News, VA 23606, U.S.A.

Abstract

Automation of DC photoinjector designs using a genetic algorithm (GA) based optimization is an accepted practice in accelerator physics. Allowing the gun cavity field profile shape to be varied can extend the utility of this optimization methodology to superconducting and normal conducting radio frequency (SRF/RF) gun based injectors. Finding optimal field and cavity geometry configurations can provide guidance for cavity design choices and verify existing designs. We have considered two approaches for varying the electric field profile. The first is to determine the optimal field profile shape that should be used independent of the cavity geometry, and the other is to vary the geometry of the gun cavity structure to produce an optimal field profile. The first method can provide a theoretical optimal and can illuminate where possible gains can be made in field shaping. The second method can produce more realistically achievable designs that can be compared to existing designs. In this paper, we discuss the design and implementation for these two methods for generating field profiles for SRF/RF guns in a GA based injector optimization scheme and provide preliminary results.

OPTIMIZATION SYSTEM OVERVIEW

Alternative Platform and Programming Language Independent Interface for Search Algorithms (APISA) [1] builds on the Platform and Programming Language Independent Interface for Search Algorithms (PISA) [2] system. PISA provides a modular way to combine GAs and problems. It uses two communicating state machines to separate the GA implementation from the problem model evaluation. It is easy to apply different GAs to a given problem because the state machine structures are well defined and the files used to communicate between the two state machines are standardized. Changing the GA only requires running the optimization scheme with a different GA state machine; the problem model is unchanged. APISA takes advantage of this compartmentalization and provides problem model evaluations customized for accelerator physics. APISA uses A Space Charge Tracking Algorithm (ASTRA) [3] or General Particle Tracer (GPT) [4] to simulate particle dynamics making it a suitable tool for injector design optimization. The version of APISA described in this paper relies on ASTRA for the beam dynamics simulations.

*Authored by JSA, LLC under U.S. DOE Contract DE-AC05-06OR23177. The U.S. Govt. retains a non-exclusive, paid-up, irrevocable, world-wide license to publish or reproduce this for U.S. Govt. purposes.

#hofler@jlab.org

FIELD MORPHING

The original version of APISA assumes that the field descriptions provided for the magnets and rf accelerating components are fixed and that the optimization can vary the amplitude and/or phase of these elements. This version of APISA, which is geared toward designing SRF/RF gun based injectors, allows the functional form of the on-axis field description of the gun to be varied.

Under the assumption that the desired field pattern resembles a π mode, the software uses a sine wave as the fundamental form for the field description. A truncated Fourier series,

$$f(z) = 1 + \sum_{n=1}^{15} a_n \cos\left(2\pi n \frac{z}{L_{\text{cavity}}}\right) + \sum_{n=1}^{15} b_n \sin\left(2\pi n \frac{z}{L_{\text{cavity}}}\right)$$

where L_{cavity} is the length of the cavity, is then applied to the fundamental form to produce the field description used in the beam dynamics simulation. Each coefficient of the series can be designated as a variable controlled by the optimization scheme or fixed to a specified value. The default value for all coefficients is zero. Other variables that can be fixed or varied are the frequency of the underlying sine function and the number of cells the underlying sine function should represent. The fractional part of the number of cells is interpreted as a gun cell, that incorporates the beam emitting cathode and generally precedes the full cells. The number of cells and the sine frequency are used to calculate L_{cavity} and the free space wavelength of the cavity.

The system computes characteristics of the generated field profile and the morphing function, $f(z)$, and these characteristics can be used as constraints or objectives in the optimization. For example, to preserve the nodes that occur between cells in a π mode, the minimum of $f(z)$ must be positive; otherwise, additional unwanted zero crossings are introduced in the generated field profile. Because $f(z)$ can change the frequency of the generated field, the system determines the resonance frequency from a Fourier transform of the field profile. The frequency can be used as a constraint and an objective to guide and restrict the frequencies of the fields produced.

Preliminary results for a PITZ-like 1.5 cell RF gun operating at 40 MV/m followed by an emittance compensation solenoid [5] indicate that the field amplitude in the half cell should be much larger than in the full cell. These results are obtained using 128 nodes of a Jefferson Lab cluster computer. Each case represents

COMPUTATIONAL MODELS FOR MICRO CHANNEL PLATE SIMULATIONS*

V. Ivanov, Muons, Inc. 522 N. Batavia Ave., Batavia, IL 60510, U.S.A#.

Abstract

Many measurements in particle and accelerator physics are limited by the time resolution with which individual particles can be detected. This includes particle identification via time-of-flight in major experiments like CDF at Fermilab and Atlas and CMS at the LHC, as well as the measurement of longitudinal variables in accelerator physics experiments. Large-scale systems, such as neutrino detectors, could be significantly improved by inexpensive, large-area photo-detectors with resolutions of a few millimetres in space and a few picoseconds in time. The invention of a new method of making micro-channel plates (MCP) promises to yield better resolution and be considerably less expensive than current techniques.

INTRODUCTION

One of the first full numerical models for MCP simulations was suggested by A.J. Guest [1]. Further improvements of this model were done by Y. Kulikov [2] in simulation of spatial resolution for light amplifiers of static images. Here, two different numerical models for short-pulse MCP simulations are suggested [3]. The semi-analytical approach is a powerful tool for the design of static image amplifiers (night vision devices, electron optical converters, streak cameras etc.). Monte Carlo simulations can be successfully used for large area photo detectors with micron and pico-second resolution range. Both approaches have been implemented in the computer codes MCPS [4] and MCS (Monte Carlo Simulator). The results of computer modelling for electric fields and MCP parameters are presented.

ELECTRIC FIELD DISTRIBUTION FOR TILTED CYLINDRICAL CHANNELS IN A DIELECTRIC MEDIUM

The chevron pair is a typical MCP configuration which can prevent ion feedback and increase the efficiency of the first strike problem. It consists of two glass plates with tilted cylindrical pores with a different orientation for each plate. The side surfaces of the plates are metalized, and the voltage V applied to them. The internal surfaces of the pores are coated with a resistive layer and secondary emitter material. Typical dimensions are: plate thickness – 0.5 mm, pore diameter 5-10 um, coatings – 10 nm, tilt angle - 8˚. The field distribution in the pore has a complex structure comparised with straight channels, where the electric field vector is parallel to the z-axis, and the field is a 1D one. This tilted field can change the gain factor of secondary emission in the pore. One can show that the field for the most internal part of the pore can be described analytically, but the fringe fields should be evaluated numerically.

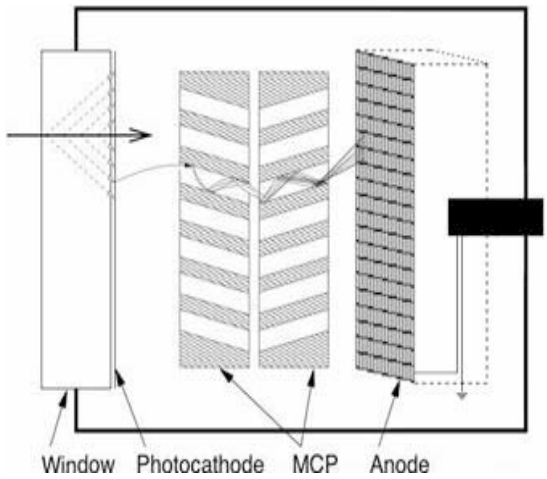

Figure 1: Chevron type MCP.

Problem 1

The potential distribution and electric field for a straight cylindrical pore in a uniform external field (Figure 1) are given by formulae

$$\varphi(\rho,\theta)=\begin{cases}-\dfrac{2\varepsilon_1}{\varepsilon_1+\varepsilon_2}E\rho\cos\theta, & \rho<R,\\ -Ex-E\dfrac{\varepsilon_1+\varepsilon_2}{\varepsilon_1+\varepsilon_2}\dfrac{R^2}{\rho}\cos\theta, & \rho>R.\end{cases} \quad (1)$$

$$E(\rho,\theta)=\begin{cases}\dfrac{2\varepsilon_1}{\varepsilon_1+\varepsilon_2}E\cos\theta, & \rho<R,\\ E-E\dfrac{\varepsilon_1+\varepsilon_2}{\varepsilon_1+\varepsilon_2}\dfrac{R^2}{\rho^2}\cos\theta, & \rho>R.\end{cases} \quad (2)$$

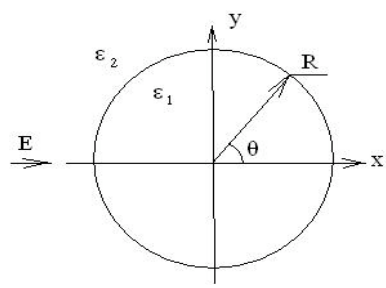

Figure 2: Cylindrical channel of radius R with dielectric constant ε_1 is in the medium ε_2 in an external electric field of strength E.

*Work supported by DoE grant #2005170.
#ivanov@muonsinc.com

RECENT IMPROVEMENT OF TRACKING CODE BBSIMC

H. J. Kim and T. Sen, Fermi National Accelerator Laboratory, Batavia, Illinois 60510, USA

Abstract

The beam-beam simulation code (BBSIMC) is a incoherent multiparticle tracking code for modeling the nonlinear effects arising from beam-beam interactions and the compensation of them using an electromagnetic lens. It implements short range transverse and longitudinal wakefield, dipole noise to mimic emittance growth from gas scattering, beam transfer function, and wire compensation models. In this paper, we report on recent improvements of the BBSIMC including a beam-beam compensation model using a low energy electron beam and a current carrying wire.

INTRODUCITON

A beam-beam simulation code BBSIMC has been developed at FNAL over the past few years to study the effects of the machine nonlinearities and the beam-beam interactions. The code is under continuous development with the emphasis being on including the important details of an accelerator and the ability to reproduce observations in diagnostic devices. At present, the code can be used to calculate tune footprints, dynamic apertures, beam transfer functions, frequency diffusion maps, action diffusion coefficients, emittance growth and beam lifetime. Calculation of the last two quantities over the long time scales of interest is time consuming even with modern computer technology. In order to run efficiently on a multiprocessor system, the resulting model was implemented by using parallel libraries which are MPI (interprocessor Message Passing Interface standard) [**?**], state-of-the-art parallel solver libraries (Portable, Extensible Toolkit for Scientific Calculation, PETSc) [**?**], and HDF5 (Hierarchical Data Format) [**?**]. The following section describes the physical model used in the simulaiton code. Some applications are presented for the Large Hadron Collider (LHC) wire compensator and the Relativistic Heavy Ion Collider (RHIC) electron lens.

PHYISCAL MODEL

In the collider simulation, the two beams moving in opposite direction are represented by macroparticles of which the charge to mass ratio is that of each beam. Fewer number of macroparticles are chosen than bunch intensity of the beam because it becomes prohivitive for few revolutions around accelerator even with modern supercomputers. They are genernated and loaded with an initial distribution for a specific simulation purpose according to the beam parameters at the interaction point, for example, six-dimensional Gaussian distribution for long-term beam evolution. The transverse and longitudinal motion of particles is calculated by transfer maps which consist of linear and nonlinear maps. In the simulations, the following nonlinearity is included: head-on and long-range beam-beam interactions, external electromagnetic force by current carrying wire, mulitipole errors due to quadrupole triplets, and sextupole strength of chromaticity correction. In the following, linear and nonlinear tracking models are described in detail.

Transportation through arc

The six-dimensional accelerator coordinates $\mathbf{x} = \left(x, x^{'}, y, y^{'}, z, \delta\right)^T$ are applied, where x and y are horizontal and vertical coordinates, $x^{'}$ and $y^{'}$ the trajectory slopes of each coordinates, $z = -c\Delta t$ the longitudinal distance from syncrhotron particle, and $\delta = \Delta p_z/p_0$ the momentuem deviation from the synchrotron. The linear rotation between two elements denoted by i and j can be written as

$$\mathbf{x}_j = \begin{pmatrix} \mathcal{M} & \hat{\mathcal{D}} \\ 0 & \mathcal{L} \end{pmatrix} \mathbf{x}_i. \tag{1}$$

Here, $\mathcal{M}$ is coupled transverse map of *off-momentum* motion defined by $\mathcal{M} = \mathcal{R}_j \tilde{\mathcal{M}}_{i\to j} \mathcal{R}_i^{-1}$, where $\tilde{\mathcal{M}}_{i\to j}$ is the uncoupled linear map described by twiss functions at i and j elements, and the transverse coupling matrix $\mathcal{R}$ is defined as

$$\mathcal{R} = \frac{1}{\sqrt{1+|C|}} \begin{pmatrix} I & C^\dagger \\ -C & I \end{pmatrix}, \tag{2}$$

where $C^\dagger$ is the 2×2 matrix and the symplectic conjugate of the coupling matrix C. The dispersion matrix is described by $\hat{\mathcal{D}} = (0, \mathbf{D})$, and the dispersion vector $\mathbf{D} = \left(D_x, D_{x'}, D_y, D_{y'}\right)$ is characterized by the transverse dispersion functions and the map $\mathcal{M}$:

$$\mathbf{D} = \mathbf{D}_j - \mathcal{M}\mathbf{D}_i. \tag{3}$$

$\mathcal{L}$ is a longitudinal map and a nonlinearity of synchrotron oscillations is applied by adding the longitudinal momentum change at rf cavity.

Beam-beam interactions

For head-on and long-range beam-beam interactions, we assume that one beam is strong and is not affected by the other beam while the other beam is weak and experiences a beam-beam force due to the strong beam during the collision, so called weak-strong beam-beam model. Besides, the charge distribution of the strong beam is assumed to be

A NEW MODEL-INDEPENDENT METHOD FOR OPTIMIZATION OF MACHINE SETTINGS AND ELECTRON BEAM PARAMETERS*

Martin J. Lee, GO AI Services, Los Altos, CA 94024, USA
Jeff Corbett and Juhao Wu, SLAC National Accelerator Laboratory, Menlo Park, CA 94025, USA

Abstract

Nonlinear programs are widely employed in particle accelerators and storage rings to compute machine settings for optimal model-predictive control of beam parameters. Conventional iterative methods today suffer from problems with finding the global optimal solution when the start solutions are outside the basin-of-attraction for a given objective function to be minimized. A new iterative matrix inversion global optimization (IMIGO) method [1] has been developed to overcome this limitation. IMIGO unlike the existing iterative nonlinear solvers, it calculates only the Jacobian vector of the objection function and not the Hessian matrix at each iteration-this unique feature has led to a new application of IMIGO for optimization of electron beam parameters for cases when a model is unavailable or only an inaccurate model is available. Some possible applications of this IMIGO-based model-independent optimization method will be presented in the paper.

INTRODUCTION

A nonlinear program is a solver typically employed to find the global minimum of a given objective function subjected to certain conditions known as constraints. For optimization of beam parameters, $(b_1, b_2, \cdots, b_n)$, the control variables are the strengths or settings of a group of accelerator elements, $(a_1, a_2, \cdots, a_m)$, that are used to control these beam parameter values. In general, an objective function is defined as a function of the beam parameters. Since each of the beam parameters is a function of the control variables, the value of a given objective function is determined by the values of the control variables, $f_{\rm obj}(a_1, a_2, \cdots, a_m)$. In beam parameter optimization, the start values of the control variables $(a_1^{\rm start}, a_2^{\rm start}, \cdots, a_m^{\rm start})$ are known. Nonlinear programs are used to find the lowest value of a given objective or 'cost' function for the values of the control variables within given bounds: $\Delta_k > (a_k - a_k^{\rm start}) > -\Delta_k$ for $k = 1, 2, \cdots, m$. When the absolute minimum value of the objective function is found, $f_{\rm obj} \Rightarrow f_{\rm obj}^{\rm min}$, the set of variable values is commonly referred to as the global minimum solution: $(a_1^{\rm sol}, a_2^{\rm sol}, \cdots, a_m^{\rm sol})$.

The inherent difficulty of using an iterative method to find the global-minimum solution is well known. In general, an iterative method requires an initial guess solution. If this start solution is too far from the global-minimum solution, the program will find only a local-minimum solution. This problem is known as the basin-of-attraction limit (BOA). A BOA is defined to be the biggest region around a given minimum solution. The problem with the existing iterative nonlinear programs is that they will only find the actual solutions for a special case in which the start solution is inside the BOA corresponding to the global-minimum solution. The new nonlinear programming method IMIGO provides a mitigation to this limitation.

Existing nonlinear programs can be classified into two basic types: One uses an analytical iterative method and the other relies on a stochastic search method such as a genetic algorithm. The inherent difficulty of using an iterative method to find the global-minimum solution is well known. In general, an iterative method requires an initial guess solution. If this start solution is too far from the global-minimum solution, the program will find only a local-minimum solution. As an illustration, a surface plot of the objective function for a minimization problem with two variables is shown in Fig. 1. This figure shows the locations of local-minimum points and the global-minimum point.

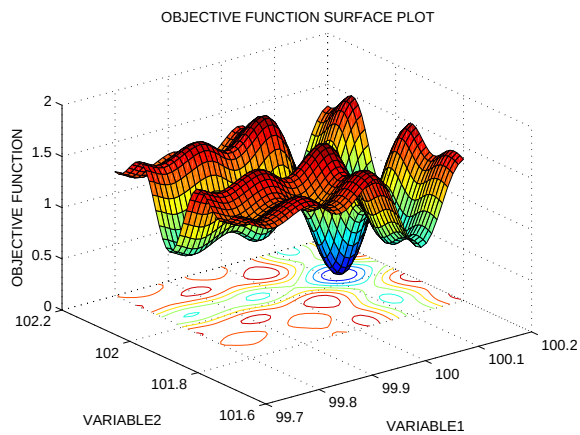

Figure 1: Object function of two variables.

AN OVER VIEW OF IMIGO

IMIGO, like conventional solvers, finds the solution by solving the following set of equations iteratively starting from a given start solution:

$$f_k(a_1, \cdots, a_m) = \partial f_{\rm obj}/\partial a_k = 0 \qquad (1)$$

for $k = 1, 2, \cdots, m$.

One unique feature of IMIGO is that it solves these equations without the using the values of the derivatives:

* JC and JW's work is supported by the US Department of Energy under contract DE-AC02-76SF00515.

RF-KICK CAUSED BY THE COUPLERS IN THE ILC ACCELERATION STRUCTURE

A. Lunin, I. Gonin, A. Latina, N. Solyak, and V. Yakovlev, Fermilab, IL 60510, U.S.A.

Abstract

In this paper new results of calculation of the RF kick from the power and HOM couplers of the ILC acceleration structure are presented. The RF kick is calculated by HFSS and CST codes. Special measures allowing the calculation of the effect are described.

INTRODUCTION

The standard 1.3 GHz SC RF cavity of the ILC linac contains 9 cells, an input coupler, and two HOM couplers, upstream and downstream, see Fig. 1.

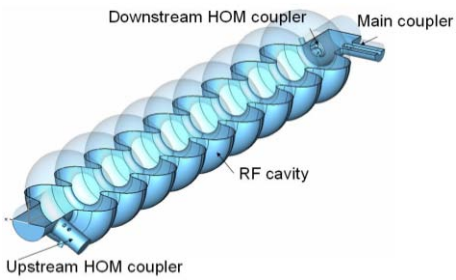

Figure 1: The ILC RF cavity with the main and HOM couplers.

The couplers break the cavity axial symmetry that causes a) main RF field distortion and b) transverse wake field. These effects may cause beam emittance dilution. RF-kick and coupler wake increase with the bunch length [1]. Calculations of the RF kick for the ILC cavity have been performed by different groups, with mismatching results, see Tab. 1.

Table 1: Results of RF-kick calculations.

	FNAL [1] $Q=3.5\times10^6$ HFSS	DESY [2] $Q=2.5\times10^6$ MAFIA	SLAC [3] $Q=3.5\times10^6$ OMEGA3P
$\frac{10^6 V_x}{V_z}$	-105.3+69.8i	-82.1+58.1i	-86.0+60.7i
$\frac{10^6 V_y}{V_z}$	-7.3+11.1i	-9.2+1.8i	-4.6+5.6i

The main reasons of the disagreement are the following: transverse fields caused by the couplers are extremely small (about 5-6 orders of magnitude smaller than the longitudinal fields); cancellation takes place between upstream and downstream coupler. Such characteristics demand for very high precision simulations of the field, better than 10^{-6}. This is a severe challenge for all numerical methods and codes.

GENERAL

In order to achieve reliable estimation for the RF kick, we used the following approaches: (i) different mesh geometry, (ii) different mesh size, (iii) different order of finite elements, (iv) different methods of the kick calculations (direct and Panofsky – Wenzel theorem), (v) different number of cells (from ½ cell to entire 9-cell geometry), and (vi) different codes (HFSS and CST).

HFSS code allows the use of a non-uniform mesh. A special three-zone mesh (see Fig. 1) was used in order to improve the field approximation near the axis. Intermediate mesh is necessary to match the fine mesh near the axis and regular mesh in the rest of the cavity.

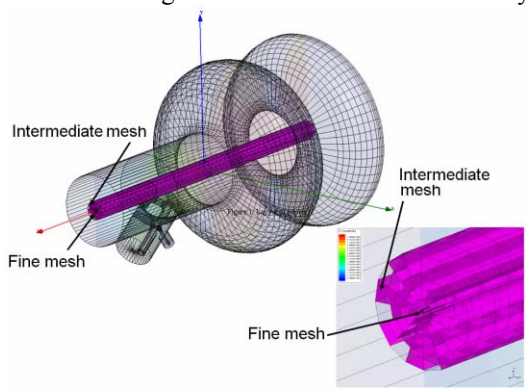

Figure 2: The three-zone mesh for HFSS used in order to improve the field approximation near the axis. Fine mesh repeats the pattern of the intermediate one.

A special symmetric mesh pattern was used in order to reduce the mesh noise. Different techniques of mesh symmetrization were used near the axis. The number of mesh nodes was up to 0.8×10^6. Cross-check of the direct RF kick were performed applying the Panofsky – Wenzel theorem. Fig. 3 shows the field pattern near the coupler.

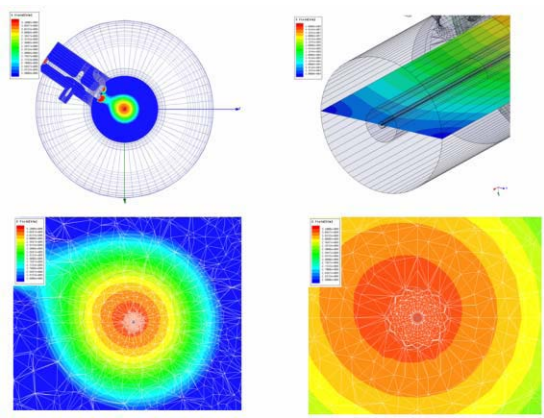

Figure 3: The field pattern near the coupler. The field asymmetry causes RF-kick.

Fig. 4 shows the results of the RF-kick HFSS simulations for upstream and downstream couplers for three cases: different finite element orders, different mesh

COMPUTATION OF A TWO VARIABLE WAKE FIELD INDUCED BY AN ELECTRON CLOUD *

A. Markoviḱ, G. Pöplau, U. van Rienen, Rostock University, Germany

Abstract

The instability of a single positron or proton bunch caused by an electron cloud has been studied using analytical and semi-analytical methods which model the influence of the cloud with the wake field to the bunch. Usually this simulations are fast because the transverse wake due to the electron cloud is being pre-computed and then it is being applied to the bunch turn after turn to simulate the head tail instability. The wake field [1] in these cases is computed in the classical sense as excited electromagnetic field that transversally distorts those parts of the bunch trailing a certain transversal offset in the leading part of the same bunch. The transversal wake force depends only on the longitudinal distance between the leading part of the bunch producing the wake force and the trailing parts of the bunch feeling the wake force. However during the passage of the bunch through the electron cloud the density of the cloud near the beam axis changes rapidly. That means that the environment changes in the time as the bunch proceeds through the cloud and therefore it is not sufficient to apply the single variable (the distance) approximation for the wake field.

In this paper pursuing the idea of K. Ohmi [2] we compute the wake forces numerically as two variable function of the position of the leading part of the bunch and the position of the bunch parts trailing the leading offset in the bunch.

INTRODUCTION

In order to simulate a single bunch instability due to the electron cloud (e-cloud) the bunch movement should be followed turn by turn until the synchrotron tune of the bunch has been resolved, which may take some thousands of turns of the bunch in the ring. At each turn along the ring, the bunch interacts with the e-cloud. A fully self-consistent beam – electron cloud interaction simulation at every turn, even with only one interaction point per turn, would inevitably lead to high computational costs. An idea to speed up the single bunch instability simulation would be to pre-compute the transverse kick of the e-cloud on the bunch. Such a pre-computed kick will be later applied on the bunch at each turn during the tracking of the bunch with the appropriate transport matrices.

Because of the nature of the beam – e-cloud interaction there is a dipole kick on the bunch only if a part of the bunch perturbs the cloud, typically if a slice of the bunch has a slight transversal offset at the entrance in the cloud of homogeneously distributed electrons. However, if the bunch enters the e-cloud with no parts transversely displaced, it does not perturbs the e-cloud asymmetrically. During its passage, it only destroys the homogeneous distribution of the electrons because it attracts them towards the beam axis. As a result, the concentration of electrons near the beam axis grows very fast during the bunch passage. As a matter of fact the electrons near the beam axis start oscillating in the beam potential while the electrons from higher radiuses are approaching the beam axis and constantly increase the number of electrons near the beam axis. Thus, if the transversal offset in the bunch occurs in the rare part of the bunch the number of electrons on the beam axis which will be perturbed by the beam offset is very high. Consequently the kick from the cloud on the following bunch slices would be expected to be stronger. On the contrary, if the transversal offset occurs in the front part of the bunch then the number of electrons that will be perturbed is not going to be that large and so the expected transverse kick on the following bunch slices would not be as strong as if the electron perturbation happens later during the bunch passage.

From this very simple consideration it is obvious that the pre-computed kick due to the interaction with the e-cloud, would depend on the longitudinal position of the bunch slice with the transverse offset and the longitudinal position of the slice that receives the transversal kick. Hence it is necessary to pre-compute the matrix of kicks from every transversally slided slab of the bunch to the trailing bunch slabs. The resulting triangular matrix can be used for the single bunch instability tracking.

3D SELF-CONSISTENT PIC SIMULATION

The interaction of two different particle species is being simulated by the particle in cell program MOEVE PIC Tracking [3]. The bunch and the cloud are represented by a 3D distribution of macro-particles in a beam pipe with elliptical cross-section. The macro-particles are defined in the six-dimensional phase space $\Psi(x, p_x, y, p_y, z, p_z)$ and typical values of their number are of order 10^6 for both species. Usually the bunch particles have a Gaussian spacial distribution. The cloud particles are assumed to be homogeneously spreaded in the 3D space bounded by the beam pipe in the transverse plane and with a certain size in longitudinal direction. The interaction is simulated during the bunch passage through the e-cloud. Figure 1 shows the longitudinal profile of the ILC bunch (blue) before it has entered in a 3D homogeneously distributed e-cloud (red).

In this paper the interaction with the electron cloud is

* Work supported by DFG under contract number RI 814/20-1

A HIGH-LEVEL INTERFACE FOR THE ANKA CONTROL SYSTEM*

S. Marsching[1], M. Fitterer[1], S. Hillenbrand[1], N. Hiller[1], A. Hofmann[1], E. Huttel[2], V. Judin[1], M. Klein[1], A.-S. Müller[1,2], N. J. Smale[2], K. G. Sonnad[1]
[1]University of Karlsruhe, Karlsruhe, Germany
[2] Research Center Karlsruhe, Karlsruhe, Germany

Abstract

ANKA is a synchrotron radiation source located near Karlsruhe, Germany. While the control system has always provided access to technical parameters, like power supply currents or RF frequency, direct access to physical parameters like tune or chromaticity has been missing. Thus the operator has to change and monitor the technical parameters manually and to calculate the physical parameters using separate tools. Therefore effort has been made to integrate the monitoring of physical parameters and simulation tools into the control system. At ANKA the MATLAB-based Accelerator Toolbox is used for simulation purposes, however the control system framework ALMA Common Software (ACS) does not support MATLAB natively. For this reason, a software bridge has been created, which provides direct access to control system components from MATLAB. Thus operators can write their own MATLAB code simultaneously using simulation code and components from the control system. This system has already been used to automate measurements, thus allowing unattended long-term measurements, which have not been possible before. Future plans include creating a graphical user interface and various monitoring and stabilization loops.

ABOUT ANKA

The ANKA facility is a synchrotron radiation facility located near Karlsruhe, Germany. A 2.5 GeV electron storage ring is used to generate synchrotron radiation for various X-ray and IR beamlines. The storage ring can be operated with different optics, in order to provide radiation for different purposes. A low emittance optic is used for normal user operation at a beam energy of 2.5 GeV [1]. A special "low alpha" optic is used to generate coherent THz synchrotron radiation for the IR beamlines in the so called "special user operation" mode [2].

CONTROL SYSTEM

The ANKA control system [3] is based on the software framework ALMA Common Software (ACS) [4, 5]. ACS uses CORBA as a communication link between components. At the moment, components written in C++, Java or Python are supported by the framework. The central ACS manager provides a naming service which is used by clients to find a component by name. The ACS manager also stores configuration information for components, thus centralizing all configuration information.

The ACS components represent technical components of the storage ring (e.g. power supplies, beam position monitors, RF generators) and are written in C++ and Java. The ACS clients (at ANKA they are all written in Java) provide a GUI for displaying data provided by the components as well as controls for changing the settings of the devices represented by the components. Apart from the lookup and configuration process, the ACS manager is not involved in the communication between clients and components. The architecture of the control system is shown in Fig. 1 (components within the box "Legacy Components").

Limitations of the legacy control system

The legacy control system is build around the hardware of the accelerator / storage ring. This means that it basically provides remote control and monitoring of all relevant devices, but it is not aware of the physics of the accelerator. The only exception is a software client specially built for performing orbit corrections. However, this client basically is just a special GUI and the code concerning physics is not part of the control system backend components.

As the ANKA storage ring has a flexible lattice and is often operated with different optics (a low-emittance, a low-alpha or a low-beta optics), having a good model for calculating the accelerator settings for different modes of operation is very important. However, without a direct connection between the model and the real acclerator, all changes calculated in the model have to be transferred into technical parameters manually.

Features of the new high-level interface

The new high-level interface allows for an easy integration of new diagnostic components. As the diagnostic components can easily access all control system parameters, task like logging tunes against beam energy can be performed very easily. Even measurements that require the change of machine parameters (e.g. chromaticity measurements) can easily be automated using the new high-level interface as it also allows for write access to most parameters.

ACCELERATOR MODEL

The Accelerator Toolbox for MATLAB (AT) provides tools to create a generic accelerator model [6]. This model

* This work has been supported by the Initiative and Networking Fund of the Helmholtz Association under contract number VH-NG-320.

PteqHI DEVELOPMENT AND CODE COMPARING

J. Maus*, R. A. Jameson, A. Schempp, IAP, Frankfurt, Germany

Abstract

For the development of high energy and high duty cycle RFQs accurate particle dynamic simulation tools are important for optimizing designs, especially in high current applications. To describe the external fields in RFQs, the Poisson equation has to be solved taking the boundary conditions into account. In PteqHI this is now done by using a finite difference method on a grid. This method will be described and simulation results will be compared to different RFQ particle dynamic codes.

PTEQHI WITH POISSON SOLVER

PteqHI is a program to simulate particle dynamics in RFQs. It has its roots in PARMTEQ and has continuously been developed and adapted to meet several problems by R. A. Jameson [1]. It describes the external field with the same multipole expansion method than PARMTEQM and it also uses the SCHEFF routine for its space charge calculation, but it uses time as the independent variable. Simulations of a set of 10 RFQs, which are similar to the IFMIF designs in terms of final energy, frequency, emittance, beam current, but with changing aperture have revealed same limitations of these original methods.
This was one of the reason to change the way the electric field is calculated along the RFQ. The new routines solve the Poisson equation directly. This is done by a Solver that uses the finite difference method on a grid.

Generating the grid

The first step is to set up the grid with the boundary conditions figuring out which grid points lie in or on the electrodes. The tip of the electrodes are found using the cell table for the geometry data and interpolating them at each z position using cubic splines. Once the tip position is known the electrode is represented by an arc with a selectable brake out angle. Since the boundary conditions at the electrodes are Dirichlet boundary condition the voltage $\pm\frac{U_0}{2}$ is assigned to the grid points which lie inside the electrodes. In order to describe the surface as smooth as possible the grid points are shifted in such manner that there is always a grid point on the surface. Longitudinal boundary conditions are more difficult to realize, because it cannot be assumed that the structure is symmetric in longitudinal direction. The small changes of the aperture and modulation which disturb the symmetry can be seen in results of the solver. To overcome this problem many cells are combined to a segment and calculated at the same time. Since the segments overlap, the regions with are influenced by the asymmetry are never used for the dynamic calculation.

Transition Region A real RFQ does not start directly with the electrodes, but with a tank wall. So we decided to let the particles start outside the tank wall, where the potential is close to zero. Then they drift through the small gap between the electrodes and the tank wall seeing the rising RF-field. The first segment of the RFQ includes the tank wall, the gap, the radial matching section and the first two regular cells of the RFQ to be able to simulate the effects of the rising RF-field.

Space charge grid The space charge effect is also calculated by solving the Poisson equation which a charge density $\rho \neq 0$. Therefore a second grid is needed which is generated in the same way as the grid for the external field, but with zero potential on the electrodes. By forcing the potential to be equal to zero on the electrodes the image effect is also taken into account directly, since the purpose of the image effect is to make sure that the potential of a conducting surface vanishes. There is also the option to ”turn off” the image effect by setting the boundary condition of the grid to a cylinder (e.g., radius m*a) with zero potential on its surface. So the effect of the image charges can be studied.

Poisson solver

For solving the Poisson equation the finite difference method is used. This method is an iterative method where at each iteration step the new value for a grid point is a function of the old value of that point and the values of the neighboring points

$$\varphi_{0,n+1} = F(\varphi_{0,n}, \Sigma_{i=1}^{6} a_i \cdot \varphi_{i,n}, \rho_0), \quad (1)$$

where φ is the potential at the point 0 and ρ_0 is the charge density at that point. Each pair of grid points has a certain distance h_i between them. The a_i are a function of these distances. In general the h_i can vary from one pair of nodes to the next, so that the shifted grid points can be taken into account in order to represent the electrodes correctly without introducing some kind of steps. From one iteration to the next the value at each node converges to the exact answer. The accuracy is limited by the h_i. This basic method is known as the Gauß-Seidel relaxation. For speeding up

* maus@iap.uni-frankfurt.de

TRACY#*

H. Nishimura
Lawrence Berkeley National Laboratory, Berkeley, CA 94720, U.S.A.

Abstract

Tracy# is a C# class library for single particle beam dynamics in full 6-dim canonical phase space. The code is based on Goemon that is a C++ version of the Tracy2 library. This paper describes the new features in Tracy# from a software engineering aspect.

INTRODUCTION

During the ALS[1] design phase, Tracy[2] was developed in Pascal for modeling and tracking studies by using embedded Pascal compiler/interpreter to parse the user logic. It evolved to a 6-dimensional version called Tracy2[3]. Subsequently its accelerator physics library was separated from Tracy and ported to C/C++ independently at multiple light sources, including SLS[4], Diamond[5], Soleil[6] and NSLS-2[7], mostly for model-based accelerator controls. At the ALS, the library was re-written in C++ as Goemon[8], which has now been re-written in C# [9] and called Tracy#.

FEATURES

Library Layers

Tracy# is a library that implements single particle beam dynamics for modeling, simulation and analysis studies.

An application built with Tracy# has 3 layers:

- Physics layer, which is Tracy# itself.
- Accelerator layer to model particular accelerators.
- Application layer.

The Physics layer is for beam dynamics and uses the following integrators:

- The 4x5 linear matrix formalism.
- The 2nd and the 4th-order symplectic integrators[10] in 6-dim.
- K-pot Hamiltonian[11] that models small rings properly.

In Tracy# these integrators were implemented in C# taking advantage of some of the important language features. For example, operator overloading is used for:

- Vector and matrix calculations.
- Differential algebra (DA) [12].
- Lattice definitions.

The second layer is to model particular accelerator structures. This is the place where virtual accelerators are built in forms of C# classes. Starting with an ideal lattice, a virtual machine is enhanced to be a practical one that provides realistic error emulations, various control knobs, and customized physics routines to calculate a range of quantities including dynamic apertures.

The application layer is for client application programs that access the virtual accelerators. These programs can use any features of the .NET libraries that cover database access, XML, networks and graphics. Tracy# is designed to be compatible with these standard .NET libraries. Actually, Tracy# needs only one external routine that is for the singular value decomposition to invert the large sensitivity matrices. We chose an open–source math library in C#[13].

Environment

Tracy# is built on the .NET Framework 3.5, and works on Windows XP SP2 as well as Vista. The development environment is Visual Studio 2008. The programming language for the physics layer is C# 3.0. The client programs are also developed in the same development environment and usually in C# 3.0. However, they can be in other .NET languages, such as Visual Basic.NET or IronPython[14] that we mention later.

Tracy# can also work non-Windows platform by using MONO[15] that is an independent, open-source implementation of the .NET Framework that covers various platforms, including Linux, Solaris and Macintosh. As Tracy# itself is a plain C# code, it is compatible with MONO. It is also possible to make its application program portable by carefully choosing the graphics components for GUI programming.

Implementation

As mentioned, Tracy# uses advanced features of the .NET Framework. In particular, .NET generics proved invaluable especially List< >. In case of Goemon in C++, we did not use C++ generics called template to keep the compile-and-link time reasonably short.

Porting the routines for vector/matrix and DA was not trivial. Goemon used local variables allocated on the memory stack to carry out calculations rapidly. This trick in C/C++ does not work with C#. Therefore the C# routines needed fine tuning to restore execution speed[9]. Currently, we are rewriting routines further to enable parallel computing as mentioned later.

Graphics is not a core part of Tracy#. Instead, the accelerator layer uses it extensively. The graphics programming was in WinForm of .NET 2.0, and is migrating to Windows Presentation Foundation (WPF) of .NET 3.0.

Tracy# also uses relational databases and XML as described in the following sections.

*Work supported by the U.S. Department of Energy under Contract No. DE-AC02-05CH11231

MODELING SINGLE PARTICLE DYNAMICS IN LOW ENERGY AND SMALL RADIUS ACCELERATORS

E. Nissen, B. Erdelyi, Department of Physics, Northern Illinois University, Dekalb, IL 60115, USA

Abstract

This research involves the development of a model of the small circumference (11.5 m) accelerator in which the earth's field has a strong effect, and in which image charge forces are also included. The code used for this simulation was COSY Infinity 9.0 which uses differential algebras to determine high order map elements, as well as quantities such as chromaticity. COSY also uses Normal Form algorithms to determine the betatron tune and any amplitude dependent tune shifts which may result. The power of COSY is that it can derive the required quantities directly form the map without costly integration and tracking. Thus determining the map for both the default elements of the ring, plus the effects of image charge forces, and the earth's magnetic field is both non-trivial, and important. This research uses the Baker Campbell Hausdorf method to determine the map of the ring with the external fields included. Furthermore COSY has the ability to directly implement misalignments within the beamline itself allowing for a study of their effects on beam dynamics. The presentation will include both coding development and applications to the University of Maryland Electron Ring.

INTRODUCTION

With the increase in demand for high current accelerators, methods for determining the effects of space charge become more important. One method for gaining experimental data on the effects of space charge is to use a low energy electron beam to model a high energy heavy ion beam, this is the approach used by the University of Maryland Electron Ring (UMER) [**?**]. UMER sends 10 Kev electrons through a storage ring that is only 11.5 meters in circumference. Currently all acceleration occurs in the electron gun, which sends the beam through a matching section and into the Y-shaped injector. This injector involves offsets on both the injection and recirculation sides, the ring then uses an additional 17 sections comprised of a bending dipole between a pair of quadrupoles, followed by a diagnostic chamber, followed by another set of quadrupoles enclosing a dipole. The arrangement of the elements in the ring are shown in Fig. 1. Due to the small radius and low energy of the beam the effects of the earth's field on the trajectory of the beam is nontrivial. Furthermore, the offsets in the injection and recirculation parts of the Y-shaped section mean that the effects of image charge on the beam should also be taken into account.

First there will be a brief introduction to COSY Infinity and its unique properties, then there will be an overview of how the earth's field, the image charge force, and unique elements contained in this particular beam are implemented. Finally there will be a brief look at some experimental observations.

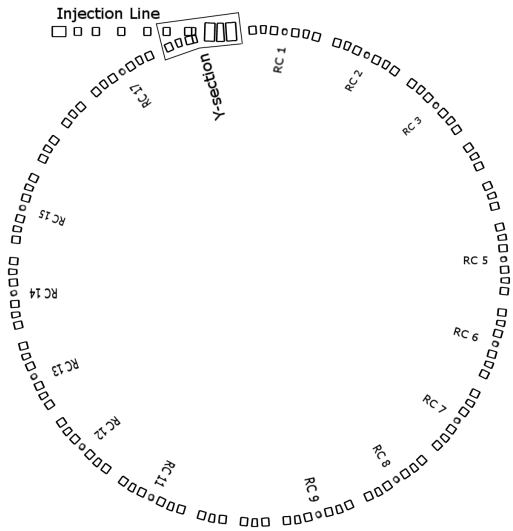

Figure 1: COSY Infinity produced diagram of the University of Maryland Electron Ring. Sections marked RC contain ring chambers which house both non-intercepting Beam Position Monitors, and intercepting Phosphor screens. Sections not marked with an RC number contain glass gaps for current monitors.

CODE DEVELOPMENT

The code used in this study is COSY Infinity 9.0. This code uses differential algebraic vectors which allow not only for an accurate calculation of numerical derivatives, but also carries them through the various mathematical operations. This behavior means that COSY can integrate a test particle through an electromagnetic field and all of the variable dependencies will be preserved, allowing for fast accurate computation of maps [**?**]. COSY also has a large library of default beam elements, so in this study they were used as often as possible.

Short Solenoid

One issue that was dealt with early on was the field profile of a short solenoid in the injection line. The field profile that was measured for the physical element was very different from the kind used in the available COSY solenoids, so the open architecture of COSY allowed us to model the solenoid using a field profile provided by fitted data. The

POSSIBILITY OF ROUND BEAM FORMATION IN RIBF CYCLOTRONS

H. Okuno#, RIKEN Nishina Center, Wako, Saitama, 351-0198, Japan
A. Adelman, PSI, 5232 Villigen, Switzerland
J. J. Yang, CIAE, Beijing, 102413, China & Tsinghua University, Beijing, 100084, China.

Abstract

Since 1997 RIKEN Nishina center has been constructing a next-generation exotic beam facility, RI beam factory (RIBF), based on a powerful heavy ion driver accelerator. Its accelerator complex was successfully commissioned at the end of 2006 and started supplying heavy ion beams in 2007. The four ring cyclotrons (RRC, fRC, IRC and SRC) connected in series accelerate the energy of the heavy ion beams up to 400 MeV/u for the lighter ions such as argon and 345 MeV/u for heavier ions such as uranium. Intensity upgrade plans are under way, including the construction of a new 28 GHz superconducting ECR ion source. The new ECR will take all the succeeding accelerators and beam transport lines to a space charge dominant regime, which should be carefully reconsidered to avoid emittance growth due to space charge forces. Beam dynamics in the low energy cyclotron, RRC was studied with OPAL-cycl a flavor of the OPAL. The simulation results clearly show vortex motions in the isochronous field, resulting in round beam formation within the first 10 turns after the injection.

INTRODUCTION

RIKEN Nishina center has undertaken construction of an RI Beam Factory (RIBF) [1] since April 1997 aiming to realize a next generation facility that is capable of providing the world's most intense RI beams at energies of several hundred MeV/nucleon over the whole range of atomic masses. The RIBF requires an accelerator complex which would accelerate the full mass range of ions and deliver ~80 kW of uranium beam at energy of 345 MeV/nucleon. Figure 1 shows a bird's eye view of

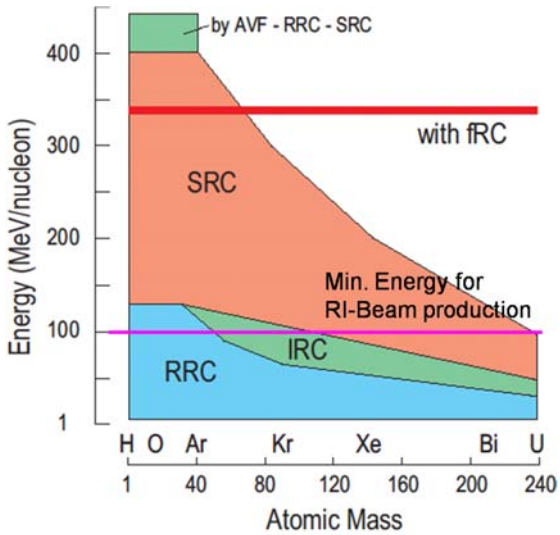

Figure 2: Performance of the RIBF accelerator complex.

RIBF. The left part is the old facility completed in 1990. Using the four-sector K540-MeV ring cyclotron (RRC), many experiments were carried with RI beams of light ions because RRC can accelerate relatively light ions up to 100 MeV/u, which is the lower limit for the RI-beam production as shown in Fig. 2. At first, the two ring cyclotrons, Intermediate Ring Cyclotron (IRC). Superconducting Ring Cyclotron (SRC) were designed as energy boosters for the RRC in order to expand the

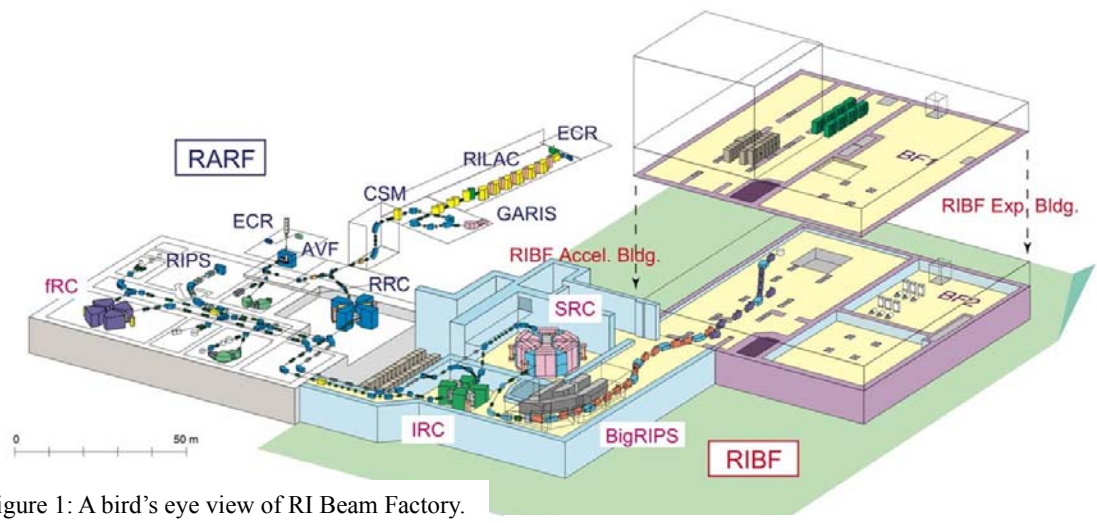

Figure 1: A bird's eye view of RI Beam Factory.

SET CODE DEVELOPMENT AND SPACE CHARGE STUDIES ON ISIS

BG Pine, DJ Adams, CM Warsop, RE Williamson
Rutherford Appleton Laboratory (STFC), Oxfordshire, UK.

Abstract

The ISIS Facility at the Rutherford Appleton Laboratory in the UK produces intense neutron and muon beams for condensed matter research. It is based on a 50 Hz proton synchrotron which accelerates ~3E13 protons per pulse (ppp) from 70 to 800 MeV, corresponding to beam powers of ~0.2 MW. Studies are under way for major upgrades in the Megawatt regime. Underpinning this programme of operations and upgrades is a study of the high intensity effects that impose limitations on beam power.

The behaviour of the beam in the 50 Hz rapid cycling synchrotron (RCS) is largely characterised by high space charge levels and the effects of fast ramping acceleration. High intensity effects are of particular importance as they drive beam loss, but are not fully understood with only limited analytical models available. This paper reviews development of a new space charge code Set, which is designed to address key issues on ISIS and similar RCS machines.

INTRODUCTION

ISIS high intensity operation is restricted by beam loss, as irradiation of equipment limits access for essential maintenance. Understanding beam loss is therefore of vital importance, however due to the complex interactions between the beam particles and their environment such understanding is challenging both analytically and numerically.

The ISIS Synchrotron Group is actively studying high intensity effects of the beam in a number of different ways, both to improve performance of the accelerator and also to enable the design of upgrades which can achieve significantly higher beam intensities. This paper focuses on developments of the beam tracking code Set.

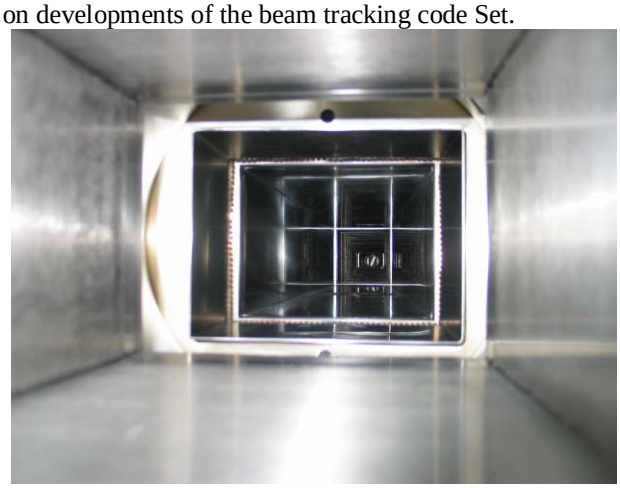

Figure 1: Rectangular ISIS vacuum vessel.

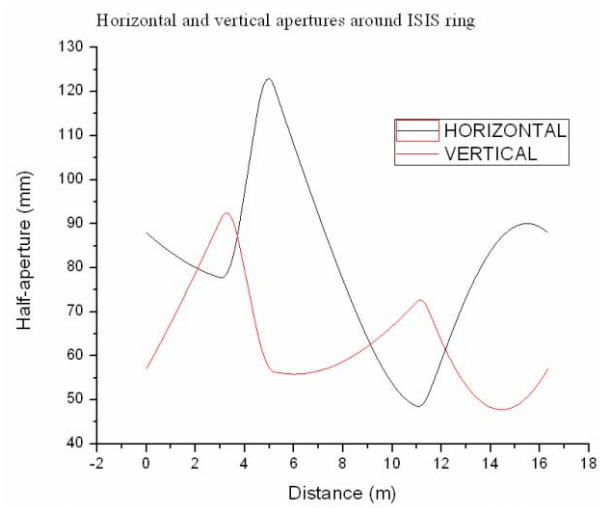

Figure 2: Profiled vacuum vessels in ISIS super-period.

SET

A new code Set is under development at ISIS. This code is intended to supplement the use of ORBIT [1] for 2D and 3D beam tracking simulations, as a tool that can be readily modified and redeployed as required to meet a given purpose. In particular, the focus is on the challenges of the ISIS RCS, including image forces from the unique profiled vacuum vessel (Figures 1 and 2), halo predictions, 2D and 3D RCS space charge effects and overall to understand and predict beam loss. Set works using either MAD input data or its own matrix routines for generating lattices, and has an FFT based Poisson-solver for calculating the beam's space charge. Early simulation work [2, 3] focused on replicating ORBIT results for the half integer resonance. Example results for the ISIS lattice (2D, coasting beam) driven with a $2Qv = 7$ resonance are shown in Figures 3, 4 and 5.

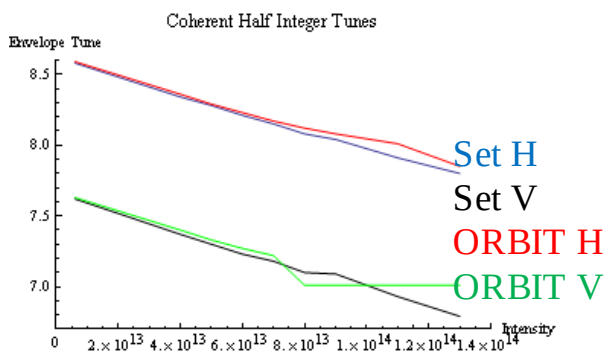

Figure 3: Envelope frequencies intensity sweep.

Figure 3 shows Set and ORBIT envelope frequencies as the intensity is swept from 1 – 14E13. Figure 4 shows the incoherent tune footprints after 100 turns, as the intensity

COMPLETE RF DESIGN OF THE HINS RFQ WITH CST MWS AND HFSS*

G. Romanov #, A.Lunin, Fermilab, Batavia, IL 60510, USA.

Abstract

Similar to many other linear accelerators, the High Intensity Neutron Source requires an RFQ for initial acceleration and formation of the bunched beam structure. The RFQ design includes two main tasks: a) the beam dynamics design resulting in a vane tip modulation table for machining and b) the resonator electromagnetic design resulting in the final dimensions of the resonator. The focus of this paper is on the second task. We report complete and detailed RF modeling on the HINS RFQ resonator using simulating codes CST Microwave Studio (MWS) and Ansoft High Frequency Structure Simulator (HFSS). All details of the resonator such as input and output radial matchers, the end cut-backs etc have been precisely determined. Finally in the first time a full size RFQ model with modulated vane tips and all tuners installed has been built, and a complete simulation of RFQ tuning has been performed. Comparison of the simulation results with experimental measurements demonstrated excellent agreement.

INTRODUCTION

Within the framework of the High Intensity Neutrino Source (HINS) program at FNAL, we plan to build and operate a portion of the Front End (up to energy of 62 MeV) as a technical feasibility proof of the proposal. A detailed description of the project and the current status is given in [1]. In the Front End test stand a four vane 325 MHz Radio Frequency Quadrupole (RFQ) will be used for bunching the beam and accelerating it from 50 keV to 2.5 MeV.

The complete beam dynamics design, resulted in a vane tip modulation table for machining, is described in [2]. The mechanical design concepts for this RFQ, tuning results, manufacturing of the RFQ in industry and the preliminary results of initial testing of RFQ at the Front End test stand are discussed in [3].

The electromagnetic design of RFQ resonators is rather complicated and requires essentially three-dimensional modeling. That, and also an additional complication with RF tuning because of some blunder made in the mechanical design of RFQ, urged us to develop a full length 3D RFQ model for simulation. Modern three-dimensional electromagnetic codes are now available and successfully used for RFQ design [4, 5, and 6]. This paper focuses exclusively on the computational technique of electromagnetic design. We report complete and detailed RF modeling on the HINS RFQ resonator using simulating codes CST Microwave Studio (MWS) and Ansoft High Frequency Structure Simulator (HFSS).

*This work was supported by the U.S. Department of Energy under contract number DE-AC02-76CH03000.

#gromanov@fnal.gov.

RFQ MODEL FOR ELECTROMAGNETIC SIMULATION

The basic parameters of the RFQ are given in table 1.

Table 1

Input energy	50 keV
Output energy	2.5 MeV
Frequency	325 MHz
Total length of vanes	302.428 cm
Average bore radius	3.4 mm

The RFQ design has several features that have been taken into account during electromagnetic simulations.

Instead of π-mode stabilizing loops (PISLs) usual for RFQs longer than ~3λ, where λ is the rf wavelength [7], FNAL's RFQ design uses the end-wall tuners - field stabilizers simpler than PISLs [8]. This method requires a precise knowledge of dipole mode spectrum, so simulating full length RFQ with end-wall tuners installed was needed.

Modulation of the vanes in the regular accelerating section of the RFQ is shown in Fig1. A variable modulation changes capacitive loading and therefore local frequency along RFQ as also reported elsewhere [4, 9, and 10]. In our RFQ the local frequency variation due to the modulation is significant, so the vane tip modulation has been included in the model.

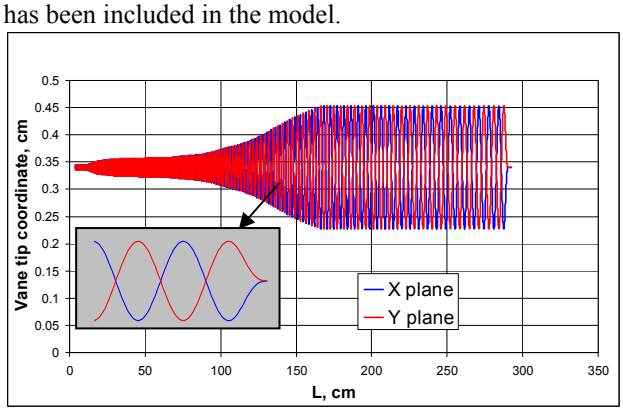

Fig.1 Vane tip modulation along RFQ. Radial matchers are excluded.

The output radial matcher is designed to form axially symmetric beam exiting the RFQ, and because of this special function it is different than the input radial matcher. Fig 2 shows profile of the output radial matcher and imposed profile of the input matcher to compare with. The RFQ ends (cutbacks) can be tuned in simulations individually, but their combined effect on field flatness must be evaluated. Besides the end-wall tuners have

H5PartROOT—A VISUALIZATION AND POST-PROCESSING TOOL FOR ACCELERATOR SIMULATIONS

Thomas Schietinger
Paul Scherrer Institut, CH-5232 Villigen PSI, Switzerland

Abstract

Modern particle tracking codes with their parallel processing capabilities generate data files of the order of 100 Gigabytes. Thus they make very high demands on file formats and post-processing software. H5PartROOT is a versatile and powerful tool addressing this issue. Based on ROOT, CERN's object-oriented data analysis framework developed for the requirements of the LHC era, and the HDF5 hierarchical data format, supplemented by an accelerator-specific interface called H5Part, H5PartROOT combines the statistical and graphical capabilities of ROOT with the versatility and performance of the HDF5 technology suite to meet the needs of the accelerator community. Providing the user with both a graphical user interface (data browser) and a shared library to be used in an interactive or batch ROOT session, H5PartROOT passes on the full power of ROOT without presupposing any knowledge about the intricacies of either ROOT or C++.

INTRODUCTION AND MOTIVATION

Three-dimensional particle simulations (e.g., OPAL [1]) follow the trajectories of a large number (up to 10^9 and more) of macro-particles through space as they are influenced by external (electro-magnetic and or gravitational) and internal (space charge) fields. The result of such a simulation is typically stored as a sequence of time steps. Each time step contains some quantities (often scalars or 3-vectors for the three spatial dimensions) describing properties of the macro-particle ensemble (bunch) as a whole (e.g., centroid position, mean particle energy etc.) and, if detailed analysis of the bunch evolution is desired, a full dump of the macro-particle phase space (i.e., positions and momenta of all macro-particles in the simulation).

With the increasing size of datasets produced by such simulations, swift post-processing becomes an issue of paramount importance. To address the problem we created a tool based on ROOT, the data analysis software used by CERN and its user community to analyze the vast amounts of data produced by the Large Hadron Collider, and HDF5, an extremely versatile and powerful data file format enjoying growing popularity throughout the scientific community. The considerable power and flexibility of both HDF5 and ROOT come at the prize of rather complex user interfaces. To spare the user the learning curves of these packages as much as possible, we built a ROOT application which allows fast extraction of statistical data and generation of publication-quality plots with just a few mouse clicks. Since it makes use of the H5Part interface to HDF5, the application is called *H5PartROOT*.

BUILDING BLOCKS

HDF5

HDF5 ("Hierarchical Data Format 5") is a highly sophisticated, "self-describing" data storage format. Originally created by NCSA, it is now supported by the HDF group [2]. The HDF5 technology suite allows the management of extremely large and complex data collections. Its versatile data model can represent very complex data objects and a wide variety of meta-data. The file format is completely portable and puts no limits on the number or size of data objects, making it an ideal format for large accelerator simulations. The HDF5 software library provides various high-level interfaces (C, C++, Fortran 90, Java) and runs on almost every computing platform, from laptops to massively parallel systems. Furthermore HDF5 comes with built-in performance features that optimize access time and storage space as well as a whole set of tools and applications for managing, manipulating, viewing, and analyzing the data.

H5Part

H5Part is a thin software layer on top of HDF5 to facilitate I/O for the simulation of particle accelerators (or any other multi-particle system that evolves in time) [3]. Designed as a portable, high-performance parallel data interface to HDF5 [4], it constrains HDF5's very general data format to a subset useful for three-dimensional particle accelerator simulations, i.e., it knows about time steps, phase space variables etc. H5Part is co-developed by LBNL and PSI.

ROOT

ROOT is an object-oriented data-processing framework developed at CERN for the requirements of the LHC era, i.e., to handle complex datasets of sizes measured in Terabytes [5]. Within the last decade, it has become the data analysis and visualization tool of choice in high-energy physics around the world.

PARALLEL SDDS: A SCIENTIFIC HIGH-PERFORMANCE I/O INTERFACE*

Hairong Shang†, Yusong Wang, Robert Soliday, Michael Borland, Louis Emery,
Argonne National Laboratory, Argonne, IL 60439, USA

Abstract

Use of SDDS, the Self-Describing Data Sets file protocol and toolkit, has been a great benefit to development of several accelerator simulation codes. However, the serial nature of SDDS was found to be a bottleneck for SDDS-compliant simulation programs such as parallel elegant. A parallel version of SDDS would be expected to yield significant dividends for runs involving large numbers of simulation particles. In this paper, we present a parallel interface for reading and writing SDDS files. This interface is derived from serial SDDS with minimal changes, but defines semantics for parallel access and is tailored for high performance. The underlying parallel I/O is built on MPI-I/O. The performance of parallel SDDS and parallel HDF5 are studied and compared. Our tests indicate better scalability of parallel SDDS compared to HDF5. We see significant I/O performance improvement with this parallel SDDS interface.

INTRODUCTION

SDDS [1] is a self-describing data file protocol developed at Argonne National Laboratory's Advanced Photon Source (APS). It is a standardized way to store and access data, and is the basis of a toolkit [2] of interoperable accelerator physics programs. Over the years, several SDDS-compliant accelerator programs (e.g, `clinchor` [3], `elegant` [4], and `shower` [5]) have been developed at the APS. Also, many existing accelerator design tools for which the source code is available have been converted to read and write SDDS files. This allows physicists to readily use several codes in combination, with greater speed, flexibility, and accuracy than otherwise possible. In addition to requiring accelerator codes to read and write SDDS files, we created a suite of generic data processing and display tools that work with SDDS files. In effect, we created a common pre- and postprocssing toolkit that is used by our codes and codes we have modified. This set of approximately 80 generic programs is referred to as the SDDS Toolkit [2].

A major advantage of using SDDS files is that data from one code can more readily be used by another. The self-describing nature of the files makes this robust, meaning that one code can be upgraded without requiring a change in the other code. The SDDS Toolkit also provides the ability to make transformations of data, which is useful when codes have different conventions (e.g., for phase-space quantities). Finally, using SDDS means that adding capabilities to a simulation code is faster and easier. The new data is simply placed in SDDS files where it can be accessed with the existing suite of tools [2].

In addition to the SDDS Toolkit, users can import SDDS data directly into programming environments like C/C++, FORTRAN, IDL, Java, MATLAB, and Tcl/Tk, using libraries created and supported by APS. These libraries, like the rest of the SDDS software and our simulation codes, are covered by an Open Source license and are available for download from our web site. The codes discussed are all available for UNIX environments, including LINUX, Solaris, and MAC OS-X, and (usually) for Microsoft Windows. The program `elegant` [4] was the first of the SDDS-compliant accelerator codes, and it is widely used for accelerator design and simulation, and is at the center of the SDDS-compliant accelerator simulation codes. The computing power of `elegant` has been enhanced significantly through recent parallelizations and optimizations [6]. However, the SDDS tools with sequential execution are a bottleneck for both memory and I/O operations. Therefore, parallel SDDS is required for large simulations, as well as for analysis and visualizations of the resulting large data sets. This paper introduces the design, implementation, and performance study on parallel SDDS. Since HDF5 [7] is another popular scientific data format, the performance of parallel HDF5 is also studied on Jazz [8] for comparison. Although HDF5 already supports parallel I/O, it is not necessarily beneficial to switch from SDDS to HDF5, given the large number of programs and applications that already use SDDS. Only if HDF5 offers a significant performance advantage over parallel SDDS would such a conversion be considered.

SDDS File Format and Data Storage

An SDDS file is referred to as a "data set". Each data set consists of an ASCII header describing the data that is stored in the file, followed by zero or more "data pages". The data may be in ASCII or unformatted (i.e., "binary"). Each data page is an instance of the structure defined by the header. That is, while the specific data may vary from page to page, the structure of the data may not. Three types of entities may be present in each page: parameters, arrays, and columns. Each of these may contain data of a single data type, with the choices being long and short integer, single-/double-precision floating point, single character, and character string. The names, units, data types, and other descriptions of these entities are defined in the header. Parameters are scalar entities. That is, each parameter defined in the header has a single value for each page. Ar-

* Work supported by the U.S. Department of Energy, Office of Basic Energy Sciences, under Contract No. DE-AC02-06CH11357.

† shang@aps.anl.gov

THE PYTHON SHELL FOR THE ORBIT CODE *

A. Shishlo, J. Holmes, T. Gorlov, ORNL, Oak Ridge, TN 37831, U.S.A.

Abstract

A development of a Python driver shell for the ORBIT simulation code is presented. The original ORBIT code uses the SuperCode shell to organize accelerator-related simulations. It is outdated, unsupported, and it is an obstacle to future code development. The necessity and consequences of replacing the old shell language are discussed. A set of core modules and extensions that are currently in PyORBIT are presented. They include particle containers, parsers for MAD and SAD lattice files, a Python wrapper for MPI libraries, space charge calculators, TEAPOT trackers, and a laser stripping extension module.

INTRODUCTION

The original ORBIT code has been very useful in the SNS ring design and in simulations of collective effects [1]. Thanks to a flexible structure, ORBIT can be extended very easily. After years of development by many scientists, ORBIT includes collimation, different types of space charge, impedances, electron-cloud effects, and numerous other features. These features are combined together by using a driving shell – the SuperCode (SC). SC is an interpreter programming language resembling C. At the time when ORBIT development started (1997), there were not many choices of driving shell language. SC was attractive because it is C-like, it is simple to learn, to understand, and to extend, and it has a set of effective auxiliary classes for arrays, vectors, strings, etc. As a result of deep integration, the ORBIT code has become inseparable from SuperCode, and SC has now become an obstacle to further ORBIT development.

There are several problems related to SC. First, SC is not an object-oriented language. This significantly slows down ORBIT development and limits the functionality of the code. All contemporary interpreters are object-oriented. Second, SC is not supported by anyone. Usually languages are surrounded by a community of users and developers, which facilitates an immediate response to problems and bugs. So, for SC the user is on his own. Finally, all auxiliary classes provided by SC have been implemented in the C++ Standard Template Library, and this implementation is probably more efficient. In SC none of these classes is protected by namespaces, and they could crush the ORBIT code compilation if there is a name conflict.

In an attempt to preserve the legacy of the ORBIT code, the PyORBIT project has been started. The motivation of PyORBIT is to replace the SuperCode driver shell by a modern interpreter language, Python [2]. Unfortunately, it is not possible to directly import the code of core ORBIT modules into the new project because of ubiquitous SC dependencies. On the other hand, this gives us an opportunity to start from scratch in the architecture and the source code development and to keep all original ORBIT physical algorithms.

DRIVER SHELL PARADIGM

PyORBIT, like the original ORBIT code, uses a driver shell language approach instead of an input file analysis, as in traditional accelerator codes like MAD, MAD-X, PTC, PARMILA, Trace3D etc. These traditional codes construct an accelerator lattice and perform calculations according to information inside specialized input files. They each use their own language created for the particular code, and the list of possible tasks is predefined and limited. PyORBIT uses another approach. We use an existing programming language and extend it with specific accelerator-related functionalities. The user can create a unique simulation code in the form of a main program or script by using a predefined set of classes and methods.

There are several requisites for a programming language that can be used for this scheme:

- The program language should be popular among physicists. There are many languages that fall under this category: FORTRAN, C, C++, Ruby, Python, and Java.
- It should be an object-oriented language with an automated garbage collection. This condition eliminates FORTRAN, C, and C++.
- It should be fast. That will eliminate Ruby and Python, which are interpreted languages.
- It should be capable of an effective usage of the Message Passing Interface (MPI) library for parallel calculations. That will remove our last candidate – Java. There are several available Java wrappers for MPI, but the overhead for array exchange makes these packages unacceptable for us.

These constraints necessitate a two-language scheme. To provide the necessary speed we must use FORTRAN, C, or C++ at the low level, and Ruby or Python to organize the calculation at the upper level. For the PyORBIT project we chose C++ for its object-oriented nature, better standardization, and better free compiler availability than FORTRAN. For the upper level we preferred Python, because its pseudo-code compilation feature makes it significantly faster then Ruby. This combination of a scripting language for orchestrating simulations and a fast compilation language to perform calculations is very popular in scientific computing [3]. Generally, code development in a scripting language is considered 3-5-10 times faster than it is in languages like C++ or Java. The downside of the two-level approach is the necessity of a “glue” code to connect the codes in the two languages.

* ORNL/SNS is managed by UT-Battelle, LLC, for the U.S. Department of Energy under contract DE-AC05-00OR22725

RECENT PROGRESS ON PARALLEL ELEGANT *

Y. Wang †, M. Borland, H. Shang, R. Soliday, A. Xiao, ANL, Argonne, IL 60439, USA

Abstract

The electron accelerator simulation software `elegant` [1] is being parallelized in a multi-year effort. Recent developments include parallelization of input/output (I/O), frequency map analysis, dynamic aperture search, and position-dependent momentum aperture determination. Parallel frequency map, momentum aperture analysis, and dyanmic aperture search provide rapid turnaround for important determinants of storage ring performance. The development of parallel Self-Describing Data Sets file (SDDS) I/O based on MPI-IO made it possible for parallel `elegant` (`Pelegant`) to take advantage of parallel I/O. Compared with previous versions of `Pelegant` with serial I/O, the new version not only enhances the I/O throughput with good scalability but also provides a feasible way to run simulations with a very large number of particles (e.g., 1 billion particles) by eliminating the memory bottleneck on the master with serial I/O. Another benefit of using parallel I/O is reducing the communication overhead significantly for the tracking of diagnostic optical elements, where the particle information has to be gathered to the master for serial I/O.

INTRODUCTION

The parallel version of `elegant`, `Pelegant`, has proved to be very beneficial to several computationally intensive accelerator research projects. Simulation with a very large number of particles is essential to study detailed performance of advanced accelerators. This was demonstrated in simulations of microbunching for FERMI [2]. In those simulations the maximum number of particles was reached at about 60M when the serial version of SDDS was used, which limited our ability to probe microbunching effects at shorter wavelengths. In the version of `Pelegant` used in those studies, the bottleneck came from the memory usage of the master CPU, which was required to hold all the particle information when simulating a diagnostic element, such as a watch point, where all the particles have to be gathered to master to be written on the disk.

The recent development of parallel SDDS [3] makes it possible for `Pelegant` to take advantage of parallel I/O through MPICH2 [4]. With parallel I/O, a common file is opened by all the processors, but each processor is only responsible for reading/writing the particles allocated to it. This technique improved I/O throughput significantly, especially on some parallel file systems, such as Parallel Virtual File System (PVFS) [5] and General Parallel File System (GPFS) [6]. `Pelegant` can also run on Network File System (NFS) file system, although the I/O performance is not as good as on the parallel file systems. The overall performance of `Pelegant` on all the file systems mentioned above has also been improved due to reduced communication overhead compared with gathering particles to master before writing to the disk with serial I/O. A nice feature of this parallel SDDS I/O is that the output/input files are the same as the files for serial I/O, which is very convenient for data analysis and exchanging data in SDDS format with other related simulation programs.

In this paper, we first describe the effort we made to integrate parallel SDDS with `Pelegant`, then we report the progress made on the parallelization of frequency map, momentum aperture analysis, and dynamic aperture optimization in `Pelegant`.

IMPLEMENTATION OF `PELEGANT` WITH PARALLEL SDDS

The simulation code `elegant` is being gradually parallelized with particle-based domain decomposition to reduce the simulation time for multi-particle beams. Beamline elements are classified in the element dictionary as parallel-capable or serial-only. Particles will be gathered to the master CPU or scattered to slave CPUs when the beam encounters a serial element or a parallelized element [7, 8], respectively. As the majority of the frequently used elements has been parallelized, `Pelegant` has been efficiently used for several important accelerator research projects [2, 9, 10, 11, 12].

Even in cases where one must use beamline elements that are not yet parallel-capable, a very significant performance improvement can be realized. However, for simulations with large numbers of particles, I/O for input, intermediate output, and final output, can consume a significant portion of simulation time. In addition to the communication overhead of gathering particles to the master, memory also becomes a problem when we simulate a very large number of particles with a central process (i.e., Master) holding all the particle information for I/O operations.

To eliminate these bottlenecks, we developed parallel SDDS [3] with MPI-IO recently. The parallel SDDS is derived from the serial version of SDDS [13], which has been successfully applied to several accelerator simulation

* Work supported by the U.S. Department of Energy, Office of Science, Office of Basic Energy Sciences, under Contract No. DE-AC02-06CH11357.

† ywang25@aps.anl.gov

BEAM FIELDS IN AN INTEGRATED CAVITY, COUPLER AND WINDOW CONFIGURATION *

Stephen Weathersby, Alexander Novokhatski
(SLAC National Accelerator Laboratory, Menlo Park, California)

Abstract

In a multi-bunch high current storage ring, beam generated fields couple strongly into the RF cavity coupler structure when beam arrival times are in resonance with cavity fields. In this study the integrated effect of beam fields over several thousand RF periods is simulated for the complete cavity, coupler, window and waveguide system of the PEP-II B-factory storage ring collider. We show that the beam generated fields at frequencies corresponding to several bunch spacings for this case gives rise to high field strength near the ceramic window which could limit the performance of future high current storage rings such as PEP-X or Super B-factories.

INTRODUCTION

The SLAC PEP-II asymmetric B-factory storage ring collider nominally collides 1700 bunches of 3.0 A of 3 GeV positrons on 2.0 A of 9 GeV electrons consisting of a low energy positron storage ring (LER) situated above a high energy electron storage ring (HER). The rings intersect at an interaction point (IP) within the BaBar detector sustaining a luminosity of $1.2 \times 10^{34}\mathrm{cm}^{-2}\mathrm{s}^{-1}$at the $\Upsilon(4S)$ resonance.

Energy lost from synchrotron radiation and wake fields is replenished to the beam with high power RF supplied to cavities. Klystrons generate the 1 MW high power 476 MHz CW RF which is transported through WR2100 waveguides into the cavities through a 1.8 cm thick 24.8 cm diameter ceramic window. The window holds the ultra-high vacuum pressure required in the cavity from the near atmosphere pressure of the waveguide while transmitting 500 kW of RF power[1, 2]. The coupler geometry places the window at a half wavelength away from a detuned short position of the cavity field to minimize reflected power at the window position[1, 2]. This works well for reflected energy at harmonics of the main generator RF frequency. For high current storage ring B-factories and light sources, higher order modes (HOMs) excited by the beam constitute a significant portion of the cavity fields. The effect of such fields on the complete cavity/coupler/window/waveguide system is examined in this study. Fields produced by the beam in the cavity enter the waveguide through the cavity coupler and excite modes with fields near the window.

* Work supported by Department of Energy Contract DE-AC02-76SF00515

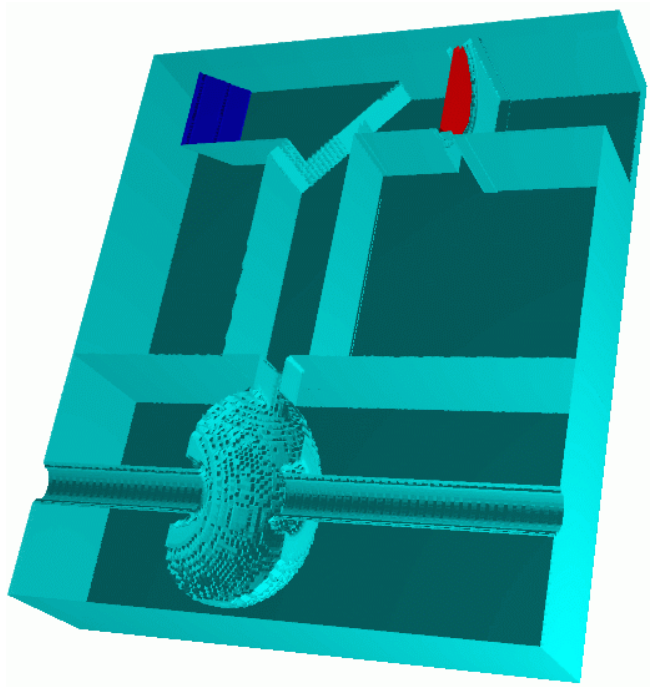

Figure 1: Model of PEP-II cavity/coupler/window/waveguide system.

RF SYSTEM MODEL

Figure 1 shows a cut plane through the full 3d model of the PEP-II cavity/coupler/window/waveguide RF system. A section of 1.5 meter long beam pipe is surrounded by a cavity which is connected through a small coupling iris into a rectangular volume which acts as a quater-wave transformer. This volume intercepts a second rectangular volume, which functions as a filter, in which there exists a dielectric ceramic window (red) of relative permittivity ε_r=9 and HOM absorbing ceramic tiles (blue) [6] with a relative permittivity of ε_r=30 and conductivity $\sigma =$ 0.918 $\mathrm{ohm}^{-1}\mathrm{m}^{-1}$. The model does not include the higher order mode dampers and detuning structures attached to the cavity. The WR2100 waveguide cuttoff frequency for the TE10 mode is 280 MHz. The beam pipe diameter is 9.5 cm with a cuttoff frequency of 1.8 GHz.

RF SYSTEM EIGENMODES

The resonant modes in the cavity/coupler/window/waveguide RF system are identified in two ways. One is by performing an eigenmode deter-

BPM BREAKDOWN POTENTIAL IN THE PEP-II B-FACTORY STORAGE RING COLLIDER

Stephen Weathersby, Alexander Novokhatski
(SLAC National Accelerator Laboratory, Menlo Park, California)

Abstract

High current B-Factory BPM designs incorporate a button type electrode which introduces a small gap between the button and the beam chamber. For achievable currents and bunch lengths, simulations indicate that electric potentials can be induced in this gap which are comparable to the breakdown voltage. This study characterizes beam induced voltages in the existing PEP-II storage ring collider BPM as a function of bunch length and beam current.

INTRODUCTION

The SLAC PEP-II asymmetric B-factory storage ring collider nominally collides 1700 bunches of 3.0 A of 3.1 GeV positrons on 2.0 A of 8.0-10.1 GeV electrons. It consists of a low energy positron storage ring (LER) situated above a high energy electron storage ring (HER). The rings intersect at an interaction point (IP) within the BaBar detector sustaining a luminosity of $1.2 \times 10^{34}\mathrm{cm}^{-2}\mathrm{s}^{-1}$at the $\Upsilon(4S)$ resonance. To monitor the beam position, hundreds of beam position monitors (BPMs) line the beam vacuum chamber. Each BPM consists of a round button electrode 15 mm in diameter which is mechanically press fitted to the 50 Ohm feed-through connector as shown in figure 1.

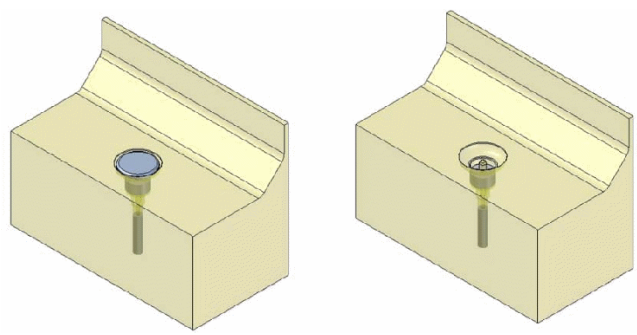

Figure 1: One quarter of the BPM geometry with and without a button. Chamber length is 9 cm. Button diameter is 15 mm.

While running at shortened bunch length (9 mm) some of the upper button electrodes heated up enough to fall off their mounts. The upper electrode fell onto the lower electrode as shown in Fig. 2 which not only shorted the underlying electrode but also became a large obstacle for the beam fields, increasing the current though the lower electrode. This then melted the feed-through (Fig.3) causing a vacuum breach.

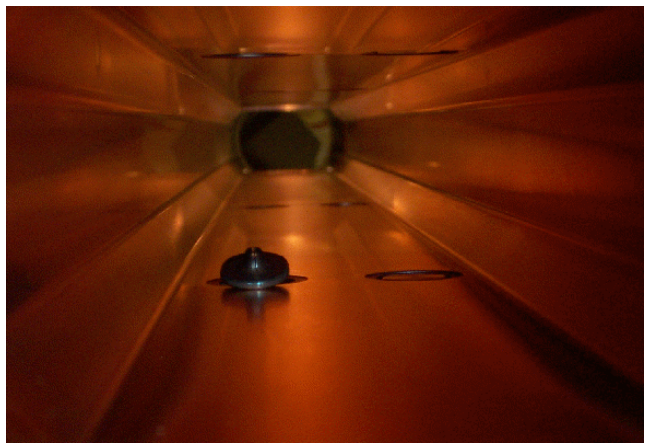

Figure 2: A button of an upper BPM fell off onto a lower button.

Figure 3: Melted feed-through of a lower button and the fallen upper button.

The origin of the heating is the wake field generated by an intense short bunch passing by the vacuum chamber discontinuity due to a BPM button. The effect of beam fields on a PEP-II BPM are examined[1]. Scattering parameter analysis reveals resonant behavior near the frequency of 7 GHz. Time domain simulations show that maximum electric fields in the BPM are located at the upbeam and downbeam extremes of the BPM button corresponding to an excited dipole resonant mode in the BPM environment. PEP-II has had a history of arcing and vacuum bursts caused by small geometric gaps in RF seals[3, 2]. It is natural to suspect that such small gap structures in the BPM design may cause the same problems. At a resonant condition when a

* Work supported by Department of Energy Contract DE-AC02-76SF00515

RECYCLER LATTICE FOR PROJECT X AT FERMILAB *

Meiqin Xiao, David E. Johnson, FNAL, Batavia, IL 60510, USA

Abstract

Projext X is an intense proton source that provides beam for various physics programs. The source consists of an 8 GeV H^- superconducting linac that injects into the Fermilab Recycler where H^- are converted to protons. Protons are provided to the Main Injector and accelerated to desired energy (in the range 60 - 120 GeV) or extracted from the Recycler for the 8 GeV program. A long drift space is needed to accommodate the injection chicane with stripping foils. The Recycler is a fixed 8 GeV kinetic energy storage ring using permanent gradient magnets. A phase trombone straight section is used to control the tunes. In this paper, the existing FODO lattice in the RR10 straight section being converted into doublet will be described. Due to this change, the phase trombone straight section has to be modified to bring the tunes to the nominal working point. A toy lattice of recycler ring is designed to simulate the end-shim effects of each permanent gradient magnet to add the flexibility to handle the tune shift to the lattice during the operation of 1.6E14 with KV distribution of the proton beam to give ~0.05 of space charge tune shift. The comparison or the combinations of the two modification ways for the Recycler ring lattice will be presented also in this paper.

INTRODUCTION

Project X [1] is an intense proton source that provides beam for various physics programs. The source consists of an 8 GeV H^- superconducting linac that injects into the Recycler where H^- are converted to protons. Protons are provided to the Main Injector and accelerated to desired energy or extracted from the Recycler for the 8 GeV program. The Recycler ring (shown in Fig. 1) is a fixed 8 GeV kinetic energy storage ring using permanent gradient magnets. RR10 is the straight section for placing the injection system and RR60 is a phase trombone straight section used to control the tunes.

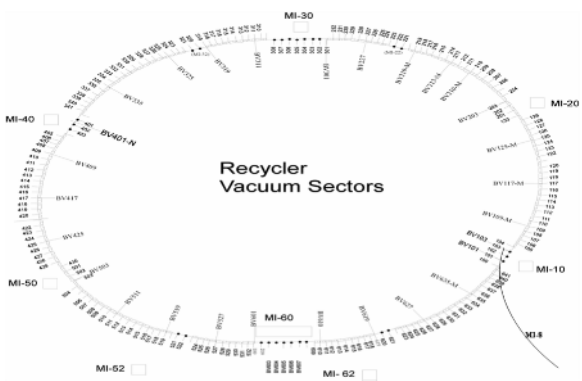

Fig. 1: Outline of the Recycler ring

Currently, In the recycler lattice for Project Run II, RR30 contains the symmetric electron cooling insert between 305 and 307 with remainder of the Recycler straight section is roughly a FODO section, but not periodic, shown in Fig. 2. This section will be replaced by a FODO lattice for Project NOvA [2], shown in Fig. 3. Notice that there are 3 quads in each D-D half-cell in RR30 due to permanent magnet quad strength limitations. To match the FODO straight section into the ring and keep the current tunes (25.425,24.415) , the lattice functions reach a peak value of 80 m.

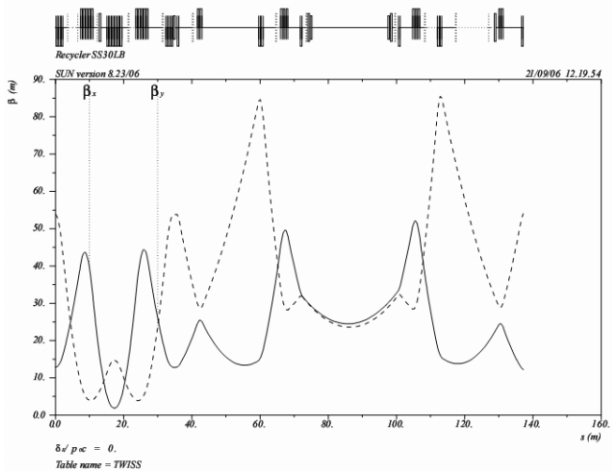

Fig.2: RR30 in the Recycler lattice for Project Run II

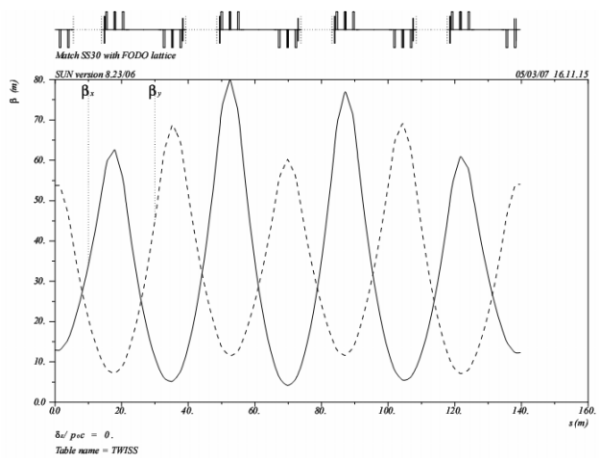

Fig.3: RR30 in the Recycler lattice for Project NOvA

The Recycler lattice for Project X will be based on The lattice for NOvA. Keep RR30 straight section as FODO cell but would lower the beta functions as the rest of the ring. We will also keep using extraction line from the Recycler to the Main Injector.

*Operated by Fermilab Research Alliance, LLC under contract No. DE-AC02-07CH11359 with the United States Department of Energy.
#meiqin@fnal.gov

ARRAY BASED TRUNCATED POWER SERIES PACKAGE*

Lingyun Yang†, NSLS-II, BNL, Upton, NY 11973, USA

Abstract

Truncated Power Series Algebra (TPSA) or Differential Algebra (DA) package has been a fundamental component for many accelerator physics simulation code, including FPP/PTC, MAD-X, BMAD and Tracy. We have developed a new algorithm to extend the ability of TPAS to handle problems with both large number of variables and high order. This package is implemented in C++ language with operator overloading, and has been integrated into PTC and MAD-X.

INTRODUCTION

Truncated Power Series Algebra (TPSA) or Differential Algebra (DA) package is a tool for Taylor series manipulation [1, 2]. It follows certain mathematical rules to do arithmatics among the Taylor series and can be used for map generating, sensitivity study, automatic differentiation and many other applications. Since it was implemented by Dr. Berz, it has been a fundamental component for many accelerator physics simulation codes, including FPP/PTC [4], MAD-X [3], BMAD and Tracy.

The package in Ref. [1] has two limitations:

- Limited index space at hign v, e.g. 39 variables can only handle up to first order[1].
- Without operator overloading, Applying DA to an existing code will need many careful translation, and introduce temporary variable. (think about translate $x = (a + b) * c/d$).

We have developed a new TPSA package in C++ recently, with a new algorithm which can expand the ability to both high number of variables and high orders. It is also more user friendly and the speed are better than the FORTRAN 77 implementation.

ALGORITHM

The Taylor series of an given function $f(x_1, \cdots, x_d)$ is given as:

$$f(x_1, \cdots, x_d) = \sum_{n_1=0}^{\infty} \cdots \sum_{n_d=0}^{\infty} \frac{(x_1 - a_1)^{n_1} \cdots (x_d - a_d)^{n_d}}{n_1! \cdots n_d!} \left(\frac{\partial^{n_1+\cdots+n_d} f}{\partial x_1^{n_1} \cdots \partial x_d^{n_d}} \right) \tag{1}$$

Given the analytic form of $f(x_1, \cdots, x_d)$, we can calculate the coefficient of Taylor series expansion, f_{x_1}, f_{x_2}, $f_{x_1 x_2}$, up to any order precisely. This can be done with finite difference method, but when going to high order, the truncation error and linear approximation may be a main obstacle. TPSA package uses a set of rule, which is complete for a field of real number and basic arithmetics. The rules can be found in Ref. [2], and we summerize here:

- Addition/Substraction. It is done between only corresponding terms (coefficients with same order or pattern of differentiation).
- Multiplication with constant. It scales all the coefficients.
- Multiplication with another series. The order of differentiation are added up for each variable. The new coefficient are added up to the new location with new pattern of order.
- Reciprocal. The coefficient is gained from the pattern of Taylor expansion of $1/x$.
- Basic functions. Such as $\sin(x)$,$\cos(x)$,$\sqrt{x}$ are just deduced from their coefficients of Taylor series expansion together with the multiplication of two series.

As we can see that +/- are trivial, and every other calculation is depending on multiplication of two TPAS series. While for multiplication the key part is how to arrange the storage of each coefficients and locate them quickly.

IMPLEMENTATION

A TPSA vector with v independent variables, each up to d degrees, will have $C(v + d, d)$ or $C(v + d, v)$ elements, where $C(n + v, v)$ are binomial coefficients defined as

$$C(v + d, v) \equiv \binom{v + d}{v} = \binom{v + d}{d} = \frac{(v + d)!}{v!d!}$$

From this we can see that, for the length of a TPSA vector, the order and number of variables are symmetric. A code can do high order with low number of variables should be

* Work supported by the Director, Office of Science, U. S. Department of Energy under Contract No. DE-AC02-05CH11231.

† lyyang@bnl.gov

[1] We can use more index function again, 3 instead of 2, to relax the limit from $(n + 1)^{v/2}$ to $(n + 1)^{v/3}$, but the performance will be lower.

MOLECULAR DYNAMICS SIMULATION OF CRYSTALLINE BEAMS EXTRACTED FROM A STORAGE RING

Yosuke Yuri
Takasaki Advanced Radiation Research Institute, Japan Atomic Energy Agency,
1233 Watanuki-machi, Takasaki, Gunma 370-1292, Japan

Abstract

It is well-known that a charged-particle beam is Coulomb crystallized in the low-temperature limit. The feasibility of beam crystallization in a storage ring has been raised by the recent progress in beam cooling techniques and in understanding of the behavior of crystalline beams. To go a step further, we here investigate the extraction and transport process of crystalline ion beams, employing the molecular dynamics simulation technique. The dependence of the stability on the lattice of the extraction beam line is explored to show whether various crystalline beams can be transported stably without collapse of the ordered structure.

INTRODUCTION

Applying a dissipative force to a charged-particle beam circulating in a storage ring, we can reduce the emittance of the beam and even expect the occurrence of a type of phase transition. In fact, the beam finally exhibits an ordered structure at the low-temperature limit if some physical conditions are fulfilled. Such an ultimate state of the beam is known as a crystalline beam [1-3] whose spatial structure is determined by the line density [4]. When the line density is sufficiently low, a one-dimensional (1D) string is formed. By increasing the line density, we can transform the string into a two-dimensional (2D) zigzag crystal and, then, eventually into a three-dimensional (3D) shell crystal. In theory, the emittance of a crystalline beam is zero (except for quantum noise) at the low-temperature limit [5, 6].

In order to form and maintain various kinds of crystalline beams, the following two conditions must be satisfied [7, 8]; the storage ring must be operated below the transition energy for crystal formation, and the average betatron phase advance must be less than 127 degrees per lattice period for crystal maintenance. In an ideal crystalline state, the Coulomb repulsive force perfectly balances with the periodic external focusing force of the ring and random interparticle collisions disappear. The crystalline state is stable and thus lasts long even after the cooling force is removed [9]. As reviewed in Ref. [10], according to many advanced theoretical and numerical works, it is now considered that crystalline beams can exist in a storage ring, at least, in theory.

Here, consider the extraction of a crystalline beam from a storage ring. The crystalline beam is additionally kicked by an extraction device such as an electrostatic deflector or a septum magnet and then transported along the (usually, nonperiodic) beam line. The periodicity of the focusing force is lost, and thus the above-mentioned maintenance condition of crystals is not fulfilled any more. We expect that the emittance of the crystalline beam is increased, or even the crystalline structure of the beam can be destroyed by the extraction process. In order to verify this expectation, molecular dynamics (MD) simulations were carried out. The present MD simulation results show the stability of extracted crystals is consistent with that defined by the maintenance condition of crystals in a ring.

SIMULATION PARAMETERS

For the present simulation study, the MD code "CRYSTAL" is employed [11]. As an extraction device, an electrostatic field can be assumed as well as a normal dipole magnetic field. The equation of motion is integrated by the code in a symplectic manner. In the present MD study, the beam is assumed to be bunched by a longitudinal radio-frequency field in the ring. The Coulomb forces among particles in a bunch are directly calculated. For more detail information on the MD code, see Ref. [10].

As a storage ring lattice, the parameters of S-LSR [12] have been adopted. The operating point of the ring assumed here satisfies the above two conditions. We have also considered several different test extraction lines that have different transverse phase advances from the extraction device to an ideal target position (length: 7.8 m) in order to see how the stability of the extracted beam depends on the lattice design. The main simulation parameters are summarized in Table 1. Here, we show only two cases of high and low phase advances.

MOLECULAR DYNAMICS RESULTS

High-phase-advance lattice

For extraction, a dipole magnetic magnet or

Table 1: Main simulation parameters.

Ring lattice	S-LSR
Ion species	40 keV $^{24}Mg^{+}$
Superperiodicity	6
Circumference	22.56 m
Ring tunes (ν_x, ν_y, ν_z)	(1.44, 1.44, 0.15)
Extraction device	Electrostatic or dipole magnetic field
Beam line length	7.8 m
Phase advances of the beam line [deg]	(110, 81), (161, 85), (174, 101), (310, 167), and, (363, 181)